Eindhoven University of Technology

MASTER

Cylinder deactivation on 4 cylinder engines

A torsional vibration analysis

Peters, G.F.A.

Award date:
2007

Link to publication

Cylinder deactivation on 4 cylinder engines

Document Version:
Publisher's PDF, also known as Version of Record (includes final page, issue and volume numbers)

Please check the document version of this publication:

• A submitted manuscript is the version of the article upon submission and before peer-review. There can be important differences between the submitted version and the official published version of record. People interested in the research are advised to contact the author for the final version of the publication, or visit the DOI to the publisher's website.
• The final author version and the galley proof are versions of the publication after peer review.
• The final published version features the final layout of the paper including the volume, issue and page numbers.

Link to publication

Cylinder deactivation on 4 cylinder engines:
A torsional vibration analysis

Gilbert Peters

DCT 2007-11

G.F.A. Peters   s0552954 (TU/e)

Supervisor: (TU/e)   Bram Veenhuizen

Summary

The project "car of the future" is a project aimed at designing a sustainable passenger car for the year 2020. Sustainability is a very broad topic, which reaches further than fuel economy and exhaust emissions. The "car of the future" uses a modularity concept to maximize the sustainability aspect of the vehicle in a broad sense. The modularity concept makes it possible to use different powertrains, creating the opportunity to adapt the vehicle to the availability of fuels, or adapt the powertrain to the demands of the user in the future. The desire for flexibility justifies the choice for an internal combustion engine as primary mover, because it can be adapted to a large variety of fuels with more or less modifications to its construction.

Reducing the fuel consumption and the related CO2 emissions is increasingly important these days. Increasing the powertrain efficiency is therefor one of the major goals within the project "car of the future". Typically, internal combustion engines operate more efficiently when the engine load is high. Engine load during daily traffic however is typically low, resulting in sub-optimal fuel consumption. Better matching of the real engine load with the optimal engine load can be obtained by applying cylinder deactivation. By deactivation of cylinders the load of the still activated cylinder is increased with improved efficiency as a consequence.

Cylinder deactivation increases the torsional vibrations of the engine because of the reduced combustion interval and increased combustion peaks. Currently, cylinder deactivation is used on multi-cylinder engines, V12, V8 or V6, where the torsional vibrations do not cause much of a problem due to the still acceptable combustion intervals and combustion peaks during deactivation. In Europe, the majority of passenger cars use a 4 cylinder engine, therefor the research has been focussed on the vibrational powertrain behavior of four cylinder engines using cylinder deactivation. The goal of this research is therefor:

"Determine the influence of cylinder deactivation on a 4-cylinder engine, regarding the vibrational behavior of the powertrain."

In order to analyze the effect of cylinder deactivation on powertrain dynamics, the important criteria regarding powertrain vibrations are analyzed. The important criteria regarding powertrain comfort which are studied are "engine shake", "gear rattle" and "vehicle shuffle". Vibrations can be suppressed or damped by using for instance a torsion damper (TD) or an integrated starter alternator damper (ISAD), which can apply a positive or negative torque to the crankshaft. The ISAD system is herein preferred because it makes other powertrain functions possible, like regenerative braking, boosting and start/stop function.

The powertrain with all its components are modeled, in order to analyze the effect of cylinder

deactivation on the powertrain dynamics. These models describe the engine dynamics, manual transmission, driveshafts, wheels and vehicle. The powertrain can be equipped with a torsion damper or ISAD system. Both powertrains are compared by analyzing the frequency responses of both powertrains. Both powertrains show different eigenfrequencies, which can interfere with the engines' excitation frequency. Interference of the eigenfrequencies with the excitation frequencies can cause resonances. Analysis will show which powertrain is best suited in combination with cylinder deactivation.

During deactivation the deactivated cylinders are being used as an "air spring". The valves of the deactivated cylinder are kept closed, to minimize the pump work by this cylinder. The trapped air in the cylinder will periodical complete a compression cycle, followed by an expansion cycles. The timing of valve closing influences the torque caused by the "air spring". Three different valve timings are being discussed, serving as a starting point for further research.

Deactivation of cylinders leads to increased powertrain vibrations. These vibrations are the cyclic speed fluctuation, primary transmission shaft acceleration, longitudinal vehicle acceleration and powertrain unit acceleration. The influence of the engine speed, engine load and gear ration on these vibrations are studied. The ISAD system can be used as a passive damper to reduce the vibrations caused by cylinder deactivation. Simulation results show how effective this damping system is.

Samenvatting

Het project "auto van de toekomst" is gericht op het ontwerpen van een duurzame personenauto voor het jaar 2020. Duurzaamheid is een breed begrip en reikt verder dan brandstofverbruik en uitlaatgas emissies. Om de duurzaamheid in een breed perspectief te kunnen garanderen wordt er gebruik gemaakt van een modulariteitsconcept. Dit modulariteitsconcept maakt het mogelijk om verschillende aandrijflijn concepten te gebruiken, waardoor ingespeeld kan worden op de beschikbaarheid van brandstoffen en op de wensen van de gebruiker en eisen van de overheid. De wens naar flexibiliteit verklaard tevens waarom er gekozen is voor een inwendige verbrandingsmotor als primaire aandrijving, welke in staat is om op meerdere brandstoffen te functioneren.

Het terugdringen van het brandstofverbruik en de daaraan gekoppelde CO_2 emissie is heden ten dagen zeer belangrijk. Het verhogen van het rendement van de aandrijflijn is dan ook een van de speerpunten binnen het project "auto van de toekomst". Het rendement van een verbrandingsmotor is in de regel het hoogst bij een hoge motorbelasting. In het dagelijkse verkeer wordt de verbrandingsmotor echter slechts licht belast, doordat de vermogensvraag gering is. Hierdoor is het rendement van de aandrijving laag. Het beter afstemmen van de optimale motor belasting met de werkelijke belasting kan worden gerealiseerd door middel van cilinder deactivatie. Door het deactiveren van een of meerdere cilinders, worden de actieve cilinders hoger belast, waardoor het rendement van deze cilinders en daarmee de totale motor toeneemt.

Het deactiveren van cilinders zorgt ervoor dat de dynamica van de verbrandingsmotor veranderd, met vibraties als gevolg. Cilinder uitschakeling wordt op dit moment alleen toegepast op grote multi-cilinder motoren, zoals V12, V8 en V6 motoren, waarbij gedurende cilinder uitschakeling het trillingscomfort gewaarborgd blijft. De meest voorkomende motor configuratie in Europa is echter de 4 cilinder motor. Het onderzoek is daarom gericht op het toepassen van cilinder uitschakeling op 4 cilinder motoren. Het doel van het onderzoek is daarom ook als volgt gedefinieerd:

"Bepalen van de invloed van cilinder uitschakeling op 4 cilinder motoren, betreffende het vibratie gedrag van de aandrijflijn."

De belangrijke aandrijflijn criteria met betrekking tot het trillingscomfort zijn bestudeerd, te weten "gear rattle", "engine shake" en "vehicle shuffle". Vibraties kunnen worden onderdrukt of gedempt door gebruik te maken van onder meer een trillingsdemper of een starter/generator, welke functioneert als demper door een positief dan wel negatief koppel aan de krukas te leveren. Gezien de extra mogelijkheden die een starter/generator met zich mee brengt heeft dit systeem de voorkeur.

Om het effect van cilinder uitschakeling op de aandrijflijn dynamica te kunnen bestuderen is de aandrijflijn met al zijn componenten gemodelleerd. Deze modellen beschrijven het dynamisch gedrag

van de verbrandingsmotor, de aandrijflijn ophanging, een manuele transmissie, aandrijfassen, wielen en het voertuig. Als vibratie dempers worden zowel de torsie demper (TD), alsook de starter/alternator (ISAD) gebruikt. Dit levert twee verschillende modellen op die op basis van frequentie responsies met elkaar vergeleken zijn. De beide aandrijflijnen vertonen eigenfrequenties die, doordat de excitatie frequentie van de verbrandingsmotor afneemt tijdens cilinder uitschakeling, samen kunnen vallen met de excitatie frequentie en zo resonantie kunnen veroorzaken. Onderzoek wijst uit welke aandrijflijn het meest geschikt is voor gebruik in combinatie met cilinder deactivatie.

Tijdens het deactiveren van cilinders, worden de uitgeschakelde cilinder(s) gebruikt als "lucht veer". De kleppen van deze cilinder(s) worden gesloten zodat ze geen pomp werk verrichten. De cilinder zal vervolgens periodiek een compressie slag gevolgd door een expansie slag ondergaan, wat resulteert in een periodiek koppel verloop. Het moment van sluiten van de kleppen blijkt van invloed op het koppel wat veroorzaakt wordt door de "lucht veer". Drie verschillende sluitingstijdstippen worden besproken.

Het deactiveren van cilinders leidt tot een toename in de aandrijflijn vibraties. Hiervoor is gekeken naar motortoerental fluctuaties, primaire transmissie as acceleratie, longitudinale voertuig acceleratie en de aandrijflijn kantel acceleratie. Gekeken is naar de invloed van het motortoerental, overbrengingsverhouding en motorbelasting op deze acceleraties en fluctuaties. De resultaten van de simulaties zijn getoetst aan criteria verkregen uit literatuur. De starter generator wordt ingezet als passief dempingsysteem, welke de trillingen kan reduceren. Simulatie resultaten laten zien hoe effectief deze wijze van demping is.

Contents

Chapter 1

Introduction

1.1 Project "car of the future"

In 2005, the Society of Nature and Environment (Stichting Natuur en Milieu) challenged the 3 Dutch Universities of Technology to design "A car of the future" for the year 2020. Its objective is to create demand for clean and clever mobility and encourages the automotive industry to speed up the development of sustainable mobility solutions. The concept car will be unveiled at the 2007 Amsterdam Motorshow, AutoRAI.

Design and development is performed by students of the 3 Universities, forming a multidisciplinary project team. Students of Delft University are responsible for the vision development, interior and exterior design, students of Twente University are responsible for vehicle intelligence, interface design and context, while Eindhoven University is responsible for vehicle dynamics and powertrain engineering of the concept car.

In total 4 students from Eindhoven University of Technology have studied a variety of powertrain pathways for the future. The powertrains studied are the fuel cell hybrid powertrain, series hybrid powertrain and a classical internal combustion engine powertrain. This Thesis deals with the classical internal combustion engine powertrain.

1.2 Thesis objective

The objective of this thesis is twofold. One objective is to design one of the powertrains for the "car of the future". Developing the complete powertrain for the "car of the future" is an enormous task, ambitious and not achievable within the given time period. Therefor the decision was made to focus on one particular topic regarding the powertrain design, cylinder deactivation.

Cylinder deactivation is a technology which can reduce emissions and increase the engine efficiency. Cylinder deactivation will change the dynamics and vibrational behavior of the engine. This will have an influence on the powertrain, therefor the problem statement is defined as:

"Determine the influence of cylinder deactivation on a 4-cylinder engine, regarding the vibrational behavior of the powertrain."

The problem statement is divided into several, more specific research questions. Answering these questions will subsequently provide the answer to the problem statement.

- What will be the benefit in terms of engine efficiency?

- What are the constraints of cylinder deactivation?

- What kind of vibration suppression methods can be used to address powertrain vibrations?

- How many cylinders can be deactivated and in what order?

- Can acceptable comfort levels be obtained by using passive or active damping in powertrains with engines with cylinder deactivation?

Cylinder deactivation in itself is nothing new, but in almost all cases it is applied to large multi cylinder engines (6 or more cylinders). These engines are typically not used in mainstream vehicles (at least not in Europe), so improving these engines will therefor not have a great influence on the total fuel consumption and emissions. The research is therefor completely focussed on cylinder deactivation for mainstream 4 cylinder engines.

1.3 Report outline and approach

This thesis is devoted to the development of the internal combustion engine powertrain, with as main topic cylinder deactivation. Several choices have been made to come to the current powertrain design which are discussed in chapter two and three. Chapter four discusses how cylinder deactivation works and what the benefits and limitations are. Due to the expected increased vibrations caused by cylinder deactivation, powertrain Noise Vibration and Harshness (NVH) is discussed in chapter five. Chapter six addresses the modeling of the powertrain, used for simulations. The results of these simulations can be found in chapters seven and eight. The report is concluded with conclusions and recommendations.

Chapter 2

Project "car of the future"

2.1 The vehicle concept

The objective of the concept car is to speed up the development of sustainable mobility solutions. Sustainable development is herein defined as:

"the development that meets the needs of the present without compromising the ability of future generations to meet their own needs." - Brundtland -

Vehicles, and the automotive industry, put a strain on the sustainability in several different areas:

- Exhausting of raw materials (e.g. oil)

- Ecological damage (e.g. mining, disposal)

- Energy consumption during mining and manufacturing

- Emissions and waste during mining and manufacturing

- Energy consumption and emissions during driving (especially technically dated vehicles)

When looking at the addressed issues, reducing the environmental impact is not just a matter of reducing fuel consumption and tail pipe emissions. However, currently tailpipe emissions and fuel consumption are the criteria of legislation in the form of EURO-emission norms and the 140 [g/km] CO_2 norm for 2008, agreed between the EU and the organization of manufacturers (ACEA). With a modularity concept it is possible to also address the other issues regarding sustainability.

The modularity concept aims at the possibility of easily upgrading the vehicle to a higher and newer specification of components, resulting in cleaner, more efficient and safer vehicles. Figure 2.1a gives an example of upgrading the powertrain to a newer spec, or adapt the powertrain to the availability of a certain fuel. Also, when the demands of the customer changes, durable parts of his current vehicle can be re-used into a "new" vehicle in order to reduce cost, material use and production energy [30]. By continuously upgrading the vehicle fleet, the total state of technology of the fleet will stay up to date. This concept also allows the customer to specify in detail the specifications of his vehicle. The consequence for the industry is that a shift occurs from manufacturing to services (leasing) and

the actual manufacturing will be done through local production. More about the modularity and leasing concept can be found in [19].

(a)   **(b)**
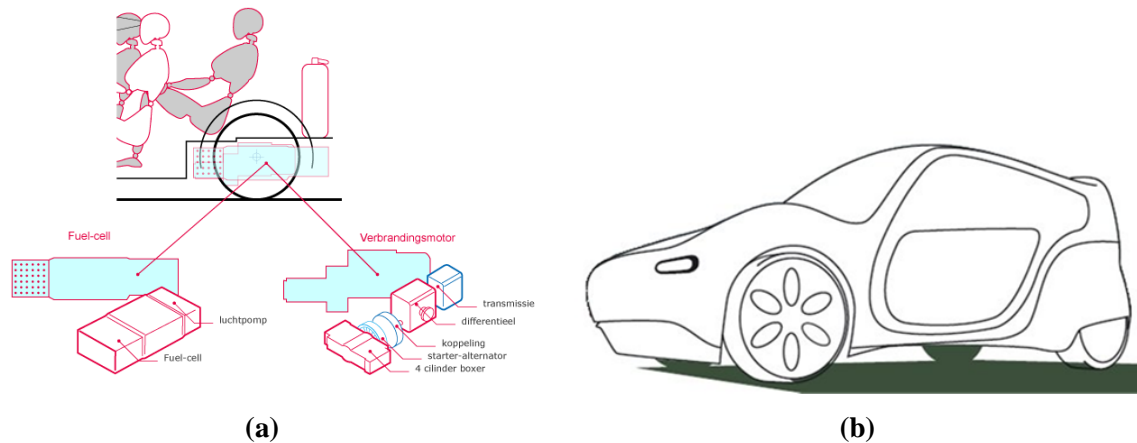
*Figure 2.1: **(a)** Example of powertrain modularity. A fuel cell system can be exchanged for an internal combustion engine with transmission. **(b)** Artist impression of the "car of the future".*

2.2 Modular powertrain

By designing the powertrain as one module, it is possible to use different powertrains for one vehicle. It makes it possible to equip the vehicle with for instance a fuel cell, a large battery pack or an internal combustion engine. By doing so, it is possible to adjust the powertrain to the availability of fuels, or adjust the powertrain to the needs of the customer. For instance, an internal combustion engine can be used for towing or when a large driving range is required. A battery powered or hydrogen fuel cell powered powertrain can be used when silent and emission free driving is required. When the entire powertrain is build up by modules, it would even be possible to upgrade the powertrain with improved components like for instance an improved and heated catalyst converter, or a particle filter system.

The modularity concept has consequences however. The different powertrain modules will have to have equal outer dimensions and share the same mounting points to the chassis and suspension. Systems that are shared by the powertrains, electrical system, cabin heating etc., will have to be normalized. This could end up in sub-optimal solutions because engineering freedom is reduced (for instance limited built space or the shape of the built space). Furthermore, different powertrains have different characteristics regarding vibrations and sound. Electric powered vehicles (battery and fuel cell) equipped with in-wheel motors require advanced (active or semi-active suspension) and strengthened suspension systems to control the increased unsprung mass of the vehicle. For the internal combustion engine powertrain however, a simpler and light weight suspension is preferred in order to keep the vehicle weight low. Further studies will have to show what the balance is between the advantages and disadvantages of this modularity concept, regarding the powertrain and other modules.

Chapter 3 explains the reason for choosing the internal combustion engine as one of the primary movers for the "car of the future".

Chapter 3

The powertrain concept

The choice for a powertrain concept (Internal combustion engine, fuel cell, or other primary mover) is mainly driven by the availability of fuels or energy carriers in the future. Which fuel or energy carrier will be used in the future is not clear and hard to predict, however there is a great desire to shift away from fossil fuels because of the political and economical instability the oil and gas market causes. The availability of fuels and energy carriers now and the uncertainty in the future requires a flexible solution regarding the powertrain of the concept vehicle. Flexibility is maximized by the modularity concept, which makes it possible to replace a complete powertrain concept in case of changed demands regarding fuel availability or state of technology.

At a lower level this flexibility can also be guaranteed within one powertrain concept, the internal combustion engine. The internal combustion engine is capable of running on various fuels with more or less adjustments to its construction. Its flexibility is also of great value to support transitions to new fuels or energy carriers. This flexible characteristic makes the internal combustion engine the primary mover of choice within this thesis. Other powertrain options like the Fuel Cell (FC) or Battery Electric Vehicle (BEV) are discussed in other theses [23].

This chapter gives insight in the choices involved to come to the internal combustion engine powertrain for the "car of the future". The design is not only focussed on optimizing the engines energy efficiency, but also on integrating the powertrain inside the vehicle in order to optimize the efficiency of the entire vehicle. New engine technology is capable of reducing engine losses, increasing efficiency and letting the engine operate in its most optimal point. Cylinder deactivation is one of those technologies.

3.1 Powertrain package and layout

By choosing a smart powertrain layout it is possible to increase the total efficiency of the vehicle. The vehicle layout is however constrained by the desired space for occupants and luggage. From an interior point of view it was desired to have an entirely flat cabin space, leaving room for powertrain and suspension between the four wheels, see figure 3.1a. Furthermore, due to the modularity requirements the position of the powertrain is also constrained by possible other powertrain configurations. Figures 3.1b to 3.2 show three possible powertrain layouts. Layout L1 represents the layout as used in the majority of passenger vehicles today. It has a front mounted engine transmission unit driving the front wheels. The fuel tanks and battery are placed in the rear, under the rear seats. Layout L2 consists of a

front mounted engine with a rear mounted transmission. Battery and fuel tanks are positioned around the transmission. Layout L3 is the opposite of layout L1. The engine and transmission is mounted at the back, below the rear passenger seats. Fuel tanks and batteries are mounted in the front of the vehicle.
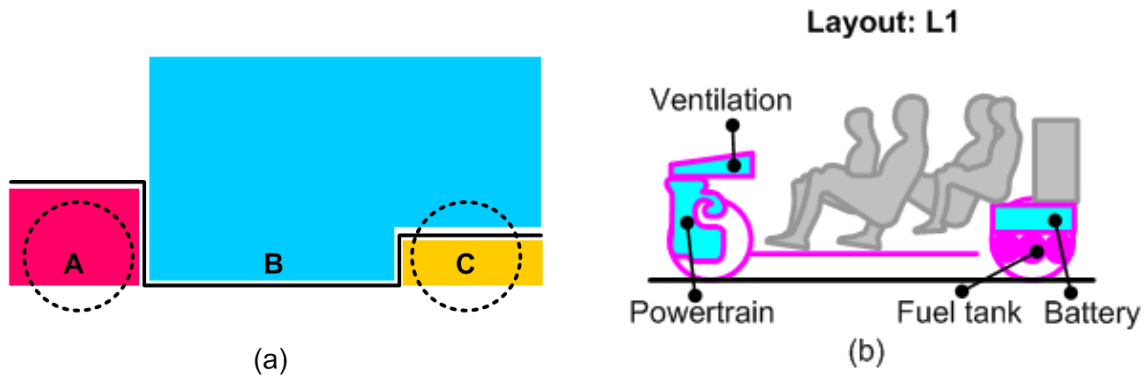
Figure 3.1: (a) Schematic representation of the vehicle and powertrain package. The volumes A and C are available for suspension and powertrain components, while B is reserved for passengers and luggage. (b) Schematic representation of layout L1, engine and transmission in the front driving the front wheels.
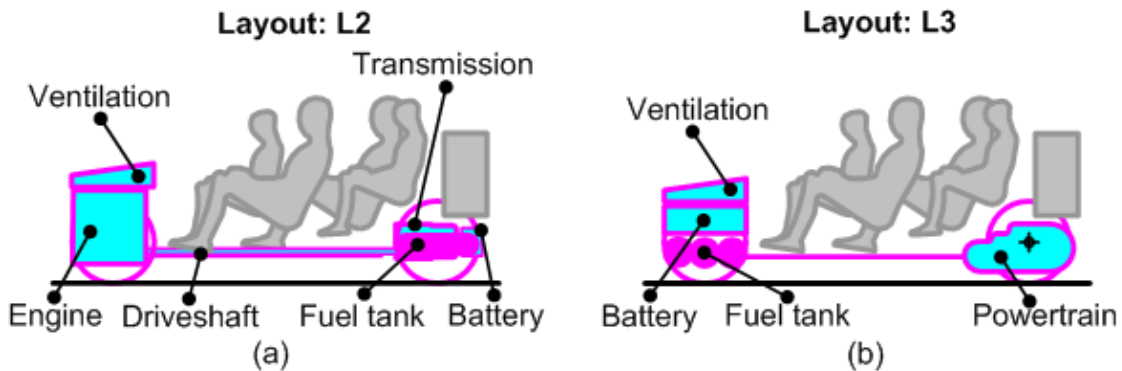
Figure 3.2: Schematic representation of (a) layout L2, engine in the front and transmission in the back. (b) layout L3, engine and transmission at the back driving the rear wheels.

Table 3.1 gives an overview of the three assessed powertrain layouts. Chosen is to use a so called mid engine setup (layout L3). The engine is placed just in front of the rear axle, driving the rear wheels, see figure 3.2b. The list emphasizes the advantages of this layout:

- Placing the engine in the rear of the vehicle improves the aerodynamic properties of the vehicle. The underside of the vehicle is not interrupted by an exhaust system. Furthermore the air flow for cooling and intake can be drawn around the rear wheels, which is already a turbulent area. The less dense heated air coming from the engine and radiator can be used to fill the void behind the vehicle in order to reduce the drag at the rear of the vehicle [27].

- Powertrain vibrations are isolated from the steering wheel, improving comfort for the driver.

- Because of the non-steering rear wheels, there is more space available between the rear wheels. This makes it possible to use a horizontally opposed engine (also known as Boxer), which has a lighter construction compared to an inline engine with the same displacement and number of cylinders [16].

- The entire vehicle concept requires the acceptance of other powertrains, for instance a fuel cell or battery electric powertrain. The frontal crash behavior of the vehicle can be more constant when more or less the same components like batteries and/or fuel tanks are placed in the front of the vehicle, no matter what powertrain is used. Also, fuel cells are very expensive and vulnerable components which will have to be protected in case of small accidents.

Disadvantages are the possibly reduced regenerative braking performance due to the reduced rear wheel load under braking and the more critical vehicle stability in extreme situations. Also, the engine build height is limited because of the rear passengers sitting on top of the engine bay. Only engines up to a certain cylinder displacement are possible.

Criteria	Layout: L1	Layout: L2	Layout: L3
Volume	-	- -	+ +
Weight	-	- -	+ +
Aerodynamics	-	-	+ +
Vibration	-	+	+
Center of gravity	+	+	+ +
Vehicle stability	+ +	-	-

Table 3.1: Assessment of powertrain layouts L1, L2 and L3.

3.2 Internal combustion engine

Over the years, under influence of public demand and stricter regulations, the internal combustion engine has significantly improved in terms of power, cost, weight, fuel economy and emissions. New insights, simulation tools, production processes, control tools and new materials provide opportunities for further improvements into the future. One of the hot topics within powertrain development is the reduction of the fuel consumption, respectively CO_2 reduction.

On average, combustion engines are overpowered for the way they are used. For instance when cruising at a speed of 80 [km/h] only approximately 6 [kW] is needed to overcome the air and rolling resistance (depending on the aerodynamic and tire properties of the vehicle), while the maximum engine output is around 75 [kW] for family cars (C-segment, e.g. Volkswagen Golf or Opel Astra). This high engine output is needed for acceleration, top speed, hill climbing or towing a heavy load.

When looking at a typical engine specific efficiency diagram, figure 3.3a, it shows that the optimal operating point is at high engine load conditions. Most of the time there is a mismatch between the optimal engine load and the required engine load, causing a non optimal fuel consumption. Hybrid powertrains, such as the Toyota Prius (power split hybrid) or the Honda Insight (parallel hybrid), are designed to optimize the engine load and engine speed by using an electrical machine as generator or as motor. The engine load can be increased for a short time by charging the batteries with the generator. The buffered electrical energy can later on be used by the motor to support the combustion
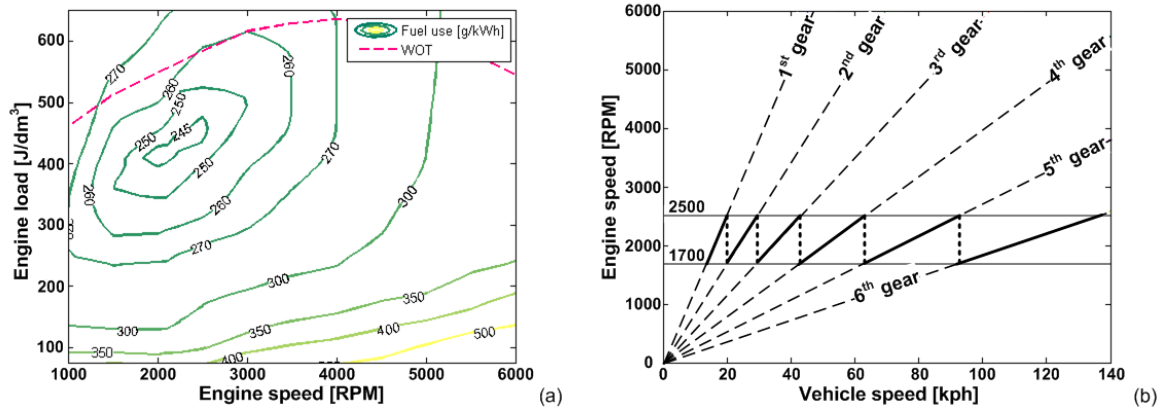
*Figure 3.3: **(a)** Typical engine efficiency diagram of a gasoline engine (WOT = Wide Open Throttle). **(b)** Relation between engine speed and vehicle speed (variogram).*

engine or for pure electric propulsion. Besides the optimal engine load strategy, the hybrid system can be used to regenerate kinetic energy during braking and provide start/stop functionality.

Future engine technology will increase the engine efficiency over a wider operating range ([17] and [8]), meaning that there is lower advantage in extra loading the engine. The advantages and disadvantages of hybrid systems make a parallel hybrid setup ideal, see table 3.2, which is still capable of start/stop operation and regenerative braking. A small system minimizes the vehicle weight penalty, minimizes conversion losses, keeps the engine temperature more leveled and minimizes the environmental load caused by battery systems and electric drives, due to the less recycle ability.

Criteria	Series hybrid	Power split hybrid	Parallel hybrid
Cost	- -	- -	+ +
Volume	- -	-	+ +
Weight	- -	+	+ +
Vibration	+ +	+	-
Package freedom	+ +	- -	-
Efficiency	+ +	+	-
Cold start emissions	-	-	+

Table 3.2: Assessment on hybrid topologies.

Table 3.3 summarizes the main engine technology which will be seen in the future on both Otto and Diesel engines. Technology already available today, will be expanded to mainstream vehicles.

3.3   Transmission

The engine power has to be transferred efficiently to the wheels through a transmission. Using a lightweight and compact transmission will help in minimizing the total weight of the vehicle. Table 3.4 shows the evaluation of several transmission systems, being the manual transmission (MT), Automated Manual Transmission (AMT), Continuously Variable Transmission (CVT) and an Automatic

Proposed technology	Area of improvement
Exhaust turbo system	engine downsizing, recovery of exhaust heat
Starter Alternator (42V) - Mild Parallel Hybrid	Increase efficiency of electrical system, start/stop operation, regenerative braking, booster function
Pump-on-demand (electrification of pumps)	reduce parasitic losses, pump flow when required, control of coolant temperature
Camless valvetrain (electro-hydraulic)	eliminate mechanical friction in valvetrain, optimizing volumetric efficiency, freedom in valve timing
Cylinder deactivation	reduce valvetrain losses, optimize engine load, reduce pumping losses

Table 3.3: Summary of future engine technology introduced to mainstream vehicles ([17] and [8]).

Transmission (AT).

Criteria	MT	AMT	AT	CVT
Engine efficiency	- -	+	+	+ +
Cost	+ +	+	-	-
Weight	+ +	+ +	-	-
Comfort	-	+	+ +	+
Package freedom	+ +	+ +	-	- -
Mechanical efficiency	+ +	+ +	-	-

Table 3.4: Assessment on hybrid topologies.

The evaluation reveals that the AMT is regarded as the ideal transmission system. It is chosen because of its lightweight construction and high mechanically efficiency. The automatic operation minimizes the human influence factor, which leads to optimal gear change operation. The gear ratios are spaced in such a way that the engine can operate in a very small engine speed range, presumed to be between 1700 and 2500 [RPM] (figure 3.3b). New engine technologies as described in table 3.3, especially the camless valvetrain technology, will result in an engine characteristic which has a high engine torque over the entire engine speed range [29]. This will compensate for the lost drivability caused by the relative wide ratio spread. Compared to other transmissions like the automatic transmission (AT) or continuously variable transmission (CVT), the automated manual transmission has a high mechanical efficiency.

3.4   Conclusion

This chapter explained a powertrain setup as proposed for the "car of the future". This powertrain uses an internal combustion engine as fuel converter because of the flexibility it offers regarding fuel use. The position and packaging of the engine helps the efficiency of the total vehicle by improving the aerodynamic efficiency and reduce vehicle weight. Several technologies are proposed which can help in increasing the fuel efficiency of the internal combustion engine.

The optimal operating point of an internal combustion engine typically lies at relative high engine loads. Increasing the engine load can be realized by using a hybrid powertrain topology, at the cost of increased volume, weight and cost. The challenge is to realize the advantages of hybrid systems, at the same time minimizing the disadvantages. Cylinder deactivation can realize an increased engine load by using camless valvetrain technology. Possible introduced vibrations can be damped by a flywheel mounted starter generator unit. The next chapter explains in detail the benefit and working principle of cylinder deactivation.
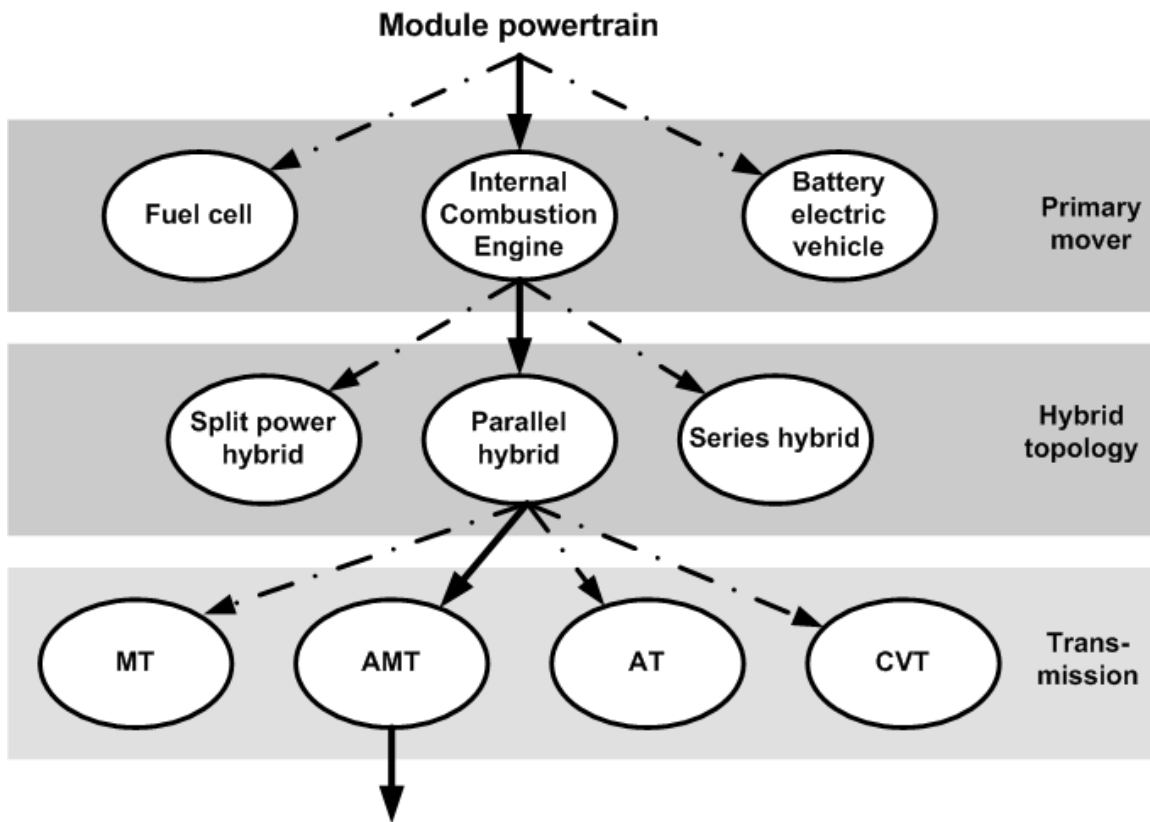

Figure 3.4: Morph structure of the powertrain module, showing the choices made within the powertrain domain. Internal combustion engine as primary mover, parallel hybrid topology coupled to an automated manual transmission.

Chapter 4

Cylinder deactivation

4.1 History

For long, cylinder deactivation is considered as a very promising technology for reducing emissions and fuel consumption. Apparently already in 1905, at the beginning of the internal combustion engine revolution, cylinder deactivation was used in the Sturtevant 38/45 six. The first mass production attempt of engines with cylinder deactivation was by GM in 1981 with the Cadillac Eldorado V8-6-4. As the name suggests, the V8 engine was capable of deactivating 2 or 4 cylinders. The technology was used for only one model year and due to electronic problems, only after 120000 produced engines, the technology went out of production.

More recently, in 1998, DaimlerChrysler re-introduced the cylinder deactivation technology (named Active Cylinder Control) on their 5.0L V8 and 6.0L V12 engines, used by Mercedes-Benz. The system is able to deactivate 4 respectively 6 cylinders. Honda is applying their so called Variable Cylinder Management since 2005 on their 3.5L V6 gasoline engine range, where one cylinder bank of 3 cylinders can be deactivated.

A clear trend is that the most attempts with deactivation are done with a cylinder count of 6 or more. One exception is Mitsubishi, who presented a 1.6L 4 cylinder in-line engine, equipped with cylinder deactivation [11] in 1992. The engine never went into production.

4.2 Working principle

Cylinder deactivation is realized by deactivating (closing) the valves and blocking injector or ignition (Otto-engine) signals. Current cylinder deactivation systems use a mechanical valvetrain, where a hydraulic control element is used to prevent the cam followers from actuating the valve. Figure 4.1a shows a mechanical/hydraulic deactivation mechanism used by General Motors. Future camless valvetrain systems, figure 4.1b, simplify cylinder deactivation by keeping the valves closed.

By closing the valves the cylinder is being used as an "air spring". This air spring performs a periodical compression and expansion cycle, which eliminates the pumping losses (apart from blow-by). There are three moments to start the deactivation, before the exhaust stroke, after the intake stroke and after the exhaust stroke. Deactivation before the exhaust stroke results in hot exhaust gases being trapped inside the cylinder. This keeps the cylinder warm and according to [18] this high
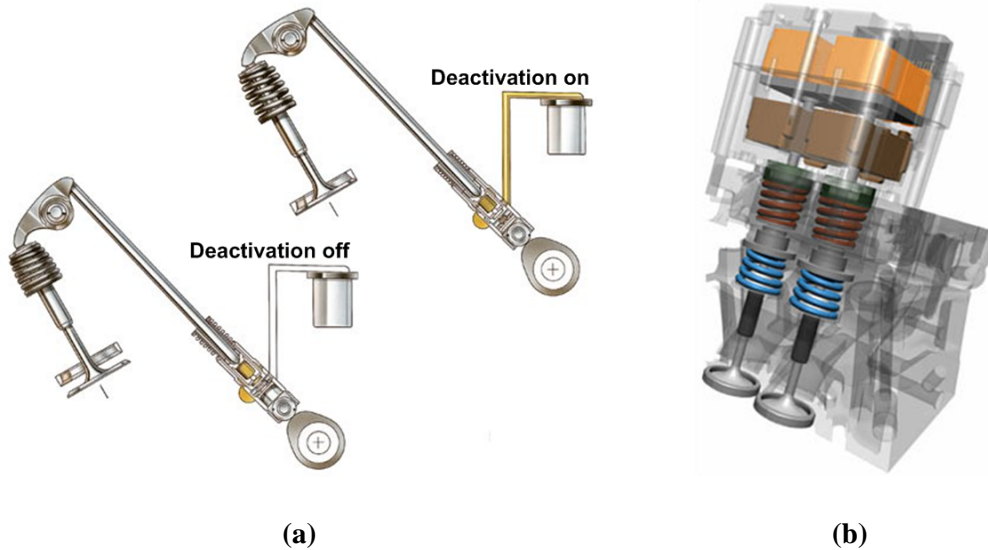
(a)   **(b)**

*Figure 4.1: **(a)** Cylinder deactivation by deactivating the pushrod (source: GM) **(b)** Electromechanical valves system concept (source: Valeo)*

temperature has advantages regarding thermal efficiency. The consequence of this timing is a higher compression end pressure. Deactivation after the intake stroke results in near ambient temperature and pressure conditions. Compression end pressure will consequently be lower. Deactivation after the intake stroke leads to even lower compression end pressures. Blow-by effects and cylinder wall heat transfer will eventually level the cylinder pressure and cylinder temperature. The effect of these three valve close timings are discussed in chapter 8 paragraph 8.3.

4.3   Benefits

Typically the power demand during normal everyday driving is low (NEDC average power demand is 5kW). Due to this low power demand, internal combustion engines operate most of the time at low engine load (low BMEP or Brake Mean Effective Pressure). The efficiency of combustion engines depends on the engine load and is at its best at high BMEP. Cylinder deactivation can help in combining those two operating conditions, high engine BMEP during low power demand. Deactivation requires the remaining active cylinders to operate at higher IMEP (Indicated Mean Effective Pressure) to provide the same overall BMEP (Break Mean Effective Pressure). BMEP is an indication of the overall engine performance, whereas IMEP is an indication of individual cylinder performance.

   A simple example will be given to show the potential and theoretically benefit of cylinder deactivation. Changes in engine friction or reduced energy consumption because of deactivated valve actuators are not taken into account. Figure 4.2a shows a normalized engine efficiency map of a 2.0L gasoline engine. Suppose a constant engine power request of 6 [kW] @ 2300 rpm, which is required to cruise at 80 [km/h]. The engine torque then equals 25 [Nm]. A common and useful notation for the engine load is the specific load, see equation 4.1 with w the specific engine work [J/dm^3], T_{engine} the engine torque [Nm] and V_{active} the active displacement [dm^3]. In the initial situation, all (4) cylinders activated, the specific engine load is equal to 79 [J/dm^3]. Table 4.1 shows the specific engine load

for the situations where 1, 2 or 3 cylinders are deactivated. The consequence regarding the engine efficiency is graphically shown in figure 4.2.

$$W = \frac{2\pi T_{engine}}{V_{active}} \qquad (4.1)$$

Active cylinders	V_{active} $[dm^3]$	w $[J/dm^3]$	SFC $[g/kWh]$	Improvement [%]
4	2.0	79	380	
3	1.5	105	334	+12
2	1.0	157	296	+22
1	0.5	314	258	+32

Table 4.1: Active displacement V_{active}, specific engine load W, specific fuel consumption SFC and fuel consumption improvement for 1, 2, 3 and 4 cylinders activated
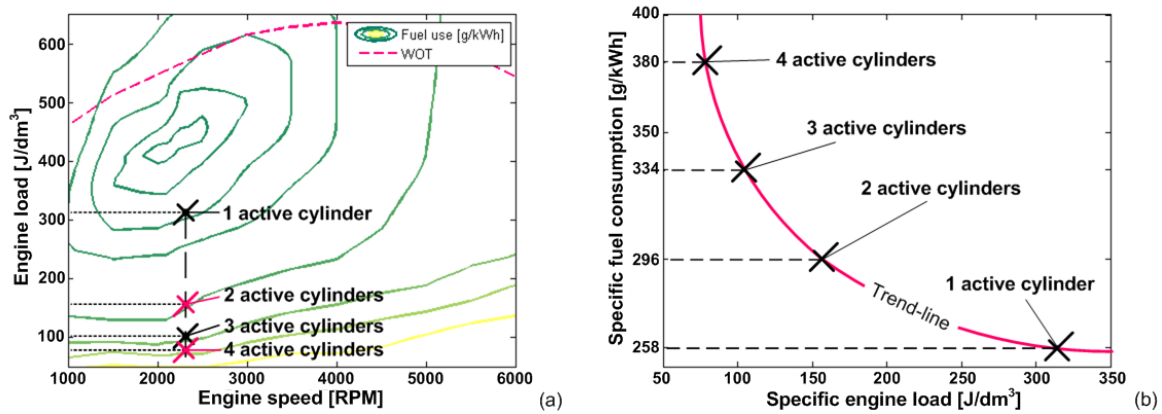

Figure 4.2: (**a**) Typical engine efficiency map of a gasoline engine. Operating points for 1, 2, 3 and 4 activated cylinders show the theoretical improvement in efficiency. (**b**) Shows the development of the specific engine load versus the specific fuel consumption.

Figure 4.2a shows that, although the operating points are not laying inside the optimal operating area, cylinder displacement shifts the operating point towards the optimal operating area which improves efficiency. The figure also shows that more cylinders with a smaller displacement, for instance 5 or 6 cylinder engines, could potentially further improve the specific fuel consumption and provide an even better match between the desired engine load and optimal engine load.

Table 4.1 shows the improvement in efficiency and decrease in fuel consumption related to the situation where all cylinders are active. The fuel consumption trend is shown in figure 4.2b. Further research will have to make clear what the benefit will be when transient operation and losses are taken into account.

Literature shows several results of cylinder deactivation applications. Reference [18] shows test results of an inline 4 cylinder gasoline engine where 2 cylinders can be deactivated. During steady state low engine load conditions an efficiency improvement of 20 % was achieved. At part load conditions, 2 bar BMEP @ 2000 [RPM] an improvement of 16% was obtained. Stationary tests also showed a HC-emission decrease of 10 - 40% for low BMEP, caused by the higher engine load and

consequently a higher cylinder temperature. At higher BMEP both the fuel consumption and HC-emissions increased slightly due to the reduction of the volumetric efficiency.

Reference [2] reports about a field test with a taxi fleet, using 4 cylinder engines capable of de-activating 2 cylinders. The taxi-drive cycle resulted in fuel consumption reductions of 20 - 30%. A 6 cylinder inline engine showed an improvement of 45% in fuel efficiency during idle. During the NEDC-cycle the reduction was 25.4%, both results where obtained with 3 cylinders deactivated.

Finally, the 5.0L V8 engine, as used by Mercedes-Benz, shows a reduction in fuel economy of 6.5% during the NEDC-cycle and 10.3% during the American FTP+HW cycle, with 4 cylinders de-activated. For Mercedes-Benz, cylinder deactivation makes it possible to combine high performance and large cylinder displacement with improved fuel economy.

4.4 Limitations

There are several constraints that limit the use of cylinder deactivation during driving. Under influence of cylinder deactivation the engines excitation order will change. The frequency of the combustion torque pulses onto the crankshaft is lowered, and the active cylinders operate under higher load to maintain the output torque, therefore the amplitude of the combustion torque pulse will be higher, see figure 4.3a. Both conditions are not preferable for systems excited by the engine, and with an eigen frequency below the engine idling frequency. Reference [20] reports situations where deactivation only can be used when driving in 3rd, 4th and 5th gear due to NVH (Noise Vibration Harshness) issues. The "lug limit" is defined as the lowest possible engine speed permitted, constrained by Noise Vibration and Harshness (NVH). Due to cylinder deactivation this "lug limit" is increased.
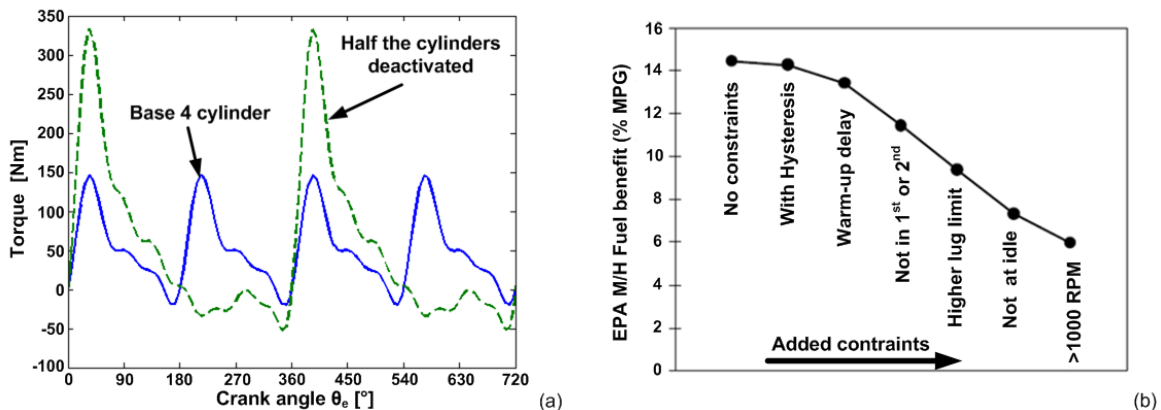
Figure 4.3: *(a) Comparison between the engine torque of the base 4 cylinder engine and when 2 cylinders are deactivated, for an average engine torque of 50 [Nm]. (b) Fuel economy penalty due to added constraints, 6.8L V10 [20]. Data obtained during EPA M/H drive cycle. Fuel consumption is given in miles per gallon (MPG).*

Cylinders will only be deactivated under low engine load conditions, above a certain engine load the system will be activating more or all cylinders. Hysteresis will have to be built in, to prevent ner-vous switching between activation and deactivation around the same engine load. According to [20] a built in hysteresis of 1 bar BMEP will cost 0.2% fuel economy. Under cold start conditions cylinder

deactivation may not be possible due to actuator limitations or emission requirements. This delay will also give a fuel economy penalty. Figure 4.3b shows the reduction in improvement with respect to the constraints, based on a study performed on a 6.8L V10 gasoline truck engine [20].

The main reason for the failure of cylinder deactivation in the past was the transient control of the torque and air/fuel ratio [20]. The introduction of electronic port fuel injection and the electronic throttle made the re-introduction of cylinder deactivation possible again, as proven by Mercedes-Benz.

Other issues regarding cylinder deactivation are the unbalanced warm-up and cooling of engine components, which could lead to thermal stresses and increased emissions when cooled down cylinders are active again. Possible solutions for unbalanced warm-up can be found in frequently reactivating cooled down cylinders and deactivating the warmed up cylinders in order to keep the entire engine equally warmed up. An electronic water pump can also help in balancing the engine temperature by reducing or even reversing the coolant flow direction. Cylinder deactivation also results in changed exhaust flow pulsations and flow. This has implications for the effectiveness of exhaust turbo systems and catalyst converters.

4.5 Conclusion

In summary, the benefit of cylinder deactivation is threefold. The deactivated cylinders operate as an air spring and therefore do not require pump work, apart from a marginal loss caused by blow-by and heat transfer. Power normally needed to operate the valves is not needed for the deactivated cylinders (holds for both cam driven and camless valvetrain). Therefore the engines mechanical loss is reduced. The third and main benefit is a result of the higher engine load, which results in less pumping losses.

Due to limitations the benefit and effect of Cylinder deactivation on engine efficiency will be reduced. With an effective NVH suppression method the engines' efficiency and deactivation time could be increased, resulting in reduced fuel consumption. Because of the importance of NVH on cylinder deactivation the next chapter is devoted to powertrain NVH.

Chapter 5

Powertrain Noise Vibration Harshness

Noise Vibration and Harshness, or NVH, addresses both comfort and durability which are important requirements for powertrain design. Cylinder deactivation has an effect on powertrain NVH, because of the increased combustion torque amplitude and lowered combustion frequency. Resonances excited by the engine can cause structures to fail under stress, and therefor will have to be prevented.

This chapter explains what kind of vibration sources are relevant for the powertrain design and what the influence of cylinder deactivation will be on these vibrations. There are several systems or methods to suppress powertrain vibrations. Three systems are discussed which can help in increasing the powertrain comfort and durability, the torsion damper, dual mass flywheel and the integrated starter alternator damper.

5.1 Sources of excitation

Powertrain excitation sources can be differentiated into internal and external sources ([4] and [28]). External excitations can be caused by the driver (pedal tip-in, pedal back-out), by road irregularities or by body-powertrain interactions.

Internal excitations are caused by engine excitations and driveline imperfections. An internal combustion engine is a source of several periodic excitations, depending on the configuration and number of cylinders. In general the excitations are caused by the reciprocating engine inertias and by the combustion torque pulses.

The engines main order of excitation, caused by the combustion pulse torque, can be determined with equation 5.1, with N_{main} [-] the engines main harmonic excitation order, num_{cyl} [-] the number of cylinders and z[-] the number of revolutions needed for one cylinder to complete one engine cycle (2-stroke = 1; 4-stroke = 2).

$$N_{main} = \frac{num_{cyl}}{z} \tag{5.1}$$

$$f_{ex} = \frac{n_e N_{main}}{60} \tag{5.2}$$

When cylinders are deactivated the engine order N_{main} changes. This has a consequence for the excitation frequency, which is linear dependant on the engine order. Equation 5.2 shows the excitation

frequency f_{ex} [Hz] with the main order N_{main} and engine speed n_e [RPM].

Driveline imperfections are caused by gear imperfections, driveshaft misalignment, imperfect universal joints or unbalanced rotating inertias. Discussing these causes of excitations lies beyond the scope of this report, because there is no relation between cylinder deactivation and these imperfections.

5.2 Response

The main vibration response is the deceleration and acceleration of the crankshaft, caused by the intermitting combustion torque pulses and inertia torque. This torsional vibration can:

- be transferred to the transmission primary shaft, where the angular acceleration causes gear rattle [12]

- cause a longitudinal vehicle accelerating called vehicle shuffle .

- cause the powertrain unit, engine block and transmission housing, to shake with respect to the vehicle body [4].

Vehicle shuffle and engine shaking are of direct influence on the comfort of the occupants. Gear rattle is caused by engine torque fluctuations, resulting in vibration of the lightly loaded components in the gearbox, such as the idler gears, synchronizer rings and sliding sleeves. Transmission of vibration from the gear shafts through bearings to the gearbox housing is the principal mechanism, radiating noise to the environment. During cylinder deactivation the firing distance will change, causing the engine sound to change also. This phenomena will be one of the major hurdles to get cylinder deactivation accepted by the "market".

Acceptable maximum values for gear rattle, vehicle shuffle and engine shaking are hard to give, because they highly depend on the occupants personal perception. Furthermore, interior damping, vehicle body structure, engine mounts and even sound deadening will dampen the vibrations which makes it hard to quantify the maximum allowable vibrations emitted by the powertrain.

Resonance occurs when the excitation frequency happens to be near or exactly on the systems eigen frequencies. Excitation with the eigen frequency will result in a rising amplitude which, when not dampened, will lead to destruction of the structure or system.

5.3 Comfort improvement solutions

Solutions for powertrain NVH problems can be categorized as followed:

Reduce or eliminate the source causing the vibration
Reducing or eliminating the vibration source can be obtained by increasing the number of cylinders, which results in lower and more frequent combustion torque pulses. This solution is opposite to cylinder deactivation and therefor leads to opposite effects.

Isolation of the source
Isolation of the source can be done by decoupling the internal combustion engine from the vehicles'

wheels. This can be obtained by a series hybrid setup, where the combustion engine drives a generator and a motor drives the wheels. The combustion torque pulses and inertia torque are no longer transmitted through the transmission to the wheels. The series hybrid setup will be covered in another thesis [6].

Tuning of the system

Tuning of the system can be done by changing the parameters of the powertrain, like inertia or stiffness. Tuning can help in shifting the systems eigenfrequencies away from the excitation frequencies, eliminating the possibility of resonances.

Damping of the source

There are several systems available to dampen the vibration source caused by the engine. The most common method to dampen torsional vibrations, in European cars, is by means of a Torsion Damper (TD) integrated into the clutch assembly. Vehicles in the upper segment or with diesel and turbo engines are equipped with a Dual Mass Flywheel (DMF), also to dampen the torsional vibrations. The Integrated Starter Alternator Damper (ISAD) is currently not yet applied to a mass produced vehicle. Besides the vibration damper function, the ISAD system has other beneficial functions making it an useful addition to the powertrain, see paragraph 5.3.3.

5.3.1 Torsion damper

A torsion damper (TD) is used to isolate the rotational vibrations from the engine to the transmission. Often it is integrated into a dry plate clutch, as used in manual transmissions, see figure 5.1a. Small coil springs transfer the engine torque from the friction elements to the transmission primary shaft.

The TD coil spring stiffness creates an extra powertrain resonance frequency, typically between 40 - 80 [Hz] (equals 1200 - 2400 [RPM] for a 4 cylinder 4 stroke engine). This resonance frequency lies within the operating speed range. It is possible to lower the eigen frequency by lowering the spring stiffness and/or by increasing the transmission inertia. However, a too low spring stiffness causes the springs to block under heavy load, resulting in a rigid connection.
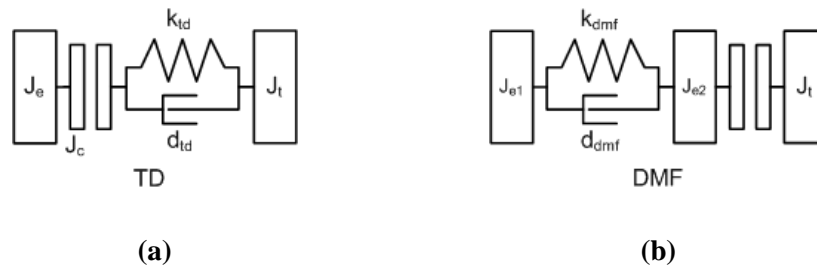

(a)   **(b)**

Figure 5.1: (a) Schematic representation of the torsion damper. (b) Schematic representation of the dual mass flywheel.

5.3.2   Dual mass flywheel

The Dual Mass Flywheel (DMF) is applied more and more in luxury vehicles and is finding its way into the turbo(diesel) engine market. A DMF flywheel consists of two inertias, connected to each other by a spring-damper system. One inertia contributes to the engine inertia, the second inertia contributes to the transmission inertia in case the clutch is closed. Due to packaging the used coil spring can be longer compared to the TD which results in a lower spring stiffness and a powertrain resonance frequency which is shifted below engine idle speed. The now lowered eigen frequency causes problems during cranking of the engine, see [3] and [5]. The amplitude of the lowered eigen frequency is also typically higher. The application of a DMF comes with a penalty in weight, volume and cost [32].

5.3.3   Integrated starter alternator damper

The Integrated Starter Alternator Damper (ISAD) is an active damping system as opposed to passive systems as the TD and DMF. The ISAD system is not used to shift resonance frequencies, but is used to dampen the vibration amplitudes. The ISAD system will replace the alternator, starter motor and flywheel with one system, mounted directly onto the crankshaft. Mechanically the ISAD system is represented by a rotor, mounted onto the crankshaft and a stator mounted to the engine block. Typically the rotor inertia is lower than the flywheel inertia it replaces.

The damper function is used to slow down the crankshaft when it is accelerated under influence of a torque pulse. By slowing down the crankshaft the alternator is generating electrical energy which can be accumulated temporarily into a capacitor. At the next compression cycle the accumulated energy is used to accelerate the crankshaft if it is rotating too slow. This results in a lower engine speed fluctuation, which in turn reduces engine shake, gear rattle and vehicle shuffle.

Besides its torsional damping function, the ISAD system has several features which makes it desirable in future powertrains. Current alternator systems can produce up to 2.5 [kW] of electrical power, limited by the belt drive. Increasing demand of electric power consumers like electric pumps and in car entertainment systems demands a higher alternator output [14], which cannot be obtained efficiently any more with the current state of art belt driven alternators [24]. The ISAD system is able to generate a higher power output at a higher electrical efficiency, at the same time increasing the vehicles system voltage from 14V to 42V.

The higher system voltage and power availability makes camless valve actuation technology possible, further improving engine efficiency. Belt driven accessoires can be replaced by pump-on-demand systems, by doing so reducing parasitic losses and provide freedom in the engine auxiliary package of the engine.

The use of pump-on-demand has another advantage, related to NVH. The stand alone pumps are not driven by the crankshaft anymore and therefor are easier to dampen. Pump systems can now be tested and designed separately from the engine, which can reduce cost in testing and simulation or make modularity possible. Electrically heated catalytic converters lower the light off time, reducing cold start exhaust emissions which are currently a major contributor to total exhaust emissions. It also could enable the use of cylinder deactivation directly after cold starts. Typical hybrid functions as start/stop, boosting and regenerative braking are possible as already mentioned in chapter 3.

Figure 5.2: Flywheel mounted integrated starter alternator damper or ISAD [source: Bosch]

5.4   Conclusion

Engine shake, vehicle shuffle and gear rattle are the three main parameters which define powertrain comfort. These parameters will therefor be used to analyze the effect of cylinder deactivation. There are several systems available to improve the vibrational behavior of powertrains, because of the additional functions the ISAD system is preferred. The next chapter describes two powertrain models which will be used to analyze the effect of cylinder deactivation. A powertrain equipped with a torsion damper will function as a benchmark, while the powertrain containing the ISAD system will represent the desired powertrain.

Chapter 6

Powertrain model

Analyzing the effects of cylinder deactivation on the vibrational behavior of the powertrain requires a dynamic model of this powertrain. This chapter gives the equations of motion of two powertrains, based upon literature [4], [25] and [22], necessary to create these models. The first powertrain is the torsion damper (TD) powertrain. The TD powertrain will serve as benchmark, since it is used most frequently on passenger cars. The model, represented in figure 6.1, describes the engine, powertrain mounts, torsion damper, transmission, driveshafts, wheels, vehicle body and road load.
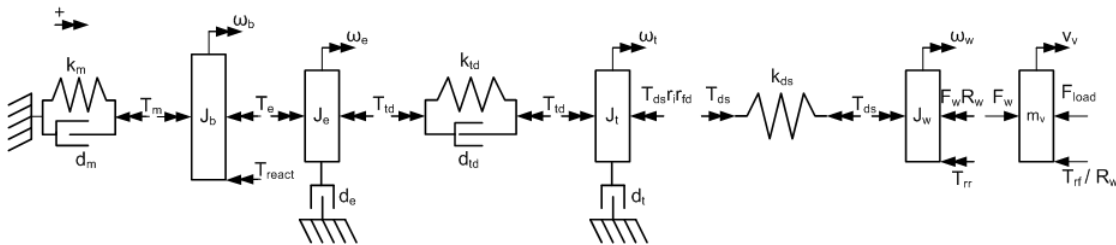

Figure 6.1: Free body diagram of the TD powertrain, containing engine, torsion damper, transmission, driveshafts, wheels and vehicle body.

The second powertrain or ISAD powertrain, differs slightly from the TD powertrain in a sense that an ISAD system is used instead of the torsion damper. Analysis will show later on if it is indeed the preferred setup when cylinder deactivation is taken into account. The ISAD powertrain is discussed in paragraph 6.7. In the following paragraphs all the powertrain components are explained in detail.

6.1   Engine

The dynamic engine torque T_e is built up by three sources. The gas pressure torque T_g represents the torque resulting from the gas pressure, caused by combustion, compression and gas exchange. The second source is the engine inertia torque T_i, caused by the rotating and reciprocating engine masses and inertias. The third source, called air spring torque or T_{spring}, is only available when cylinder are deactivated and replaces the gas pressure torque of the deactivated cylinder. The air spring torque is caused by the cyclic compression and expansion cycle completed by the deactivated cylinder. All three torques depend on the crank angle rotation θ_e and the crank-conrod geometry. Both the inertia and gas

21

pressure torque are modeled by a Fourier algorithm. A detailed explanation about the gas pressure, inertia and air spring torque can be found in appendix B. The influence of the engine geometry on the engine vibrations will not be studied. Engine friction d_e is assumed to be lineair dependant on the engine speed ω_e [1]. The total engine torque reduced by the engine friction and engine load T_{td} causes the engine inertia J_e to accelerate or decelerate. The equation of motion is given by equation 6.2.

$$T_e(\theta_e) = T_g(\theta_e) + T_i(\theta_e) + T_{spring}(\theta_e) \tag{6.1}$$

$$J_e\dot{\omega}_e = T_e - T_{td} - d_e\omega_e \tag{6.2}$$

6.2   Powertrain mounts

The powertrain unit, engine block and transmission housing, is connected to the vehicle body through 3 powertrain mounts. Figure 6.4 shows typical mounting points of a boxer engine and an inline engine.
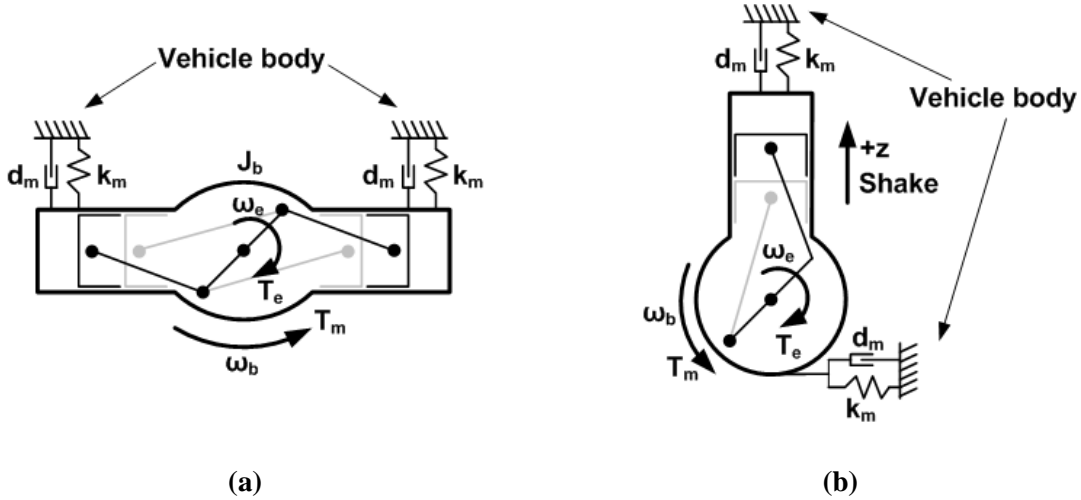

(a)   **(b)**

Figure 6.2: Powertrain unit mounting for (a) Boxer engine and (b) inline engine

The difference in vibrational behavior between a boxer engine and an inline engine is caused by the inertia torque of the engine and is therefor not related to cylinder deactivation. This means that one model can be used for both inline and boxer engines. The difference between the vibrational behavior of both engines is discussed in appendix B.4.

The engine torque T_e and transmission reaction torque T_{react} will cause a torsional vibration motion ω_b of the powertrain unit with respect to the vehicle body. the resultant torque T_m is supported by the powertrain mounts. The powertrain mounts will be represented by a spring-damper system, with stiffness k_m and damping d_m. The equations of motions become:

$$J_b\dot{\omega}_b = T_m - T_e - T_{react} + d_e\omega_e \tag{6.3}$$

The torque amplification caused by the transmission ratio r_i and final drive ratio r_{fd}, leads to a reaction torque T_{react}. Figure 6.3c shows this reaction torque, defined by equation 6.4.

$$T_{react} = T_{td}(\frac{1}{r_i r_{fd}} - 1) \tag{6.4}$$

The powertrain unit mount is defined with equation 6.5.

$$T_m = -k_m \theta_b - d_m \omega_b \tag{6.5}$$

6.3 Clutch

The "car of the future" is equipped with a 6 speed automated manual transmission (AMT). A dry plate clutch is used to decouple the engine from the transmission during shifting. Three operating modes can be distinguished, open clutch, slipping clutch and a fully closed clutch. Ratio changes are not included in the cylinder deactivation analysis, therefor the fully closed clutch state is of interest, consequently simplifying the model in terms of DOF. Under closed conditions the engine and clutch are considered as a rigid system.

6.3.1 Torsion Damper

Manual transmissions are normally equipped with an torsion damper (TD) integrated into the clutch plate. The TD's main function is to isolate the transmission from the engine periodic vibrations as explained in paragraph 5.3.1. The TD is represented by a spring-damper system, with spring stiffness k_{td} and damper constant d_{td}. The movement of the powertrain unit with respect to the vehicle body causes an extra rotation motion, represented by θ_b and ω_b. A schematic representation of the TD is pictured in figure 6.3.

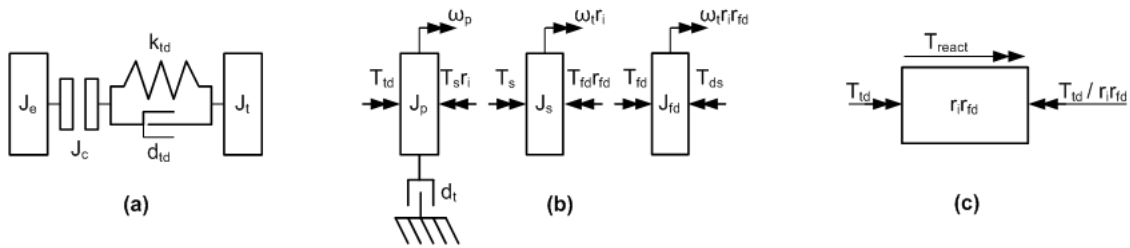$$T_{td} = k_{td}(\theta_e - (\theta_t + \theta_b)) + d_{td}(\omega_e - (\omega_t + \omega_b)) \tag{6.6}$$

Figure 6.3: (a) Schematic representation of the torsion damper. (b) Schematic representation of the lumped transmission model, build up by primary shaft J_p, secondary shaft J_s and final drive / differential inertia J_{fd}. (c) Schematic representation of the reaction torque of the powertrain unit.

6.4 Transmission and driveshaft

The powertrain concept is based on a automated manual transmission (AMT) with a combined final drive / differential unit. The transmission ratio r_i is defined by equation 6.7, with index i indicating the selected gear while the final drive ratio is defined by r_{fd}. The transmission friction d_t is assumed to be linear dependant on the speed ω_t of the primary transmissions shaft [26].
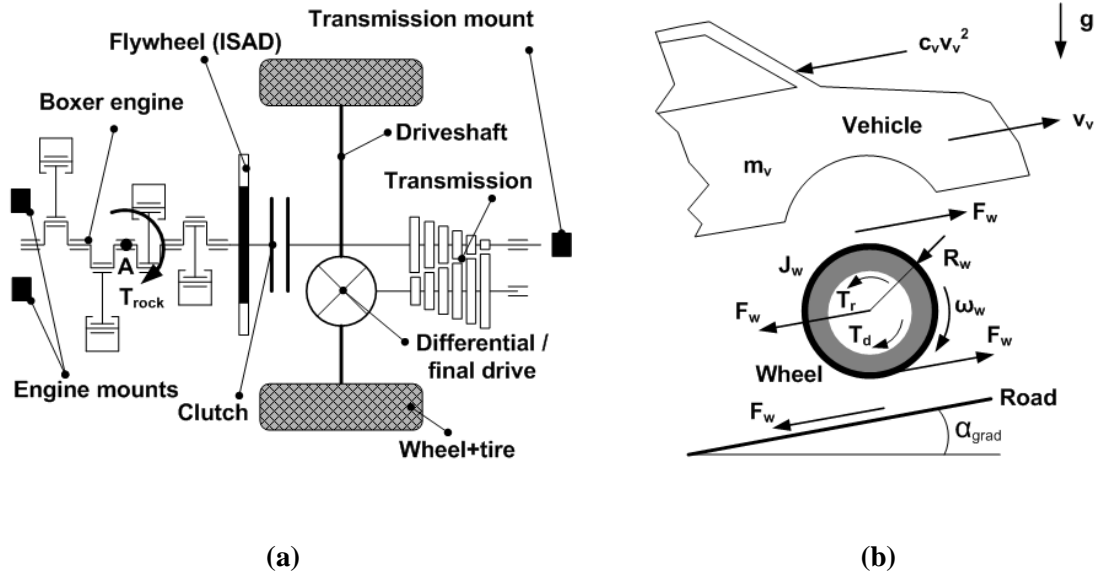
Figure 6.4: (a) Schematic representation of the powertrain as proposed for the "car of the future". (b) Road-wheel-vehicle interaction, from [25].

$$r_i = \frac{\omega_{out}}{\omega_{in}} \tag{6.7}$$

The transmission consists of a primary inertia J_p, secondary inertia J_s and final drive inertia J_{fd}, together forming the lumped transmission inertia J_t, figure 6.3. The transmission inertia J_t changes with the transmission ratio r_i, see equation 6.8. All inertias are herein reduced to the engine side.

$$J_t = J_p + J_s r_i^2 + J_{fd} r_i^2 r_{fd}^2 \tag{6.8}$$

The equation of motion for the transmission becomes:

$$J_t \dot{\omega}_t = T_{td} - T_{ds} r_i r_{fd} - d_t \omega_t \tag{6.9}$$

The vehicles driveshafts are modeled as a combined flexible spring with stiffness k_{ds}, between the transmission and the wheels. The movement of the powertrain unit with respect to the vehicle body causes an extra rotation motion, represented by θ_b. Equation 6.10 shows the driveshaft torque due to driveshaft rotation.

$$T_{ds} = k_{ds}((\theta_t r_i r_{fd} + \theta_b) - \theta_w) \tag{6.10}$$

6.5 Wheels and tires

The tire tractive force F_w describes the forces from the rear tires onto the road and depends on the normal force ($m_{vr}g$ and the tire-road friction coefficient μ. Coefficient μ is a function of the wheel slip ψ and is approximated to be lineair up to 15% wheel slip, with coefficient b_w [25].

$$F_w = \mu(\psi) m_{vr} g \cos(\alpha_{grad}) \tag{6.11}$$

$$\mu(\psi) = b_w \psi \tag{6.12}$$

Wheel slip is necessary to translate the forces from the tire to the road and visa versa. The wheel slip for driving wheels is defined by equation 6.13.

$$\psi = 1 - \frac{v_v}{\omega_w R_w} \tag{6.13}$$

Rolling resistance acts on both the front (T_{rf}) and rear (T_{rr}) wheels and depends on the normal force and the tire deformation length x_l.

$$T_{rf} = x_l m_{vf} g \cos\alpha_{grad} \tag{6.14}$$

$$T_{rr} = x_l m_{mr} g \cos\alpha_{grad} \tag{6.15}$$

The equation of motion for the rear wheels become:

$$2 J_w \dot\omega_w = T_{ds} - F_w R_w - T_{rr} \tag{6.16}$$

The front wheels have no contribution regarding traction, due to the rear wheel drive concept. The front wheels are therefor regarded as simple inertias causing drag due to rolling resistance. In order to reduce the models DOF, the inertias of the front wheels are added to the vehicle mass, as shown in equation 6.17.

$$m_{lumped} = m_v + \frac{2 J_w}{R_w^2} \tag{6.17}$$

6.6 External load

The previous paragraph already discussed the rolling resistance T_r. Together with the air resistance and gradient resistance they form the external vehicle load. Air resistance F_{air} is defined according to:

$$F_{air} = c_v v_v^2 \tag{6.18}$$

The air resistance constant c_v is defined by:

$$c_v = \frac{1}{2} \rho_{air} c_d A_v \tag{6.19}$$

Herein is ρ_{air} the air density, c_d the vehicles drag coefficient, A_v the frontal area of the vehicle and v_v the vehicle speed.

The gradient load depends on the vehicle weight and the road gradient α_{grad}.

$$F_{grad} = m_v g \sin\alpha_{grad} \tag{6.20}$$

The total external vehicle load becomes:

$$F_{load} = F_{air} + F_{grad} \tag{6.21}$$

With this the equation of motion regarding the vehicle dynamics becomes:

$$m_{lumped} \dot{v} = F_w - T_{rf}/R_w - F_{load} \tag{6.22}$$

6.7 Integrated Starter Alternator Damper powertrain

The ISAD powertrain requires a slightly adapted model compared to the TD powertrain. Although the ISAD powertrain can be equipped with a TD, it is of interest what the behavior of the powertrain will be in a setup without TD. Literature also specifically reports, [32], that the ISAD system can be regarded as a replacement for other vibration absorbers in the powertrain.
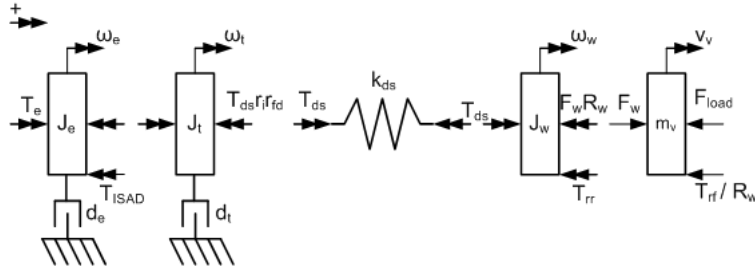

Figure 6.5: Free body diagram of a powertrain with an ISAD system, containing engine, transmission, drive-shafts, wheels and vehicle body.

The rotor of the ISAD system is mounted directly to the engines' crankshaft, replacing the flywheel. The torque produced by the ISAD system, T_{ISAD}, acts onto the engines' crankshaft. The rotor speed equals the engine speed ω_e. The stator is mounted to the engine block and therefor is always stationary. Compared to the TD powertrain, there is no spring damper system placed between the engine and transmission, reducing the DOF, see figure 6.5.

The ISAD system has numerous functions as described in paragraph 5.3.3, making the control of the system complicated. The controller of the ISAD system must:

- be able to provide optimal damping and reduce the speed fluctuations of the engine

- adapt itself to variation in powertrain dynamics (vehicle load, gear ratio, etc.)

- provide electrical power for onboard electrical consumers (camless valvetrain, electric pumps, etc)

- make sure that T_{ISAD} is limited to T_{max}

- assure that the power contribution over one engine revolution is zero. Otherwise the ISAD system is propelling the vehicle and thereby reducing the engine load.

The ISAD system can be used as an active damper or as a passive damper. Using the ISAD system as an active damper requires closed loop control, figure 6.7. Herein represents $H(s)$ the powertrain plant, $S(s)$ the sensor dynamics, $C(s)$ the controller and $P(s)$ the ISAD electric dynamics (from [31], [9]). The engine torque T_e represents the disturbance, n is sensor noise and ω_{e0} is the average engine speed over one revolution. Controller design requires detailed knowledge of the capabilities of the ISAD system, which are not available. For this thesis only the damping function is of interest, therefor passive damping is used. Passive damping is also easier to implement into the model. Further research on control and energy management is required in the future.
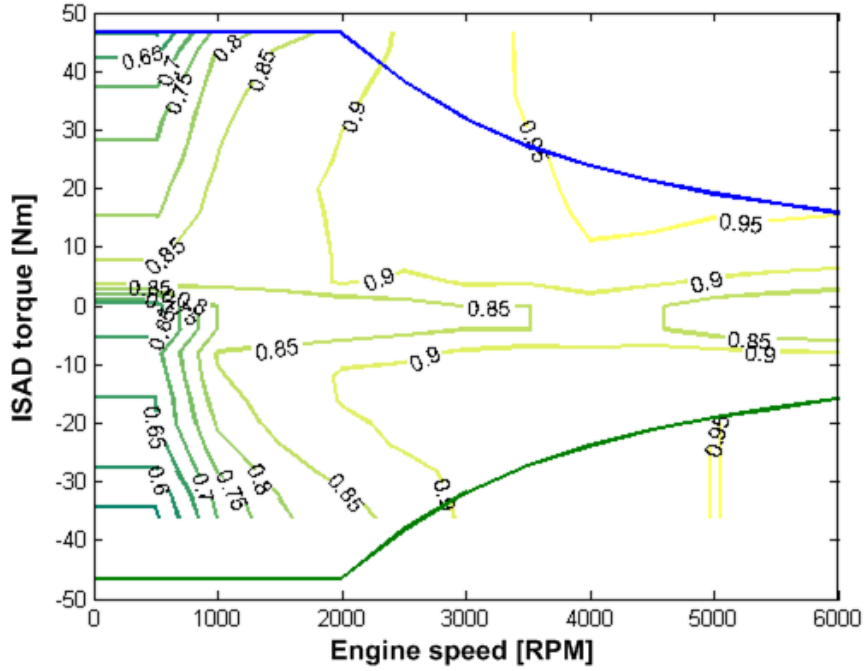
Figure 6.6: Maximum torque characteristic and efficiency map of a starter generator system (from $ADVISOR^{TM}$ Honda Insight data). Positive torque is motor mode, negative torque is generator mode.

The damping values are chosen in such a way that T_{ISAD} never exceeds the maximum torque values as shown in figure 6.6. The result and effect of the ISAD system depends highly on the torque capacity of the starter generator. The used maximum torque data is taken from the 10 [kW] starter alternator system of the Honda Insight mild hybrid vehicle, which has the same parallel hybrid powertrain setup as required for the "car of the future". The reaction time of the ISAD system is assumed to be infinite fast, while sensor dynamics are not taken into account. The damper is only used to prove the concept of damping vibrations caused by cylinder deactivation, therefor the system dynamics are neglected for now.

The engine and transmission inertia are lumped because of the removed torsion damper with respect to the TD powertrain. The ISAD torque depends on the variable damper constant $d_{isad}(\omega_{e0}, r_i)$ and the engine speed error $(\omega_e(t) - \omega_{e0})$. Because the engine speed error depends on the transmission ratio and engine speed, the damping is also ratio and engine speed specific.

$$T_{ISAD} = (\omega_e(t) - \omega_{e0})d_{isad}(\omega_{e0}, r_i) \tag{6.23}$$

$$\omega_e = \omega_t \tag{6.24}$$

The engines' equation of motion for the ISAD powertrain changes from 6.2 to:

$$(J_e + J_t)\dot{\omega}_e = T_e - T_{ds} - (d_e + d_t)\omega_e - T_{ISAD} \tag{6.25}$$
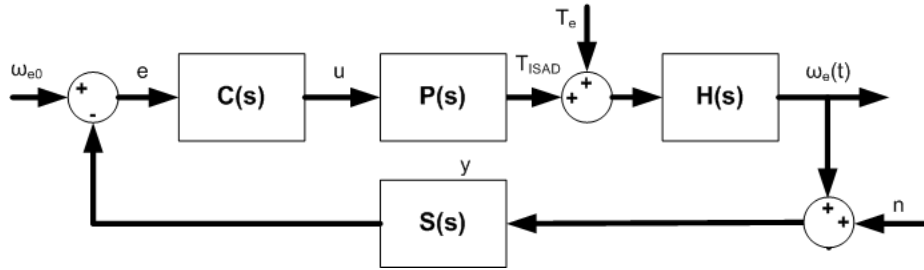
Figure 6.7: Block diagram of the closed loop active damping using controller $C(s)$.

6.8 Conclusion

Two powertrain setups, the TD powertrain and the ISAD powertrain, are described in detail. The equations of motion can be used to make numerical models of the powertrains, see appendix C. With these models frequency and time domain simulations can be executed to analyze the effect of cylinder deactivation on powertrain vibrations. The ISAD powertrain uses a starter alternator as vibration damper instead of a torsion damper. The ISAD system has been modeled as a simple passive damper. Sensor and ISAD system dynamics are not taken into account in order to simplify the models. Further research on controllers and energy management is necessary to integrate the damper function with other hybrid functions.

Chapter 7

Frequency domain response

Deactivation of cylinders causes the engines' excitation frequency to change, possibly interfering with the powertrains resonance frequency. A frequency response gives information about resonances and magnitudes at certain excitation frequencies. Excitation frequencies around the eigen frequency of the powertrain must be prevented, because resonances can cause fatigue, wear or immediate damage of powertrain components.

The previous chapter described two different powertrain setups, the TD powertrain and the ISAD powertrain. Frequency analysis will show which powertrain is best suited for cylinder deactivation and what can be done to improve the powertrain behavior.

7.1   State space model

In order to obtain the frequency response plots, a state space model is made with the powertrain models from the previous chapter. The TD powertrain is described by 8 linear and non-linear differential equations, whereas the ISAD powertrain is described by 6 linear and non-linear differential equations. The system is linearized around stationary points of interest, meaning engine speed and fixed gear ratio. The steps of the linearization process are described in detail in appendix C. The system states and input vector are shown below for the TD powertrain, equation 7.1:

$$x = [\omega_b.T_m, \omega_e, T_{td}, \omega_t, T_{ds}, \omega_w, v_v]^T$$
$$y = [T_e]$$

$$(7.1)$$

And for the ISAD powertrain, equation 7.2:

$$x = [\omega_b, T_m, \omega_e, T_{ds}, \omega_w, v_v]^T$$
$$y = [T_e]$$

$$(7.2)$$

7.2 Frequency plot

Figures 7.1 and 7.2 show the magnitude and phase plots of both the TD powertrain (benchmark) and the ISAD powertrain. The data is acquired in 5th gear with the engine speed set to 2300 RPM, which equals a vehicle speed of 80 km/h. Relevant outputs are ω_e, $\dot{\omega}_b$, $\dot{\omega}_t$ and $\dot{v}_v$ relevant for respectively engine speed fluctuation, powertrain unit vibration, gear rattle and vehicle shuffle.
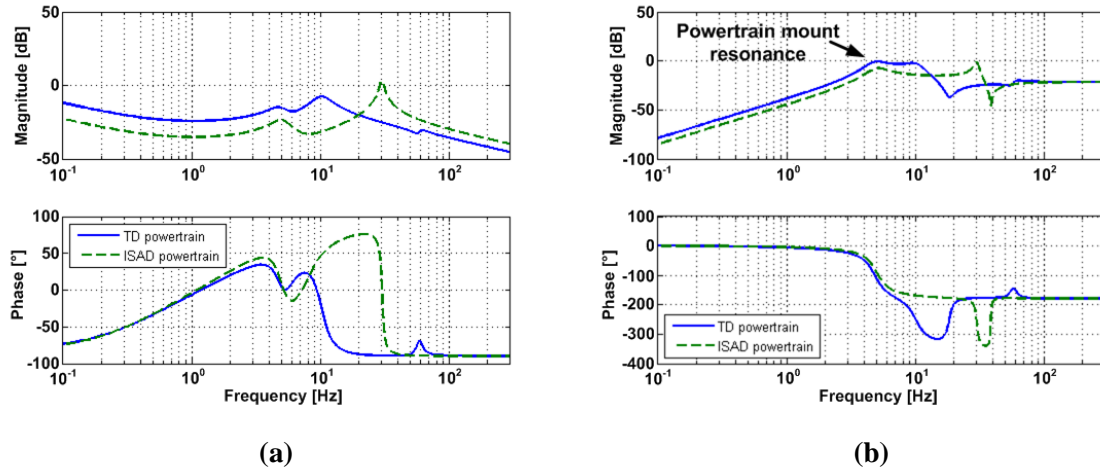

Figure 7.1: (a) Frequency response diagram from T_e to ω_e. (b) Frequency response diagram from T_e to $\dot{\omega}_b$.
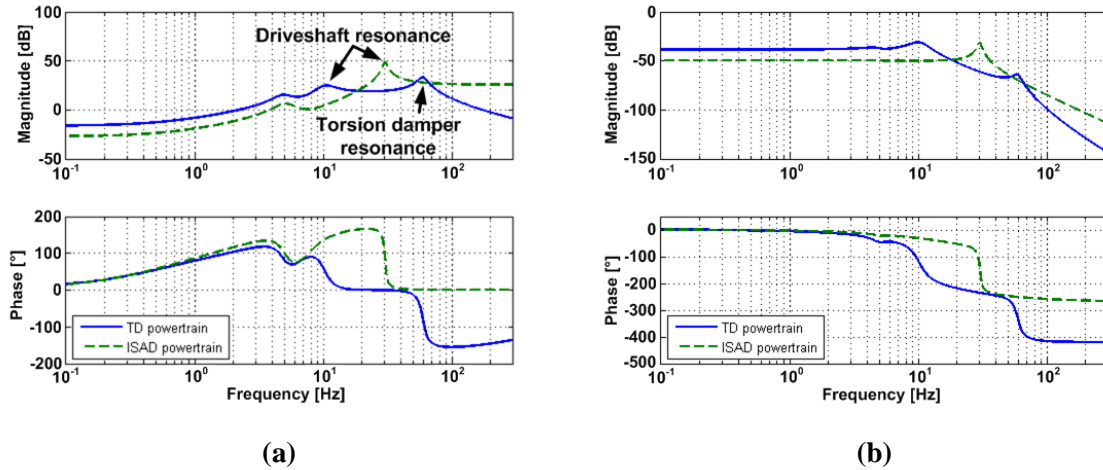

Figure 7.2: (a) Frequency response diagram from T_e to $\dot{\omega}_t$. (b) Frequency response diagram from T_e to $\dot{v}_v$.

Figure 7.1a shows the magnitude and phase response of T_e to ω_e. The magnitude frequency response (MFR) of the TD powertrain shows two eigen frequencies at 10 [Hz] and 59 [Hz]. The ISAD powertrain only shows one eigen frequency at 31 [Hz]. The magnitude of the ISAD resonance frequency is higher than the two TD resonances. At low excitation frequencies the magnitude of the ISAD powertrain is better compared to the magnitude of the TD powertrain, while at higher frequencies the magnitude is worse compared to the TD powertrain.

Figure 7.1b shows the magnitude and phase response of T_e to $\dot{\omega}_b$. The MFR response of the ISAD powertrain is lower at low frequencies, but higher at frequencies over 13 [Hz]. After the driveshaft resonance at 30 [Hz], the magnitude of the ISAD response drops below the TD response. At frequencies above 100 [Hz] both powertrains show an equal response. Both the TD powertrain and ISAD powertrain show a eigenfrequency at 5 [Hz]. This frequency can be checked by using equation 7.3. This eigen frequency is visible in all frequency responses and is equal for all gear ratios.

$$f_{mount} = \frac{1}{2\pi}\sqrt{\frac{k_m}{J_b}} \tag{7.3}$$

The response of T_e to $\dot{\omega}_t$ can be seen in figure 7.2a. Again, the MFR of the TD powertrain is lower at high frequencies, providing better vibration suppression. The MFR and PFR of T_e to $\dot{\omega}_t$ is equal to T_e to $\dot{\omega}_e$ because the engine and transmission are coupled to each other in case of a closed clutch.

Figure 7.2b shows the MFR and PFR of T_e to $\dot{v}_v$. Equally to T_e to $\dot{\omega}_e$ and T_e to $\dot{\omega}_t$ the TD powertrain proves to be better at higher frequencies. All four TD plots show two resonance frequencies. The meaning of the first and second resonance frequencies are explained in the next paragraphs.

Powertrain parameters like gear ratio, enlarged engine inertia or changed vehicle load have an effect on the resonance frequencies and on the shape of the response. The influence of parameter changes on the transfer function is discussed in appendix E.

7.2.1 1st resonance frequency

Both the TD and ISAD powertrain show a resonance frequency as a result of the driveshaft stiffness k_{ds}. Figure 7.3 represents the simplified undamped TD powertrain model with 3 DOF, with J_{load} as the total equivalent vehicle inertia, J_e the total engine inertia and J_t the lumped transmission inertia. Clearly visible is the opposite motion of J_{load} with respect to J_e. J_t has only a small motion in the same direction as J_{load} and is almost stationary with respect to J_e during this resonance frequency.
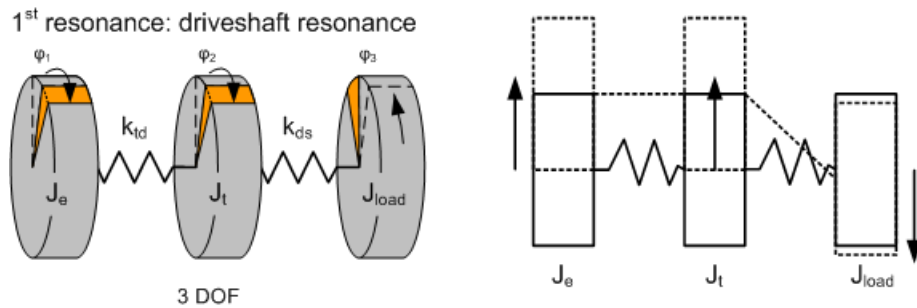

Figure 7.3: (left) 3D representation of the 1st resonance eigen mode (driveshaft resonance)of the TD powertrain, (right) schematic representation where the vibration is represented as a vertical vibration motion

The simplified undamped ISAD powertrain, figure 7.4, shows that the combined vehicle inertia J_{load} moves in the same direction as the lumped engine inertia. The first resonance (or in case of the ISAD powertrain the only resonance) is also known as "driveshaft resonance" [4].
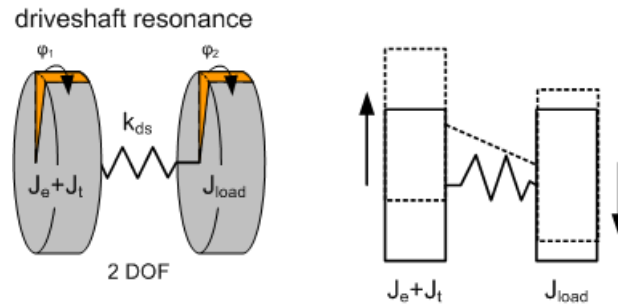
Figure 7.4: (left) 3D representation of the only resonance eigen mode (driveshaft resonance)of the ISAD powertrain, (right) schematic representation where the vibration is represented as a vertical vibration motion

7.2.2 2nd **resonance frequency**

Figure 7.5 shows the vibration motion of the second resonance frequency, which only occurs for the TD powertrain. The transmission inertia J_t vibrates in opposite direction with respect to the engine inertia J_e and the vehicle inertia J_{load}. This resonance frequency is also known as the "torsion damper resonance" [4].
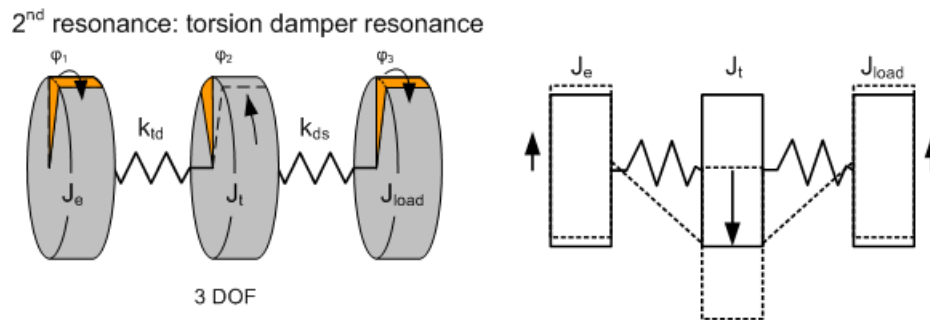

Figure 7.5: (left) 3D representation of the 2nd resonance eigen mode (torsion damper resonance) of the TD powertrain, (right) schematic representation where the vibration is represented as a vertical vibration motion

7.3   Frequency response and cylinder deactivation

During cylinder deactivation the order of excitation changes.Five different deactivation situations are being distinguished, indicated by "*System x*", where "*x*" stands for the active cylinder(s):

- System 1234: All cylinders activated (firing distance 180°/180°)

- System 134: 1 cylinder deactivated, in this case cylinder 2 (firing distance 180°/360°)

- System 14: 2 cylinders deactivated, in this case cylinders 2 and 3 (firing distance 360°/360°)

- System 13: 2 cylinders deactivated, in this case 2 and 4 (firing distance 180°/540°)

- System 1: 3 cylinders deactivated, in this case cylinders 2, 3 and 4 (firing distance 720°/720°)

System 134 represents all combinations where one cylinder is deactivated (*System 124*, *System 123*, *System 234* etc.), the resulting engine torque is equal in all cases. This also holds for *System 1*, which represents all combinations where 3 cylinders are deactivated. Deactivation of 2 cylinders can be obtained with *System 14* (constant firing distance of 360°/360°) or with *System 13* (alternating firing distance of 180°/540°), which results in a different engine torque, as can be seen in figure D.2.

Table 7.1 shows the main engine order for situations where cylinders are deactivated. The orders are obtained from frequency analysis of the engine torque during deactivation, see figures D.1 to D.3 in appendix D. The transmission ratios are dimensioned in such a way that the engine can be operated within an engine speed range of 1700 - 2500 [RPM]. Within this engine speed range the efficiency of the engine is potentially the best (although engine specific). Chapter 8 will show what will happen when the engine is operated outside this engine speed range. With equation 7.4 the main engine orders can be translated to excitation frequency when the optimal engine speed range is taken into account. Assumed is that during acceleration up to 1700 [RPM] all cylinders are activated in order to produce sufficient power. All system show 2nd and 4th engine orders, caused by the engines' inertia torque.

Active cylinders ("System x")	Main engine order(s) - N_{main}	f_{ex} [Hz] @ 1700 [RPM]	f_{ex} [Hz] @ 2500 [RPM]
System 1234	2	57	83
System 134	$\frac{1}{2}$, 1, 2	14	83
System 14	1, 2	28	83
System 13	$\frac{1}{2}$, $1\frac{1}{2}$, 2	14	83
System 1	$\frac{1}{2}$, $1\frac{1}{2}$, 2	14	83

Table 7.1: The table shows the main engine orders for every deactivation system. The lowest excitation order corresponds to a minimal excitation frequency at 1700 [RPM].

$$f_{ex} = \frac{n_e N_{main}}{60} \tag{7.4}$$

When analyzing the frequency response of the TD and ISAD powertrain, figures 7.1 and 7.2, it becomes clear that the driveshaft resonance frequency of the ISAD powertrain lies within the engine excitation frequency range during deactivation of 1, 2 or 3 cylinders.

Figure 7.6 is the result of combining all resonance frequencies and engine excitation frequencies into one graph. The overlapping colored areas represent the excitation frequency range caused by cylinder deactivation. For example, the lowest main engine order for *System 1* is $\frac{1}{2}$, which means that the excitation frequency is equal to 14 [Hz] at 1700 [RPM]. The figure also shows the resonance frequencies of the ISAD powertrain (triangles) and TD powertrain (1st resonance = circles, 2nd resonance = squares). The driveshaft resonance frequency of the ISAD powertrain lays within the excitation frequency range during 1, 2 and 3 deactivated cylinders. The second resonance of the TD powertrain also lies within the operating range, however as figures 7.1 to 7.2 show, the TD powertrain shows lower magnitudes at higher frequencies compared to the ISAD powertrain. The first TD resonance frequencies are not interfering with the excitation frequency range.

Clearly, the eigenfrequency of the ISAD powertrain constrains the application of cylinder deactivation which is of course not favorable. The resonance can be dampened by the ISAD system,

however the torque capabilities of the ISAD are limited (+45 Nm to -45 Nm), which limits the damping capabilities. In conclusion, figure 7.6 shows that the dynamical behavior of the ISAD powertrain will have to be improved in order to maximize the benefit of cylinder deactivation. The next paragraph proposes solutions which can improve the dynamical behavior of the ISAD powertrain.
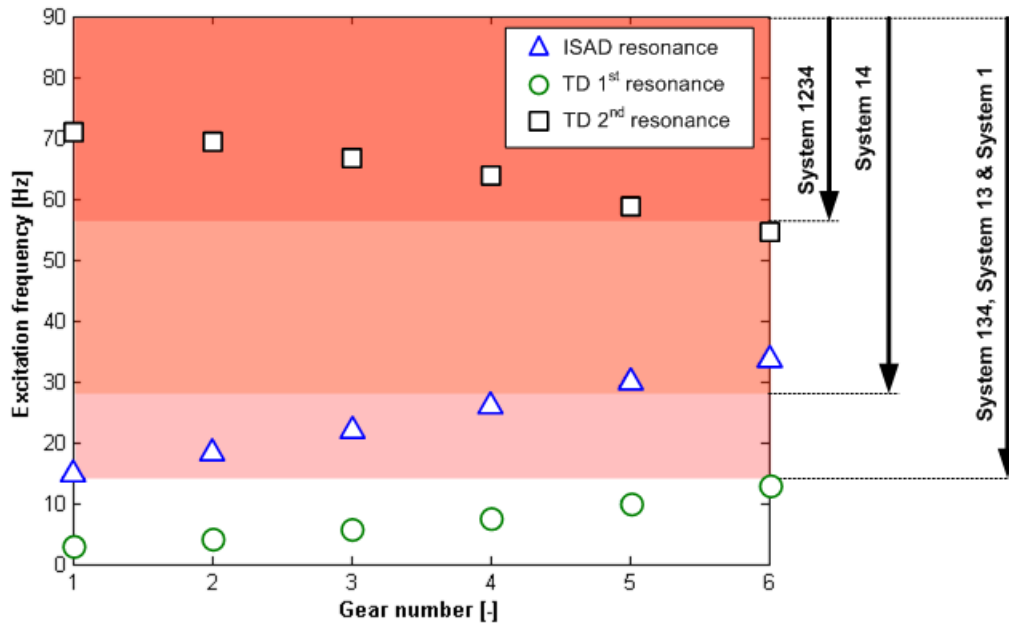

Figure 7.6: Eigen frequency analysis of the TD and ISAD powertrain. The shaded areas represent the excitation frequency range of the optimal engine speed band (1700 - 2500 RPM). The squares, circles and triangles represent the eigenfrequencies of the analyzed powertrain systems.

7.3.1 Solution

Chapter 5.3 described several solutions to improve the dynamical behavior of the powertrain:

- Increasing the torque capabilities of the ISAD system (damping of the source)

- Increasing engine and/or transmission inertia (tuning of the system)

- Dual Mass Flywheel (isolation of the source)

- Adding a torsion damper (isolation of the source)

By increasing the torque capabilities of the ISAD system it would be possible to suppress the resonance amplitude. The torque capacity will still be small (+/- 45 [Nm]) compared to the gas pressure torque peaks (up to 700 [Nm] for 1 cylinder operation). Increasing the torque capability of the ISAD system goes hand in hand with an increase in the weight, volume and cost of the ISAD system and electric buffer.

Parameter analysis shows, appendix E, that the ISAD powertrain resonance frequency can be shifted down by increasing the engine inertia or the transmission inertia. Increasing the inertia increased the weight, cost and volume of the powertrain which is not desired. Increasing the engine and transmission inertia with 50 % only reduces the resonance frequency from 30 [Hz] to 21 [Hz] in 5th gear. Figure 7.6 shows immediately that this frequency reduction is still not enough to shift the eigen frequency out of the operating speed range. Increasing the inertia also comes with the penalty of reduced engine response.

A dual mass flywheel (DMF) as described in paragraph 5.3.2, introduces an additional powertrain eigenfrequency. Compared to a torsion damper, this eigenfrequency is lower and therefor causes resonances at low engine excitations. Furthermore, it requires additional build space and increases the powertrain weight.

Placement of a spring-damper system between the engine and transmission improves the dynamical behavior of the powertrain. It introduces a second resonance frequency as seen with the TD powertrain. By adding this spring-damper a combination between the TD powertrain and ISAD powertrain is created. The responses will be equal to that of the TD powertrain, only now with the damping function of the ISAD. This solution will be used from this moment on for further analysis.

7.4   Conclusion

Two different powertrains are analyzed, the proposed ISAD powertrain for the "car of the future" and the TD powertrain as benchmark powertrain. The frequency responses showed that the dynamical behavior of the proposed ISAD powertrain is inferior to the benchmark powertrain. Together with cylinder deactivation, which changes the order of excitation, this causes an inferior dynamical behavior compared to the benchmark powertrain. In order to improve the dynamical behavior of the ISAD powertrain, a spring-damper system is added, combining the properties of both the ISAD powertrain with the TD powertrain. The powertrain mounts show a consistent eigenfrequency of 5 [Hz], independent of the used powertrain or transmission ratio.

The next chapter discusses the simulations results of this improved powertrain.

Chapter 8

Simulation results

Simulations are executed in order to gain information about comfort levels, relevance of air spring torque and relevance of the deactivation order. This chapter describes how the simulations are executed and discusses the results of these simulations. With these simulations the timing of valve closing is studied as well as the possible order of deactivation.
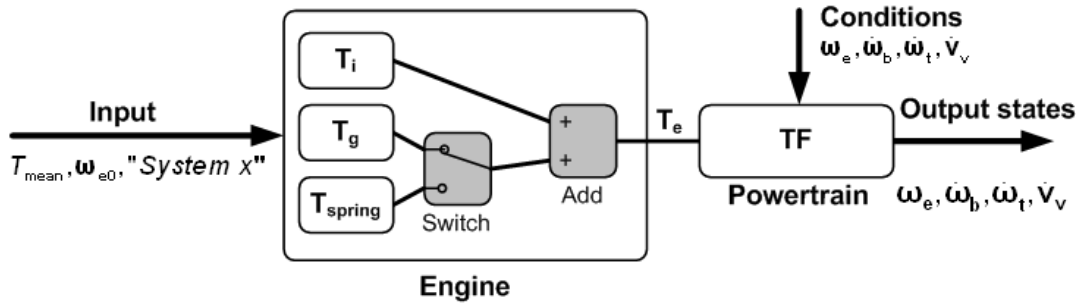

Figure 8.1: Schematic representation of an engine and powertrain model, used in Matlab/Simulink. Engine represents 1 cylinder.

8.1 Simulation model

The time domain simulations are executed with Matlab/Simulink. Figure 8.1 gives a schematic representation of the used model. The input for this model is the gas pressure torque T_g, inertia torque T_i, and in case of cylinder deactivation air spring torque T_{spring}. Together they form the engine torque T_e, which is the input for the powertrain transfer function.

$$T_e(\theta_e) = T_g(\theta_e) + T_i(\theta_e) + T_{spring}(\theta_e) \tag{8.1}$$

Both the gas pressure torque and the inertia torque are approximated by a Fourier series algorithm. Appendix B describes in greater detail the gas pressure torque, inertia torque and the air spring torque. The dynamic engine torque of the internal combustion engine will change when cylinder deactivation is used. Figure 8.2 shows the inertia torque of a 4 cylinder engine. The inertia torque is proportional with ω_e^2 and therefor gets dominant with higher engine speeds. The inertia torque is not influenced

by cylinder deactivation. Figure 8.3 shows the gas pressure torque of one single cylinder. The gas pressure torque depends on the engine load and is periodic for every two engine revolutions (720°). When a cylinder is deactivated, the gas pressure torque is replaced by the air spring torque like figure 8.4. The magnitude of the air spring torque depends on the compression start pressure, which can be influenced by the valve closing timing. More about the valve closing timing in paragraph 8.3.
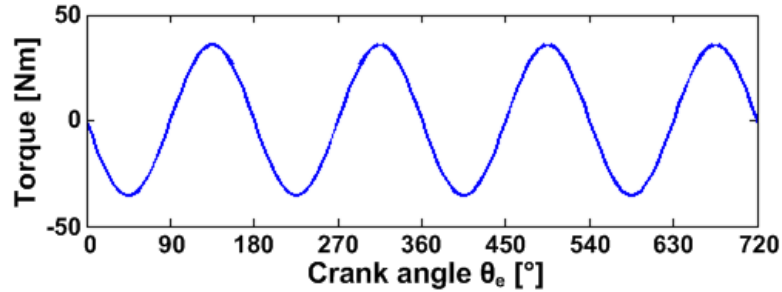

Figure 8.2: Inertia torque for 4 cylinders at 2000 [RPM]. Inertia torque is proportional to ω_e^2.
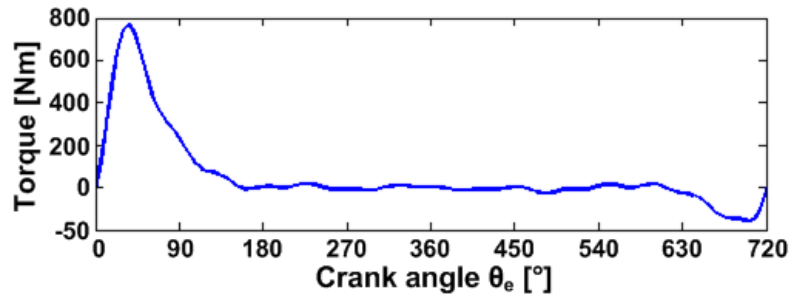

Figure 8.3: Gas pressure torque of one cylinder. Average engine torque is 50 [Nm].

The powertrain is described by a set transfer functions, which are determined from the state space notation, see appendix C. Every simulation is executed at a fixed gear ratio r_i and constant wheel slip, defined by v_{v0} and ω_{w0}. Simulations are executed under steady state conditions, meaning fixed average engine speed and fixed engine load, because comfort issues are noticed best under these conditions [12].

8.2 Cylinder deactivation order

The number of deactivated cylinders is determined by the required engine load and required powertrain comfort. The order of deactivation however can be freely chosen. When two cylinders are deactivated there are two different variants possible (*System 14* or *System 13*), see figure 8.5. *System 14* represents the activated cylinders 1 and 4, whereas *System 13* represents the situation where cylinders 1 and 3 are active. The combustion interval of *System 14* is constant at 360 crank angle degrees, the combustion distance of *System 13* is inconsistent with intervals of 180° and 540°. *System 1* always
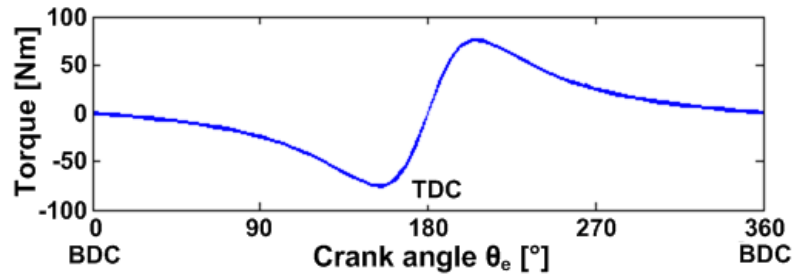
Figure 8.4: Air spring torque of one individual cylinder, which replaces the gas pressure torque in case of a deactivated cylinder. Compression start pressure 1 bar.

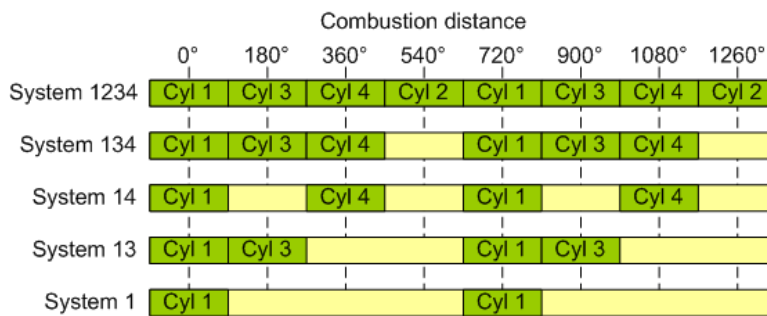has a combustion distance of 720°, independently of the activated cylinder.

Figure 8.5: Deactivation diagram showing the combustion intervals during deactivation for all deactivation Systems. For two cylinder deactivation two different systems are available, System 14 *and* System 13

Figures F.1 to F.3 from appendix F show the total engine torque and engine speed error in 5th gear at 2000 [RPM], without ISAD damping. The average engine torque is 50 [Nm]. *System 1234*, figure F.1a, shows a very moderate engine speed error. The torque pulsations are equally spaced with a relative low torque amplitude. Because of one missing combustion torque pulse, *System 134* has a larger speed error. *Systems 14* and *System 13* show a different response due to the difference in the combustion pulse interval. *System 14*, figure F.2a, delivers a relative smooth engine torque compared to *System 13* with a lower peak-to-peak engine speed error. The engine torque peaks are also higher for *System 13*, which can be explained with figure F.4. With *System 13*, cylinders 2 and 4 operate as air spring. The air spring torque pulse and the gas pressure pulse complement each other and thus increasing the engine torque peak. With *System 14* this is not the case. Due to superior response, *System 14* will be used in the remaining of the report when two cylinders are deactivated.

8.3   Valve closing timing

When cylinders are deactivated the intake and exhaust valves are closed. The deactivated cylinder will repeatedly complete a compression stroke followed by an expansion stroke. The cylinder operates then as a so called "air spring", which has a nett energy cost of zero (energy required for compression is released during expansion, losses not included). As reported already in chapter 4.2, there are several

moments to close the valves of a deactivated cylinder. The numbers listed below correspond to the numbers in the engine cycle of figure 8.6a:

1. Before the exhaust stroke

2. After the intake stroke

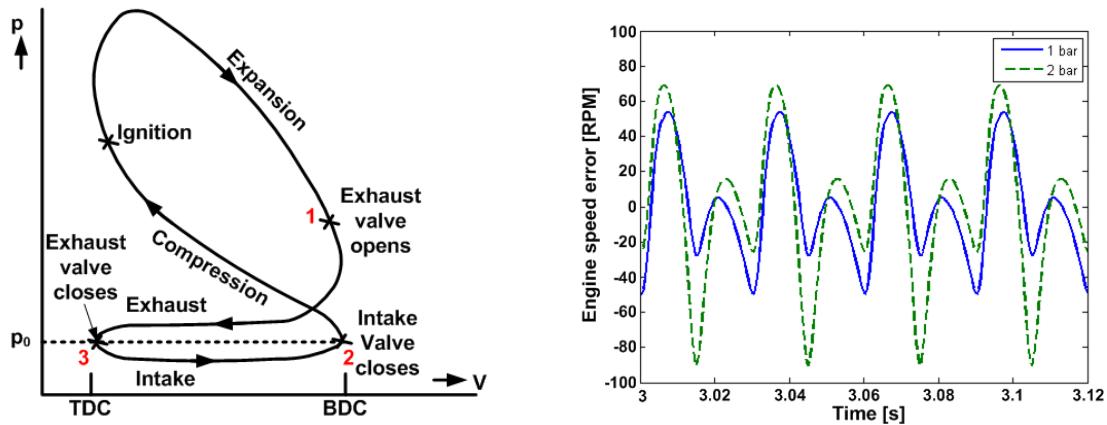3. After the exhaust stroke and before the intake stroke

Figure 8.6: (a) p-V diagram showing the gas exchange cycle of a spark ignited engine. The numbers represent the valve closing moments. (b) Comparison between the engine speed error of timing 1 and 2.

The timing of valve closing has consequences for the air spring torque T_{spring}, because of the changed compression start pressure. Valve timing 1 keeps the pressurized and hot gases from the expansion stroke trapped, which leads to a higher compression start pressure. The compression start pressure is variable and depends on the combustion pressure, expansion ratio and gas temperature. For the simulations the combustion start pressure is assumed to be 2 [bar]. The actual pressure level is of less interest because it is only used to analyze the effect of increased compression start pressure. Timing 1 has the advantage that the hot trapped exhaust gases keep the cylinder warm, which is beneficial for the thermodynamic efficiency according to [18]. The compression start pressure of timing 2 depends on wether the intake flow is being throttled, if pressure charging is used (exhaust gas turbo or compressor) and the valve timing. During the simulations atmospheric pressure p_0 is assumed, approximated at 1 [bar]. The third valve timing results in a pressure below atmospheric pressure (vacuum). The compression start pressure will therefor be approximately 0.05 [bar], and the compression end pressure will be approximately atmospheric pressure. Blow-by is not incorporated into the simulations. Further more detailed research is required on the exact timing of the valves, influence of blow-by and the influence of pressure charging.

To verify which timing is preferred from a powertrain dynamics point of view, two simulations have been executed.

- Comparing 1 bar compression start pressure with 2 bar compression start pressure (comparing timing 1 and 2), figure 8.7a.

- Comparing 1 bar compression start pressure with 0.05 start pressure (comparing timing 2 and 3), figure 8.7b.

Comparing timing 1 to timing 2 reveals that the amplitude of the air spring torque increases with the compression start pressure, leading to an increased peak-to-peak engine torque as shown by figure 8.7a. Comparing timing 2 with timing 3 reveals that the air spring torque of timing 3 is hardly noticeable, caused by the low compression start pressure. Timing 3 results in the least peak-to-peak engine torque, leading to the lowest engine speed error, figure 8.7b. Timing 3 will be used during the remaining simulations.
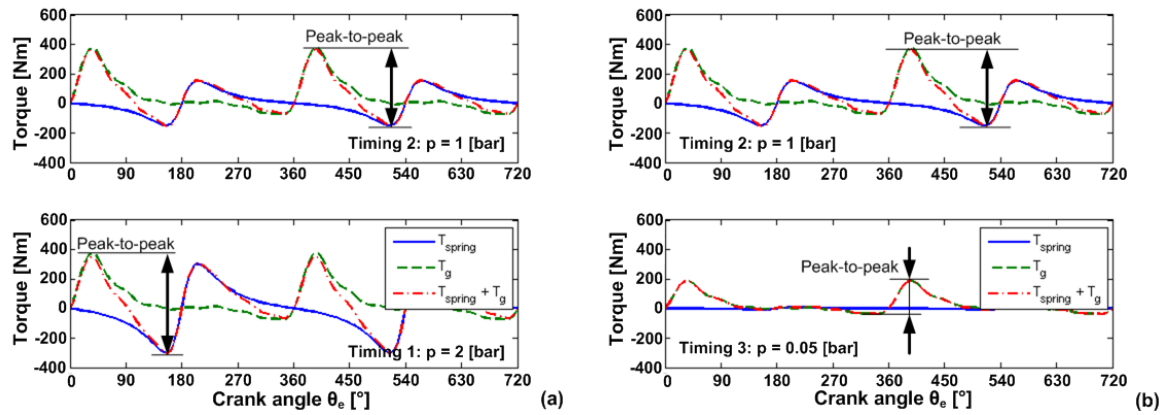

Figure 8.7: (**a**) *Comparison between timing 1 and timing 2.* (**b**) *Comparison between timing 2 and timing 3. Shown are the gas pressure torque, air spring torque and combined gas pressure torque for 2 deactivated cylinders (*System 14*). Mean engine load is 50 [Nm].*

Cylinder blow-by and heat transfer of the deactivated cylinder are not taken into account during the simulation. Due to the pressure difference between the engine sump and the deactivated cylinder, a certain amount of gases will be blown from the cylinder to the sump or from the sump back to the cylinder. This will lower the pressure in the cylinder when timings 1 or 2 are used and increase the cylinder pressure for timing 3. The increasing pressure for timing 3 will increase the air spring torque, which is not beneficial because of the increased peak-to-peak torque. Further research will have to show what the amount and rate of blow-by is and how this will effect the air spring torque.

An air damper effect could be created by keeping the valves slightly open, by doing so create an air spring torque which dampens the gas pressure torque of the other cylinders. This effect creates pumping losses however, which offset the benefit of cylinder deactivation. Further research is necessary to investigate the usefulness of the air damper and what the cost will be in engine efficiency.

8.4 Simulation responses

The previous paragraphs showed what the ideal valve timing is regarding the air spring torque and what the best deactivation order is in case of deactivation of two cylinders. These results are now used to analyze the response of cylinder deactivation on the cyclic engine speed fluctuation (c_{fluc}), gear rattle ($\dot{\omega}_t$) and vehicle shuffle ($\dot{v}_v$). The following situations and conditions will be analyzed and discussed:

- Analyze the response with respect to the engine speed.

- Analyze the response with respect to the engine load.

- Analyze the effect of transmission ratio.

- Analyze the effect of passive ISAD damping.

8.4.1 Cyclic speed fluctuation

The cyclic speed fluctuation is an indicator of the running smoothness of the engine, which is a measure for engine shake. The cyclic speed fluctuation, c_{fluc} as defined by equation 8.2, is regarded as the main criteria regarding powertrain comfort. Large fluctuations result in engine shake (not investigated in this report), high transmission shaft accelerations and high vehicle accelerations. According to [7] the recommended limit is 0.25 [-], to ensure a certain comfort level.

$$c_{fluc} = \frac{\omega_{e.max} - \omega_{e.min}}{\omega_{e.mean}} \tag{8.2}$$

Figure 8.8a shows the cyclic speed fluctuation in relation to the engine speed in 5th gear and at a mean engine load of 20 [Nm]. In 5th gear 20 [Nm] is representative for cruising at 80 [km/h] on a flat road. The figure shows four different responses, representing the cyclic speed fluctuation of the four systems. As expected, deactivation of cylinders results in an increase of the cyclic speed fluctuation. Due to the fact that the engine torque of *System 134* and *System 1* contains lower engine excitation orders, resonance peaks are visible at 1200 [RPM] representing driveshaft resonances at 10 [Hz]. Because of this resonance peak the response of *System 134* proves to be worse than *System 14*. At higher engine speeds the behavior is nearly identical. When taking the above into consideration, it would not be logical to deactivate one cylinder, instead always immediately deactivate two cylinders. This is more efficient because the resulting cylinder load of the two active cylinders is higher than the cylinder load when three cylinders are activated, as explained in chapter 4 paragraph 4.3. The cyclic engine speed fluctuation of a three cylinder engine from [7] shows resemblance with respect to the speed fluctuation of *System 134*.
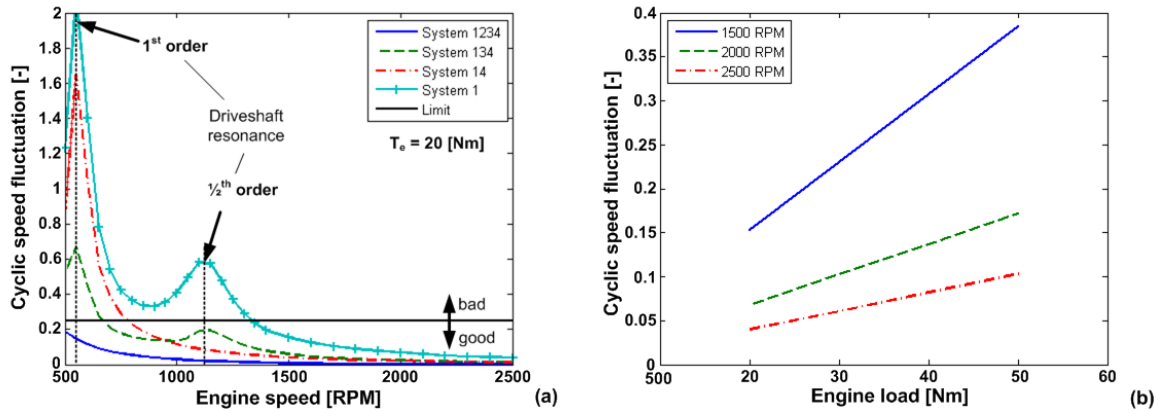

Figure 8.8: **(a)** *Speed irregularity of the TD powertrain during cylinder deactivation in 5th gear and 20 [Nm] engine load.* **(b)** *Influence of the engine load on the cyclic speed fluctuation.*

The horizontal line in figure 8.8a represents the recommended cyclic speed fluctuation limit of 0.25 [-]. Responses below this limit are considered as acceptable regarding comfort. The engine speed at the point where the response crosses the limit is defined as the "lug limit", as introduced in [20]. The "lug limit" is the lowest possible engine speed where cylinder deactivation is still possible. Below this speed one or more cylinders should be activated again to lower the response. The figure shows that the "lug limit" increases because of cylinder deactivation. At higher engine speeds the inertia torque gets dominant, reducing the influence of cylinder deactivation on the dynamic engine torque. Figure 8.8b underlines this by showing the speed fluctuation of *System 1* at different engine loads and engine speeds. At low engine speeds (1500 [RPM]) the change in speed fluctuation is relatively large when the engine load is increased. Comparing this to higher speeds, 2500 [RPM], it is clear that the influence of the engine load is reduced.

Figure 8.9 gives the relation between the cyclic speed fluctuation and the transmission ratios for *System 1*. The "lug limit" increases with an increase in gear ratio, at the same time reducing the peak magnitude. This figure tells that, concerning the "lug limit", deactivation at low engine speeds is better suited in low gears. Table 8.1 gives the "lug limit", lowest possible engine speed, for every system and transmission ratio at 20 [Nm].

System	1st gear	2nd gear	3rd gear	4th gear	5th gear	6th gear
1234	<500	<500	<500	<500	<500	<500
134	770	800	860	960	840	850
14	770	780	800	820	870	940
1	1040	1060	1090	1190	1370	1570

Table 8.1: Lug limit at 20 [Nm] average engine load, minimal allowable engine speed where comfort is still preserved.
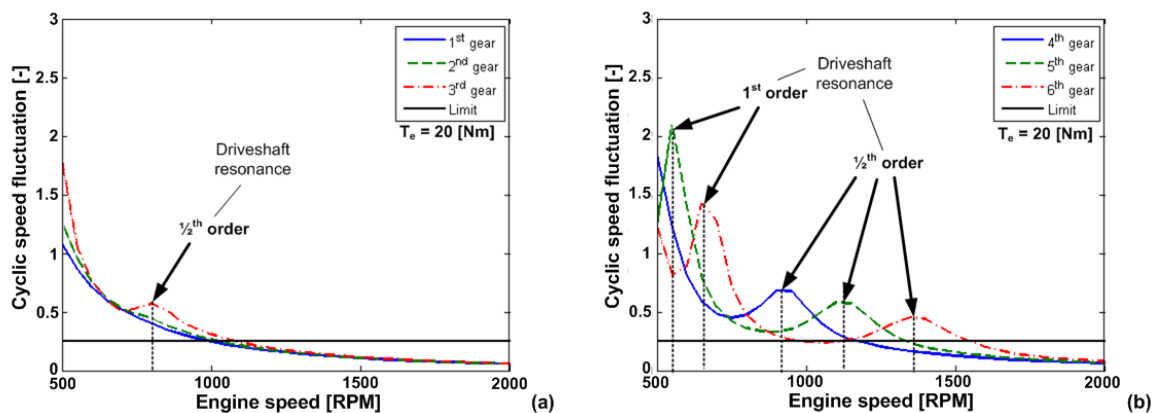

Figure 8.9: Influence of the transmission ratio on the cyclic speed fluctuation for (a) 1st, 2nd and 3rd gear (b) 4th, 5th and 6th gear.

The ISAD system can be used to dampen the speed fluctuation. Figure 8.10 shows the result on engine speed fluctuation at 20 [Nm] when passive damping is used. Clearly visible is that the effect of damping is the largest around the resonance frequencies. This can be explained by figure E.10a, showing the effect of damping on the frequency response of T_e to ω_e. Damping has mainly an

influence on the 1st resonance frequency (driveshaft resonance). *System 1* and *System 134*, showing this first resonance, therefor have the largest benefit.
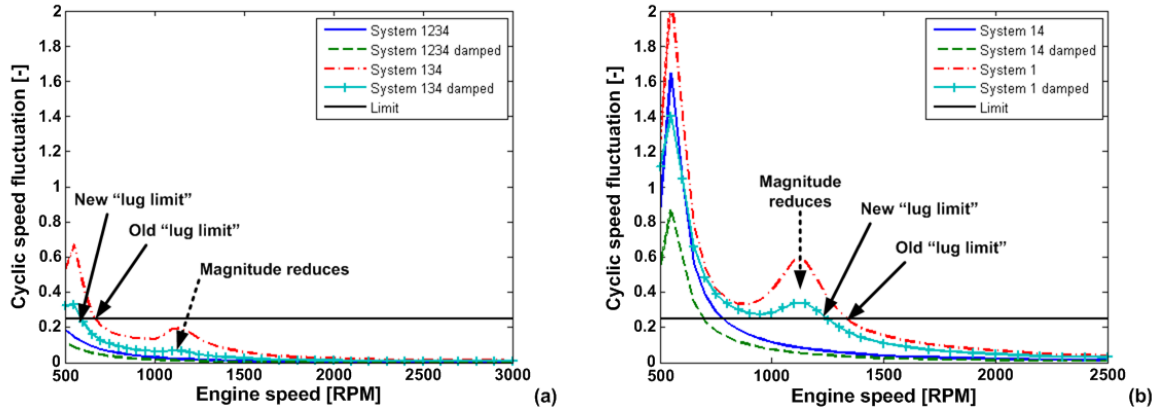

Figure 8.10: Effect of damping on the cyclic speed fluctuation for (a) System 1234 and System 134, (b) System 14 and System 1.

8.4.2 Engine shake

Engine shake describes the movement of the powertrain unit with respect to thevehicle body. Vibrations are transmitted through the engine mounts to the vehicle body. This response only addresses the angular acceleration $\dot{\omega}_b$ of the powertrain unit around the crankshaft, caused by the transmission reaction torque and engine torque. Figure 8.11a shows the maximum acceleration $\dot{\omega}_b$ related to the engine speed in 5th gear at 20 [Nm]. $\frac{1}{2}^{th}$ order resonance frequencies are visible for *System 134* and *System 1*. The response increases after approximately 2500 [RPM]. Further research will have to explain the difference in response of *System 1234* compared to *System 134*, *System 14* and *System 1* at engine speeds above 2500 [RPM].
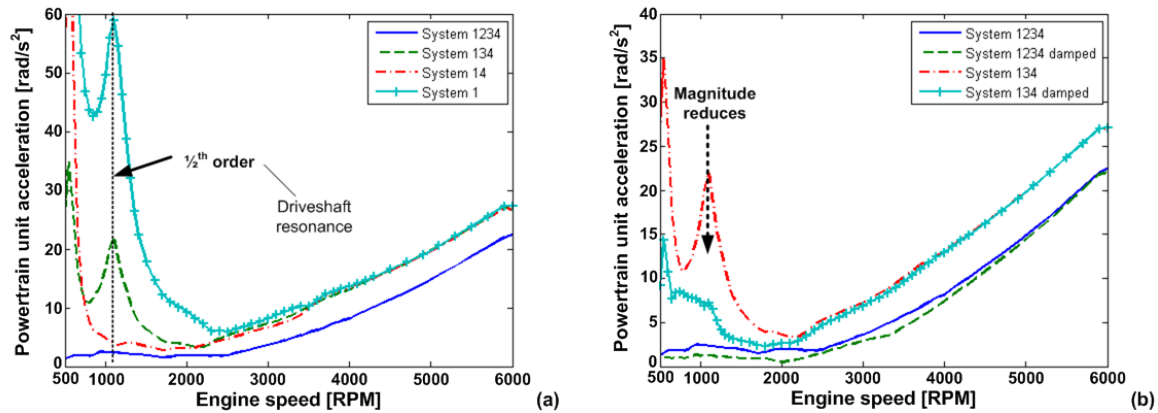

Figure 8.11: (a) Powertrain unit acceleration during cylinder deactivation in 5th gear and 20 [Nm] engine load. (b) Result of ISAD damping on transmission acceleration for System 1234 and System 134.

Figure 8.11b shows that the ISAD system is also capable of reducing the response related to engine

shake. Again, the damping is most effective around the resonance peaks.

8.4.3 Gear rattle

Gear rattle is the third comfort related criterion which is determined by the maximum primary transmission shaft acceleration $\dot{\omega}_t$. Gear rattle expresses itself by audible noise transmitted by transmission components [15]. Figure 8.12a shows the maximum transmission acceleration in relation to the engine speed, in 5th gear and at 20 [Nm]. Deactivation of cylinders increases the response, the difference between deactivated systems and the non deactivated system (*System 1234*) is fairly large, especially at lower engine speeds. Several resonance peaks are visible. caused by the 2nd powertrain resonance frequency (torsion damper) at 59 [Hz].
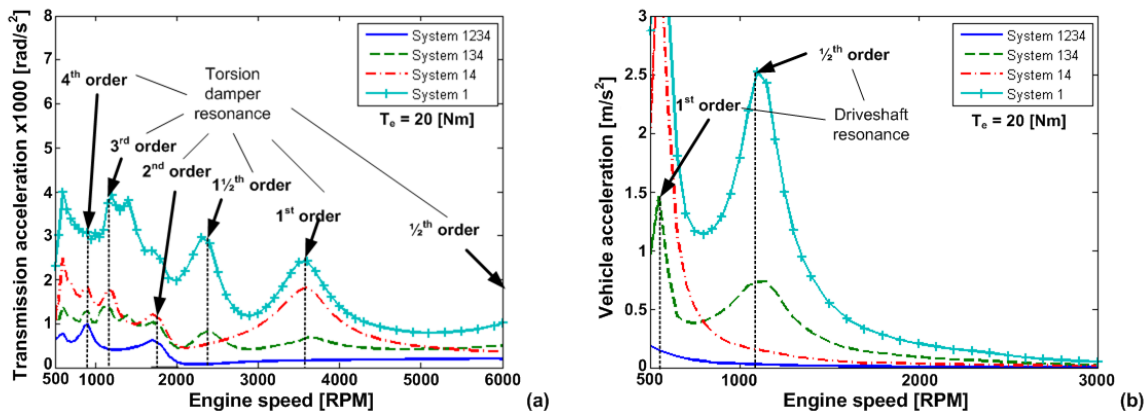

Figure 8.12: (**a**) *Maximum transmission primary shaft radial acceleration during cylinder deactivation.* (**b**) *Maximum vehicle acceleration caused by cylinder deactivation (5th gear and 20 [Nm] engine load).*
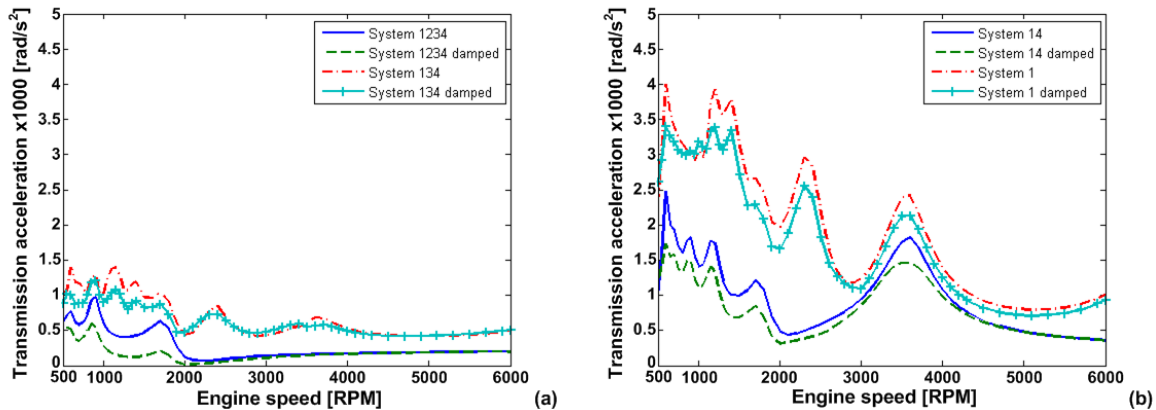

Figure 8.13: *Result of ISAD damping on transmission acceleration for* (**a**) *System 1234 and System 134,* (**b**) *System 14 and System 1.*

The effect of the passive ISAD damping on the response is visible but minimal. Figure E.9a shows the frequency response of T_e to $\dot{\omega}_t$ under influence of ISAD damping. The second resonance is minimally damped, in contrast to the first resonance. Reducing the transmission acceleration therefor is

not effective with the ISAD system. Reducing the transmission acceleration can be obtained by reducing the 2nd powertrain resonance frequency. This can be done for instance with a dual mass flywheel, which increases the transmission inertia. Another solution would be lowering the torsion damper stiffness. Reference [15] reports about acceleration values of 2300 [rad/s^2] without occurrence of gear rattle. Further research is needed to determine the maximum allowable value of the primary transmission acceleration regarding comfort. This requires a detailed model of the powertrain, able to determine the exact accelerations of idler gear, sleeves and synchronizers.

8.4.4 Vehicle shuffle

The last comfort related criterion is the maximum vehicle acceleration $\dot{v}_v$ or vehicle shuffle. With conventional powertrains, without cylinder deactivation, vehicle shuffle often only occurs at specific load change conditions (pedal tip-in, back-out). Due to the changed engine torque dynamics it could be possible that this phenomena, longitudinal vehicle accelerations, occurs constantly under influence of cylinder deactivation.

Figure 8.12b shows the response of the maximum vehicle acceleration, with respect to engine speed, in 5th gear at 20 [Nm]. The figure shows strong resemblance to the speed fluctuation response, figure 8.8a. The visible resonance peaks are caused by the 1st powertrain resonance frequency. At higher engine speeds the amplitude reduces.
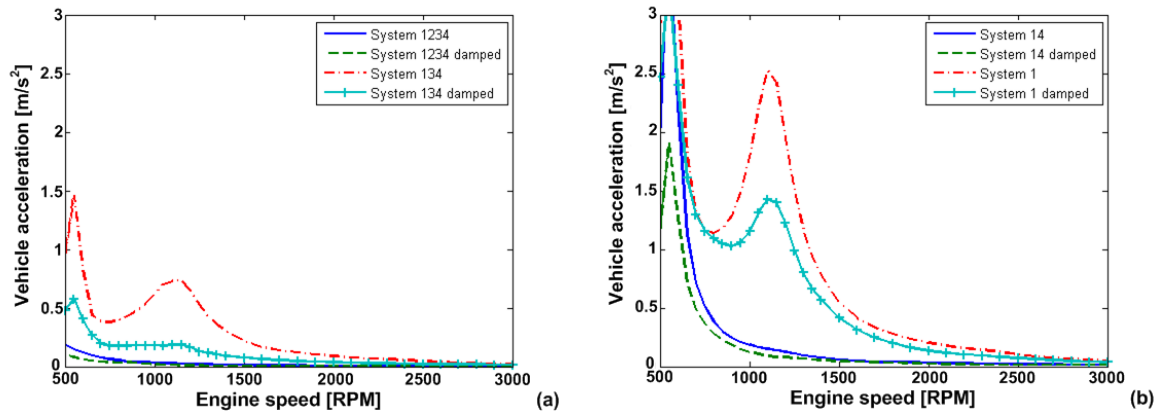

Figure 8.14: Result of ISAD damping on vehicle acceleration for (a) System 1234 and System 134, (b) System 14 and System 1.

The effect of ISAD damping is highest around the resonance peaks, figure F.2, as already concluded for the cyclic speed fluctuation response. Changes to the powertrain to improve the speed fluctuation response during deactivation will also have a positive influence on vehicle shuffle. The model used in the simulation does not incorporate longitudinal damping of the suspension and the interior. Further research is needed to determine acceptable vehicle acceleration values and investigate other components affecting vehicle shuffle.

8.5 Conclusions

Simulations made clear that the timing of cylinder deactivation, regarding valve closing, has an influence on the peak-to-peak engine torque. The valve timing determines the compression start pressure of the air spring torque cycle. Preferable is to keep this pressure around the ambient pressure, achieved when the valves are closed after the intake stroke.

Deactivation of two cylinders can be achieved with two different configurations. The difference between these two configurations is the interval between consecutive combustion events. When using an inconsistent combustion interval, *System 13*, the peak-to-peak engine torque is increased leading to increased engine speed fluctuations. *System 14* has an evenly spaced combustion interval and due to the lower peak-to-peak engine torque this system is preferred in case of two cylinder deactivation.

Four different comfort criteria have been analyzed, cyclic speed fluctuation, gear rattle, vehicle shuffle and engine shake. Resonances are visible in all responses, but only the gear rattle response shows resonances within the engine speed range of 1700 - 2500 [RPM]. The resonance in the speed fluctuation and vehicle acceleration are caused by the driveshaft resonance, whereas the torsion damper resonance causes resonance peaks in the transmission acceleration response. From literature a maximum allowable cyclic speed fluctuation limit was found. When cylinder deactivation is evaluated with this limit, it is possible to deactivate up to three cylinders above 1600 [RPM]. The cyclic speed fluctuation and vehicle acceleration also show that the response of two cylinders deactivation is better than the response of one cylinder deactivation. One cylinder deactivation has therefor not much use, when taking the fuel efficiency benefit of two cylinder deactivation into account (only based upon cyclic speed fluctuation criteria).

The level of damping by the ISAD system is not good enough to obtain the same comfort level under deactivation as under normal operation (*System 1234*). The best damping performance is obtained around the first powertrain resonance frequency. The relative effect of damping is the highest when less cylinders are deactivated. Modifications to the powertrain setup are needed in order to bring the comfort level during deactivation back to the non-deactivation level.

Literature is used to verify the obtained responses from simulations. The obtained data regarding cyclic speed fluctuation are comparable with those found in literature. The other responses show values which are in range with values found in literature. However, further verification and validation is required.

Chapter 9

Conclusions and recommendations

9.1 Conclusions regarding project "car of the future"

The project "car of the future" is a project aimed at designing a sustainable passenger car for the year 2020. The concept of the "car of the future" is based upon a modularity concept, creating flexibility in exchanging different powertrains. This flexibility makes it possible to adapt the vehicle to the availability of different fuels and demands. Because of the fuel flexibility an internal combustion engine is used as primary mover for the "car of the future".

Placing the powertrain at the rear of the vehicle offers advantages regarding vehicle aerodynamics, vehicle dynamics, vehicle weight and space. Mounting the engine in the back creates the possibility of using a boxer engine configuration. The boxer engine provides advantages regarding engine weight, center of gravity and vibrations.

An automated manual transmission is regarded as the ideal transmission in combination with a parallel hybrid setup and future improved engine technology. The transmission ratios are dimensioned in such a way that it is possible to let the engine operate in its optimal engine speed range.

9.2 Conclusions regarding cylinder deactivation

The objective of this thesis is to:

"Determine the influence of cylinder deactivation on a 4-cylinder engine, regarding the vibrational behavior of the powertrain."

With cylinder deactivation it is possible to increase the engine efficiency by increasing the cylinder load of the active cylinders. Cylinder deactivation results in reduced mechanical losses in the valvetrain, further increasing the engine efficiency. Pumping losses are minimized by keeping the valves of the deactivated cylinders closed.

Deactivation of cylinders will reduce the engines' excitation frequency and increase the combustion torque peaks. The reduced excitation frequency causes powertrain resonances when the engine is operated in its optimal engine speed range. Frequency analysis showed that a torsion damper is

required to shift the driveshaft eigen frequency outside of the engines' excitation frequency range.

Simulations showed a large influence of cylinder deactivation on the vibrational behavior of the powertrain. Due to cylinder deactivation responses are factors higher than the non-deactivation response at low engine speeds. At higher engine speeds however the difference is reduced due to the increasing dominance of the engines inertia torque. Deactivation of up to 3 cylinders is possible, from 1600 [RPM] onwards, when using cyclic speed fluctuation values from literature as comfort benchmark. The integrated starter alternator damper (ISAD) can be used to dampen the increased responses caused by cylinder deactivation. The ISAD system proved to be unable to reduce the vibrations under deactivation back to the level of the non deactivated level. The effect of damping was most noticeable around the first powertrain eigen frequency.

The valves of the deactivated cylinder are kept closed, to minimize the pumping losses of this cylinder. The deactivated cylinder will then function as an air spring. The timing of closing the valves influences the engine torque peaks. Closing of the valves can be done at three different moments. Closing of the valves before the intake stroke results in the lowest peak-to-peak engine torque, leading to less torsional vibrations.

9.3 Recommendations and future work

A start has been made in developing and researching the classic powertrain for the project "Car of the future", with the focus on cylinder deactivation of 4 cylinder engines. This research has answered some questions regarding cylinder deactivation, but a lot of questions are still unanswered.

This research showed that the transmission acceleration and vehicle accelerations increased under influence of cylinder deactivation, possible causing gear rattle and vehicle shuffle. Further detailed research is necessary about gear rattle and vehicle shuffle. Simulation models will have to be extended with a detailed transmission model to verify gear rattle. Extending of the model with damping dynamics of the vehicles suspension and the interior, provides the opportunity to investigate vehicle shuffle. Real world testing is needed to verify the obtained results.

Other powertrain topologies need to be studied, including different transmission systems like continuously variable transmissions, to analyze if the gear rattle, vehicle shuffle and engine shake can be further reduced. At the same time, more knowledge is needed about acceptable limits of engine shake, gear rattle and vehicle shuffle.

A study is needed about the energy management of the ISAD system. Smart control can both improve the damping effect of the ISAD system and reduce the energy needed for damping. It could be integrated into the powertrain control for the mild parallel hybrid setup as proposed for the car of the future project. More detailed analysis is needed on the unbalanced warmup of the engine, on the air spring torque and on the behavior of cylinder deactivation on turbo charging.

The air spring torque has a large influence on the total engine torque. The compression start pressure is influenced by, for instance valve overlap, blow-by, cylinder temperature, compression ratio and pressure charging (turbo). Further research in this area could be helpful to get a better understanding about the influence of the air spring torque on cylinder deactivation.

Bibliography

[1] BADREDDINE, B., ZAREMBA, A., AND SUN, J. Active damping of engine idle speed oscillation by applying adaptive pid control. *SAE-paper 2001-01-0261* (2001).

[2] BASSHUYSEN, R. Zylinderabschaltung und ausblenden einzelner arbeitszyklen zur kraftstoffersparnis und schadstoffminderung. *MTZ 54* (1993).

[3] DE COCK, J. Prognosis of the starting behaviour of a dual mass flywheel. Tech. rep., TU Eindhoven, 2002.

[4] DE COCK, J. Vibration analysis and synthesis off the brake/impulse shift transmission technology. *DCT 2004-97* (2004).

[5] DE METSENAERE, C. Fracture analysis of dual mass flywheel arc springs. Tech. rep., TU Eindhoven, 2002.

[6] DE VRIES, B. Work in progress. Master's thesis, TU Eindhoven, 2007.

[7] GRAF ET AL., B. 100 hp / 200 nm diesel motorcycle with 6 speed automated manual transmission. *SAE-paper 2004-32-0069* (2004).

[8] GRAVES ET AL., R. Stretch efficiency in combustion engines with implications of new combustion regimes. *Advanced Combustion Engine R&D - FY 2004 Progress Report* (2004).

[9] GUSEV ET AL., S. Active flywheel control based on the method of moment restrictions. *American Control Conference, 0-7803-3832-4/97* (1997).

[10] HAFNER, K., AND MAASS, H. *Theorie der Triebwerksschwingungen der Verbrennungskraftmachine*. Springer-Verlag, 1979.

[11] HATANO ET AL., K. Ein neuer mehrphasen-motor mit variabler ventilsteuerung. *MTZ 54* (1993).

[12] HEINRICHS, R., AND BODDEN, M. Perceptual and instrumental description of the gear rattle phenomenon for diesel vehicles. *6th International congress on sound and vibrations 1999* (1999).

[13] HEISLER. *Advanged Engine Technology*. Arnold, 1995.

[14] JAHED, A., HOUSELY, A., AND SPOONHOWER, J. Sema 42-volt report.

[15] KIM, T., AND SINGH, R. Dynamic interactions between loaded and unloaded gear pairs under rattle conditions. *SAE-paper 2001-01-1553* (2001).

[16] KODAMA ET AL., M. Subaru new horizontally opposed 4-valve engine. *SAE-paper 890471* (1989).

[17] KOLLMANN ET AL., K. Perspektiven zur zukunft der verbrennungsmotoren - wohin fuerth die weiterentwicklung der ottomotoren? *MTZ 59* (1998).

[18] KREUTER ET AL., P. Meta - cvd, an electro-mechanical cylinder and valve deactivation system. *SAE paper 2001-01-0240* (2001).

[19] LAMMERS, J. Common automobility in 2020. Master's thesis, TU Delft, 2006.

[20] LEONE ET AL., T. Fuel economy benefit of cylinder deactivation - sensitivity to vehicle application and operating constraints. *SAE paper 2001-01-3591* (2001).

[21] SASTRY. *Nonlinear systems*, vol. 10. Springer, 1999.

[22] SCHEEPERS, B. The virtual engine. Master's thesis, TU Eindhoven, 2003.

[23] SCHEFFER, N. Work in progress. Master's thesis, TU Eindhoven, 2007.

[24] SCHMIDT ET AL., M. Potential of regenerative braking using an integrated starter alternator. *SAE-paper 2000-01-1020* (2000).

[25] SERRARENS, A. *Coordinated Control of The Zero Inertia Powertrain*. PhD thesis, Technische Universiteit Eindhoven, 2001.

[26] SERRARENS, A., DASSEN, M., , AND STEINBUCH, M. Simulation and control of an automotive dry clutch. *Proceedings of the 2004 American Control Conference* (2004).

[27] SHARKE, P. Smooth body. *Mechanical Engineering 10/1999* (1999).

[28] SHIH ET AL., S. Drivetrain noise and vibration troubleshoooting. *SAE paper 2001-01-2809* (2001).

[29] TAI ET AL., C. Increasing torque output from a turbodiesel with camless valvetrain. *SAE-paper 2001-01-1108* (2001).

[30] W., M., AND M., B. *Cradle to Cradle: Remaking the Way We Make Things*. North Point Press, 2002.

[31] ZAREMBDA, A., AND DAVIS, R. Control design for active engine damping using a starter/alternator. *Proceedings of the American Control Conference* (2000).

[32] ZEYEN ET AL., K. Isad - a computer controlled integrated starter-alternator-damper-system. *SAE-paper 972660* (1997).

Appendix A

Abbreviations, symbols and subscripts

Abbreviations

Abbreviation	Definition
$ACEA$	European Automobile Manufacturers Association
AMT	Automated Manual Transmission
$BMEP$	Brake Mean Effective Pressure
CVT	Continuously Variable Transmission
DMF	Dual Mass Flywheel
DOF	Degree Of Freedom
EPA	U.S. Environmental Protection Agency
$IMEP$	Indicated Mean Effective Pressure
$ISAD$	Integrated Starter Alternator Damper
MFR	Magnitude Frequency Response
MPG	Miles Per Gallon
MT	Manual Transmission
$NEDC$	New European Drive Cycle
NVH	Noise Vibration Harshness
PFR	Phase Frequency Response
TD	Torsion Damper
WOT	Wide Open Throttle

Symbols - Greek

Symbol	Definition	Unit
α	gradient	[rad]
β	conrod angle	[rad]
γ	specific heat ratio	[-]
θ	angle	[rad]
λ	crank - conrod ratio	[-]
μ	friction coefficient	[-]
ρ	density	[kg/m^3]
ϕ	phase shift	[rad]
ω	angular speed	[rad/s]

Symbols - Roman

Symbol	Definition	Unit
d	damping	[Nms/rad]
w	specific engine work	$[J/dm^3]$
r	ratio	[-]
k	stiffness	[N/m or Nm/rad]
l	length	[m]
m	mass	[kg]
n	speed	[rpm]
p	pressure [bar]	
D	diameter	[m]
J	inertia	$[kgm^2]$
R	radius	[m]
T	torque	[Nm]
V	volume	$[m^3]$
W	work	$[J/dm^3]$

Subscript

Symbol	Definition
b	brake
c	clutch
$crank$	crankshaft
$disp$	displacement
ds	driveshaft
e	engine
ex	excitation
f	flywheel
fd	final drive
$fluc$	fluctuation
$fric$	friction
g	gas
$grad$	gradient
i	inertia
p	primary
r	roll
rec	reciprocating
rot	rotor
s	secondary
t	transmission
td	torsion damper
v	vehicle
w	wheel

Appendix B

Engine vibrations

This appendix describes the dynamic engine torque, used as excitation source for the time domain simulation. There are 3 methods to acquire the dynamics engine torque, needed to obtain the responses of the powertrain.

1. Measure the dynamic torque on an existing engine by adding a torque sensor at the crankshaft.

2. Obtain dynamic torque data form literature.

3. Use an algorithm to create an dynamic torque curve.

Measuring the engine torque requires test facilities and an engine which can deactivated cylinders. Measuring torque data for the entire speed and load range is time consuming. Data is also only applicable for similar engines, as the one used during the measurements. Torque data from literature 2 is often not sufficient enough to model the entire engine operating range. Using algorithms makes it possible to change the shape of the dynamic torque curve rather easily and is therefor preferred. It also is an easy method to transform into a model.

The dynamic engine torque is a combination of the gas pressure torque and inertia torque. In case of a deactivated cylinder the gas pressure torque is replaced by the air spring torque.

B.1   Inertia torque

The reciprocating parts in an internal combustion engine generate a torque due to constantly acceleration and deceleration of the reciprocating engine masses. The reciprocating engine mass m_{rec} consist of the piston mass m_{piston} and roughly one third of the conrod mass m_{conrod}. Because of the crank conrod mechanism, the reciprocating masses undergo both a primary and secondary motion, resulting in a odd looking sine wave, see figure B.1.

$$m_{rec} = m_{piston} + \frac{1}{3}m_{conrod} \tag{B.1}$$

The inertia torque T_i can be modeled with the Fourier algorithm ([4], [22] and [10]) from equation B.2, where R_{crank} represents the crank radius.

$$T_i(\theta) = m_{rec}R_{crank}^2\omega_e^2(C_1 sin\theta + C_2 sin2\theta + C_3 sin3\theta + ...) \tag{B.2}$$

The coefficients C_1, C_2 and C_3 are defined below, with λ being the conrod/crankthrow ratio as defined in equation B.4.

$$C_1 = \frac{1}{4}\lambda + \frac{1}{16}\lambda^3 + \frac{15}{512}\lambda^5 + ...$$
$$C_2 = -\frac{1}{2} - \frac{1}{32}\lambda^4 - \frac{1}{32}\lambda^6 - ...$$
$$C_3 = -\frac{3}{4}\lambda - \frac{9}{32}\lambda^3 - \frac{81}{512}\lambda^5 ...$$

$$\tag{B.3}$$

$$\lambda = \frac{R_{crank}}{l_{conrod}} \tag{B.4}$$

When multiple cylinders are used, equation B.2 is extended to:

$$T_i(\theta) = m_{rec} R_{crank}^2 \omega_e^2 \sum_{j=1}^{N_c} (C_1 sin(\theta + \phi_j) + C_2 sin2(\theta + \phi_j) + C_3 sin3(\theta + \phi_j) + ...) \tag{B.5}$$

with ϕ_j the relative crank throw angle relative to cylinder 1.

$$\phi_1 = 0$$
$$\phi_2 = \pi$$
$$\phi_3 = \pi$$
$$\phi_4 = 0$$

$$\tag{B.6}$$
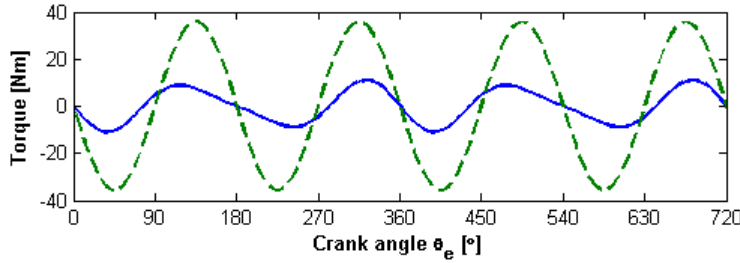
Figure B.1: 1 cylinder inertia torque (solid -) compared to the combined 4 cylinder inertia torque (dashed - -), for 2 revolutions at 2000 [RPM]

As can be seen in equation B.5, the inertia torque is proportional to ω^2. Figure B.1 shows the inertia torque for one cylinder and 4 cylinders at 2000 [RPM]. The combined 4 cylinder inertia torque shows a perfect sine wave while the 1 cylinder inertia torque shows a somewhat disturbed sine wave with a lower magnitude. The nett energy in both cases is zero because of the average zero inertia torque.

B.2 Gas pressure torque

The gas pressure torque is a result of the gas pressure working on top of the piston, incorporating the combustion pressure, compression and gas exchange pressures. The gas pressure torque can be modeled by a Fourier algorithm, equation B.7. Several engine load conditions can be simulated by varying the average engine torque T_{mean}. The shape of the engine torque depends on the used engine and is adjustable by changing the coefficients U_n and V_n. Figure B.2 shows the harmonic coefficients U_n and V_n (from [22]), representing a 1.6L gasoline engine.

$$T_g(\theta) = T_{mean}(1 + \sum_{n=\frac{1}{2},1,1\frac{1}{2},...}^{n=\infty} U_n \sin(n\theta) + V_n cos(n\theta)) \tag{B.7}$$

If multiple cylinders are being used equation B.7 can be changed into equation B.8, with α_j being the firing distance. For a 4 cylinder 4 stroke engine the firing distance is evenly spaced with an interval of π and an firing order of 1342.

$$T_g(\theta) = \sum_{j=1}^{N_c} T_{mean}(1 + \sum_{n=\frac{1}{2},1,1\frac{1}{2},...}^{n=\infty} U_n \sin(n(\theta + \alpha_j)) + V_n cos(n(\theta + \alpha_j))) \tag{B.8}$$

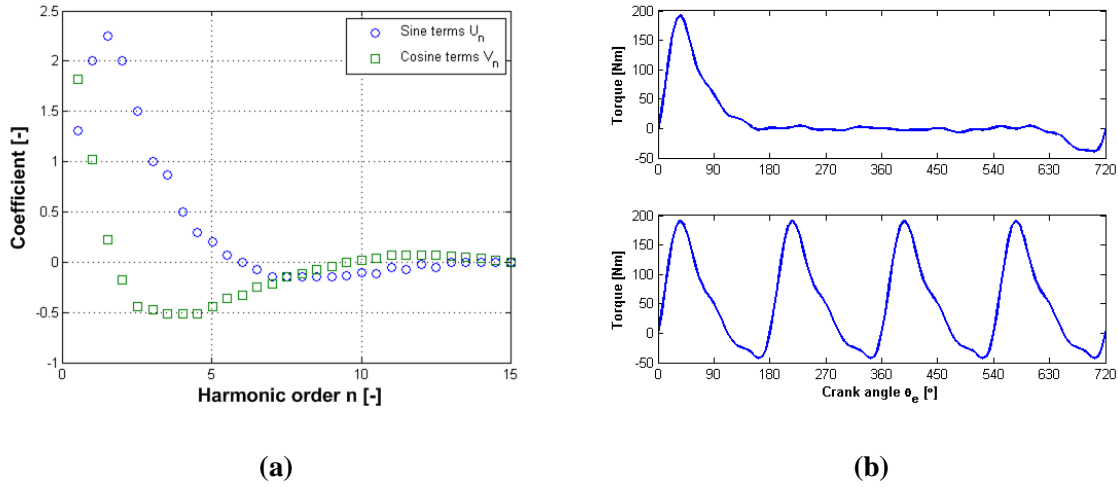(a)   (b)

*Figure B.2: (**a**) Harmonic coefficients U_n and V_n for determining the gas pressure torque. (**b**) Gas pressure torque of one cylinder (above) and gas pressure torque of 4 combined cylinders (below).*

with α_j:

$$\alpha_1 = 0$$
$$\alpha_2 = 3\pi$$
$$\alpha_3 = \pi$$
$$\alpha_4 = 2\pi$$

(B.9)

B.3   Air spring torque

During cylinder deactivation the intake and exhaust valves remain closed, letting the cylinder function as an air spring. The deactivated cylinders will complete periodically a compression stroke followed by an expansion stroke. The expansion and compression pressure will result in a periodic torque pulsation. The transformation from cylinder pressure to air spring torque is explained by equations B.10 to B.18. Figure B.3 gives the graphical representation of these equations.

$$F_{piston} = p_{piston} \frac{\pi}{4} D_{piston}^2$$

(B.10)

$$F_t = \frac{F_{piston} \sin(\theta + \beta)}{\cos \beta}$$

(B.11)

$$T_{spring} = \frac{p_{piston} \frac{\pi}{4} D_{piston}^2 R_{crank} \sin(\theta + \beta)}{\cos \beta}$$

(B.12)

The compression and expansion stroke are both described by a reversible and isentropic (adiabatic) process, where no heat transfer and blow-by is taken into consideration in order to simplify the model. The isentropic process can be modeled with equation B.13, where p_1 and p_{piston} are the compression start and compression end pressures, ϵ is the compression ratio and γ the specific heat ratio of the exhaust gas.

$$p_{piston}(\theta) = p_1 \epsilon^\gamma(\theta)$$

(B.13)

$$\epsilon(\theta) = \frac{V_{cylinder}}{V_{cylinder} - V_{disp}(\theta)}$$

(B.14)

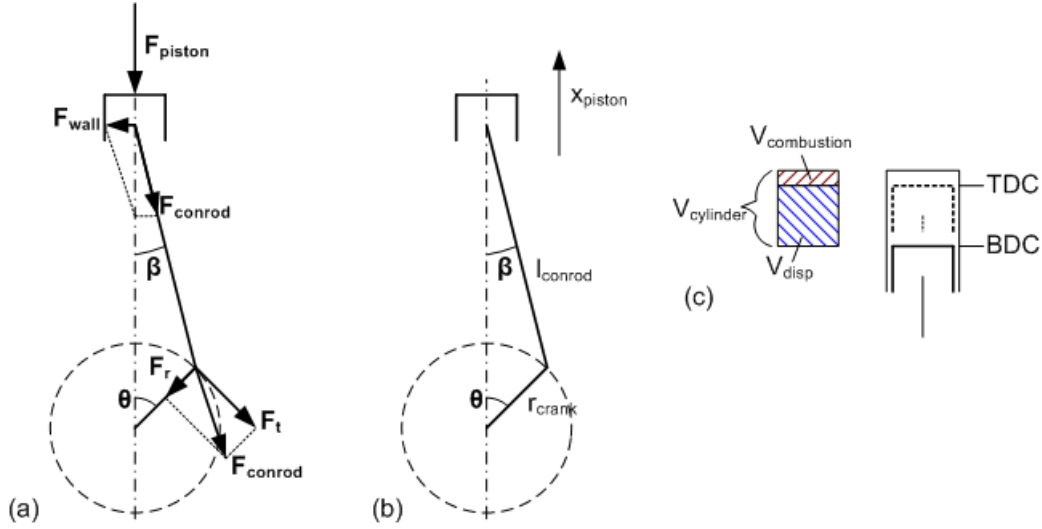$$V_{disp}(\theta) = x_{piston}(\theta) \frac{\pi}{4} D_{piston}^2$$

(B.15)

Figure B.3: Piston force diagram

$$x_{piston}(\theta) = R_{crank} \cos\theta + l_{conrod} \cos(\beta) \tag{B.16}$$

$$\beta = \arcsin(\lambda \sin\theta) \tag{B.17}$$

Substituting equations B.13 to B.17 into equation B.12 gives the following equation:

$$T_{spring} = \frac{p_1 \left(\dfrac{V_{cylinder}}{V_{cylinder} - \frac{\pi}{4} D_{piston}^2 (R_{crank} \cos\theta + l_{conrod} \cos(\arcsin(\lambda \sin\theta)))} \right)^{\gamma} R_{crank} \sin(\theta + \arcsin(\lambda \sin\theta))}{\cos(\arcsin(\lambda \sin\theta))} \tag{B.18}$$

Figure B.4 shows the resulting air spring torque. The specific heat ratio γ is considered constant during expansion and compression at 1.3 [-], the engines static compression ratio is defined to be 10 [-], which is an acceptable value for an Otto engine.
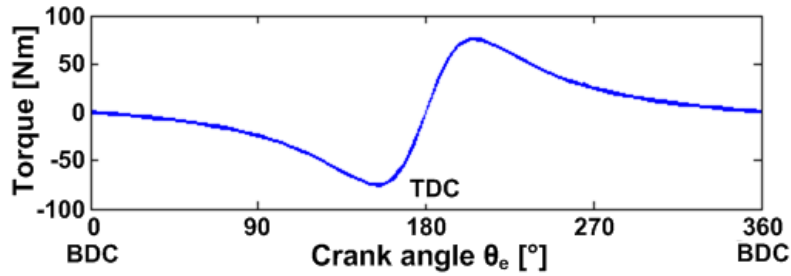
Figure B.4: Air spring torque of a deactivated cylinder, for one engine revolution.

Engine torque T_e is the sum of the inertia torque T_i, gas pressure torque T_g and the air spring torque T_{spring}.

B.4   Boxer versus inline engine

When comparing a 4 cylinder boxer engine with a 4 cylinder inline engine, figure B.5 and B.6, it becomes clear that both engines have two pistons going from bottom death center (BDC) to top death center (TDC) and two pistons going from TDC to BDC. The rotational forces caused by the inertia torque and gas pressure torque is therefor equal for both engines.

The rotational vibrational analysis as executed in this report is therefor valid for both boxer and inline 4 cylinder engine.
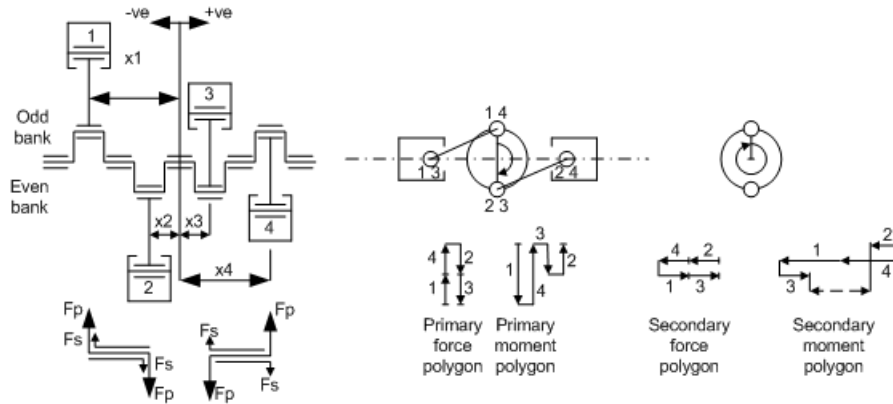

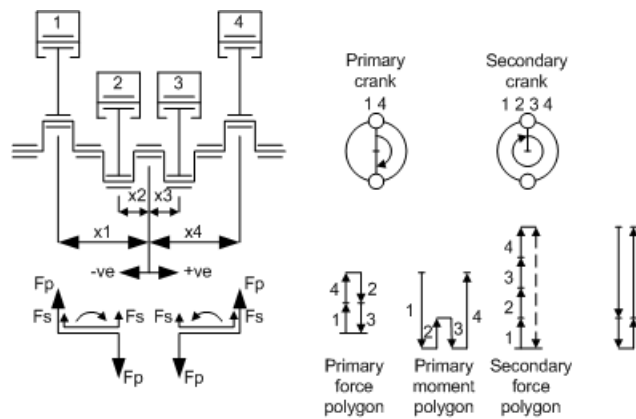*Figure B.5: Force balance diagram of a 4 cylinder boxer engine (from [13]).*

Figure B.6: Force balance diagram of a 4 cylinder inline engine (from [13]).

Figure B.5 and B.6 show the force balance of the primary and secondary inertia forces. The primary motion is caused by the reciprocating the reciprocating motion of the piston, while the secondary force is caused by the swinging motion of the conrod.

The primary fores of the boxer engine are completely balanced. The secondary forces however cause a moment around the vertical axis, perpendicular to the crankshaft and cylinders. This moment can be minimized by minimizing the center bore distance between the cylinders. Typically small balance weights are used to reduce the bending stress caused by this moment.

The primary forces of the inline engine also are balanced out completely. The secondary forces are directed in the same direction. causing a vertical vibration of the entire engine (engine shake).

Appendix C

Powertrain models

A powertrain model consist of continuous (in time) and discrete states (one fixed state). Such a system is called a hybrid dynamical system. In the case of the powertrain model, the hybridization is caused by the following discrete events, states and inputs:

1. Engine speed is constrained between 500 [RPM] and 6000 [RPM]

2. The engine torque is constrained between the drag torque and the torque at wide open throttle (WOT)

3. The plate clutch can be disengaged, engaged or slipping

4. Transmission ratio is determined by six discrete ratios

5. Tire-road interaction is described for driving and driven wheels

Changing to another discrete state in a model can cause difficulties and increase the complexity of the model. In order to reduce the complexity of the model only the situation with an engaged clutch is investigated. Cylinder deactivation also only applies to the situation where the wheels are driving the vehicle, so only the tire-road interaction is only of interest during driving.

The entire powertrain can be described by a set of first order differential equations, linear or non-linear.

C.1 TD powertrain model

Powertrain unit and mounts

$$J_b \dot{\omega}_b = T_m - T_e - T_{react} + d_e \omega_e \tag{C.1}$$

$$T_{react} = T_{td}(\frac{1}{r_i r_{fd}} - 1) \tag{C.2}$$

$$\dot{T}_m = -k_m \omega_b - d_m \dot{\omega}_b \tag{C.3}$$

Engine

$$J_e \dot{\omega}_e = T_e - T_{td} - d_e \omega_e \tag{C.4}$$

$$T_e = T_g + T_i + T_{spring} \tag{C.5}$$

Torsion damper

$$\dot{T}_{td} = k_{td}(\omega_e - (\omega t + \omega_b)) + d_{td}(\dot{\omega}_e - (\dot{\omega}_t \dot{\omega}_b)) \tag{C.6}$$

Transmission

$$J_t \dot{\omega}_t = T_{td} - T_{ds} r_i r_{fd} - d_t \omega_t \tag{C.7}$$

$$J_t = J_p + J_s r_i^2 + J_{fd} r_i^2 r_{fd}^2 \tag{C.8}$$

Driveshafts

$$\dot{T}_{ds} = k_{ds}((\omega_t r_i r_{fd} + \omega_b) - \omega_w) \tag{C.9}$$

Wheels and tires

$$2J_w \dot{\omega}_w = T_{ds} - FR_w - T_{rr} \tag{C.10}$$

$$F_w = b_w m_{vr} g \cos(\alpha_{grad})(1 - \frac{v_v}{\omega_w R_w}) \tag{C.11}$$

Vehicle

$$(m_v + 2J_w/R_w^2)\dot{v}_v = F_w - \frac{T_{rf}}{R_w} - c_v v_v^2 - m_v g \sin(\alpha_{grad}) \tag{C.12}$$

Linearized model

With the obtained equations of motions, a set of linearized differential equations can be put in state space form:

$$\dot{x}(t) = f(x(t)) + Bu(t) \tag{C.13}$$

Vector x is represented by the system states and the external input vector is defined as u.

$$x = [\omega_b, T_m, \omega_e, T_{td}, \omega_t, T_{ds}, \omega_w, v_v]^T$$
$$u = [T_e]$$
$$\tag{C.14}$$

and with equations C.26 to C.34

$$\dot{\omega}_b = \frac{T_m - T_e + d_e \omega_e - T_{react}}{J_b} \tag{C.15}$$

$$\dot{T}_m = -k_m \omega_b - d_m \dot{\omega}_b \tag{C.16}$$

$$\dot{\omega}_e = \frac{T_e - T_{td} - d_e \omega_e}{J_e} \tag{C.17}$$

$$\dot{T}_{td} = k_{td}(\omega_e - \omega_t) + d_{td}(\dot{\omega}_e - \dot{\omega}_t) \tag{C.18}$$

$$\dot{\omega}_t = \frac{T_{td} - T_{ds} r_i r_{fd} - d_t \omega_t}{J_t} \tag{C.19}$$

$$\dot{T}_{ds} = k_{ds}(\omega_t r_i r_{fd} - \omega_w) \tag{C.20}$$

$$\dot{\omega}_w = \frac{T_{ds} - F_w R_w - T_{rr}}{2J_w} \tag{C.21}$$

$$\dot{v}_v = \frac{F_w - c_v v_v^2}{m_v + 2J_w/R_w^2} \tag{C.22}$$

Because the differential equations are not linear, linearisation around a nominal trajectory is necessary. The pertubations δx and δu around the stationary state x_0 with input u_0 are assumed to be small enough to remain in close proximity of the equilibrium state x_0. Therefor the dynamics of these pertubations may be described as the first order approximation [21].

$$\dot{\tilde{x}}(t) = \frac{\partial f}{\partial x}|_{\tilde{x}(t),\tilde{u}(t)}\tilde{x}(t) + \frac{\partial f}{\partial u}|_{\tilde{x}(t),\tilde{u}(t)}\tilde{u}(t) = A(t)\tilde{x}(t) + B(t)\tilde{u}(t) \tag{C.23}$$

Matrix $A(t)$ is determined by:

$$A(t) = \frac{\partial f}{\partial x}|_{\tilde{x}(t),\tilde{u}(t)} = () \tag{C.24}$$

The linearization is done around a stationary point, so the matrices become constant as seen in equation C.25

$$A(t) = A, \, B(t) = B \tag{C.25}$$

$$A(1,1) = 0$$

$$A(1,2) = \frac{1}{J_b}$$

$$A(1,3) = \frac{d_e}{J_b}$$

$$A(1,4) = -\frac{1-r_i}{/}J_b$$

$$A(1,5) = 0$$

$$A(1,6) = -\frac{1-r_{fd}}{J_b}$$

$$A(1,7..8) = 0$$

$$A(2,1) = -k_m$$

$$A(2,2) = -\frac{d_m}{J_b}$$

$$A(2,3) = -\frac{d_m d_e}{J_b}$$

$$A(2,4) = \frac{d_m(1-r_i)}{J_b}$$

$$A2,5 = 0$$

$$A(2,6) = \frac{d_m(1-r_{fd})}{J_b}$$

$$A(2,7..8) = 0$$

$$A(3,1..2) = 0$$

$$A(3,3) = -\frac{d_e}{J_e}$$

$$A(3,4) = -\frac{1}{J_e}$$

$$A(3,5..8) = 0$$

$$A(4,1) = -k_{td}$$

$$A(4,2) = -\frac{d_{td}}{J_b}$$

$$A(4,3) = k_{td} - \frac{d_{td}d_e}{J_e} - \frac{d_{td}d_e}{J_b}$$

$$A(4,4) = -\frac{d_{td}}{J_e} - \frac{d_{td}}{J_t} + \frac{d_{td}(1-r_i)}{J_b}$$

$$A(4,5) = -k_{td} + \frac{d_{td}d_t}{J_t}$$

$$A(4,6) = \frac{d_{td}r_i r_{fd}}{J_t} + \frac{d_{td}(1-r_{fd})}{J_b}$$

$$A(4,7..8) = 0$$

$$A(5,1..3) = 0$$

$$A(5,4) = \frac{1}{J_t}$$

$$A(5,5) = -\frac{d_t}{J_t}$$

$$A(5,6) = -\frac{r_i r_{fd}}{J_t}$$

$$A(5,7..8) = 0$$

$$A(6,1) = k_{ds}$$

$$A(6,2..4) = 0$$

$$A(6,5) = k_{ds}r_i r_{fd}$$

$$A(6,6) = 0$$

$$A(6,7) = -k_{ds}$$

$$A(6,8) = 0$$

$$A(7,1..5) = 0$$

$$A(7,6) = \frac{1}{2J_w}$$

$$A(7,7) = -\frac{b_w v_{v0} m_{vr} g \cos\alpha_{grad}}{2J_w \omega_{w0}^2}$$

$$A(7,8) = \frac{b_w m_{vr} g \cos\alpha_{grad}}{2J_w \omega_{w0}}$$

$$A(8,1..6) = 0$$

$$A(8,7) = \frac{R_w b_w v_{v0} m_{vr} g \cos\alpha_{grad}}{(m_v R_w^2 + 2J_w)\omega_{w0}^2}$$

$$A(8,8) = -\frac{b_w R_w m_{vr} g \cos\alpha_{grad} + 2c_v R_w^2 v_{v0}\omega_{w0}}{(m_v R_w^2 + 2J_w)\omega_{w0}}$$

$$B(1,1) = -\frac{1}{J_b}$$

$$B(2,1) = \frac{d_m}{J_b}$$

$$B(3,1) = \frac{1}{J_e}$$

$$B(4,1) = \frac{d_{td}}{J_e} + \frac{d_{td}}{J_b}$$

$$B(5..8,1) = 0$$

C.2   ISAD powertrain model

Powertrain unit and mounts

$$J_b \dot{\omega}_b = T_m - T_e - T_{react} + (d_e + d_t)\omega_e \tag{C.26}$$

$$T_{react} = T_{ds}(1 - r_i r_{fd}) \tag{C.27}$$

$$\dot{T}_m = -k_m \omega_b - d_m \dot{\omega}_b \tag{C.28}$$

Engine

$$T_{ISAD} = d_{isad}(\omega_e(t) - \omega_{e0}) \tag{C.29}$$

$$(J_e + J_t)\dot{\omega}_e = T_e - T_{ds} - (d_e + d_t)\omega_e - T_{ISAD} \tag{C.30}$$

Driveshafts

$$\dot{T}_{ds} = k_{ds}((\omega_t r_i r_{fd} + \omega_b) - \omega_w) \tag{C.31}$$

Wheels and tires

$$2J_w \dot{\omega}_w = T_{ds} - F_w R_w - T_{rr} \tag{C.32}$$

$$F_w = b_w m_{vr} g \cos(\alpha_{grad})(1 - \frac{v_v}{\omega_w R_w}) \tag{C.33}$$

Vehicle

$$(m_v + 2J_w/R_w^2)\dot{v}_v = F_w - \frac{T_{rf}}{R_w} - c_v v_v^2 - m_v g \sin(\alpha_{grad}) \tag{C.34}$$

Linearized model

Due to the lack of a TD, the state vector is reduced to:

$$x = [\omega_b, T_m, \omega_e, T_{ds}, \omega_w, v_v]^T \tag{C.35}$$

$$\dot{\omega}_b = \frac{T_m - T_e + (d_e + d_t)\omega_e - T_{react}}{J_b} \tag{C.36}$$

$$\dot{T}_m = -k_m \omega_b - d_m \dot{\omega}_b \tag{C.37}$$

$$\dot{\omega}_e = \frac{T_e - T_{ds} - (d_e + d_t)\omega_e - d_{isad}(\omega_e(t) - \omega_{e0})}{J_e + J_t} \tag{C.38}$$

$$\dot{T}_{ds} = k_{ds}(\omega_e r_i r_{fd} - \omega_w) \tag{C.39}$$

$$\dot{\omega}_w = \frac{T_{ds} - F_w R_w - T_{rr}}{2J_w} \tag{C.40}$$

$$\dot{v}_v = \frac{F_w - c_v v_v^2}{m_v + J_w/R_w^2} \tag{C.41}$$

The matrices A and B become:

$$A(1, 1) = 0$$

$$A(1, 2) = \frac{1}{J_b}$$

$$A(1, 3) = \frac{d_e + d_t}{J_b}$$

$$A(1, 4) = -\frac{1 - r_i r_{fd}}{J_b}$$

$$A(1, 5..6) = 0$$

$$A(2, 1) = -k_m$$

$$A(2, 2) = -\frac{d_m}{J_b}$$

$$A2, 3 = -\frac{d_m(d_e + d_t)}{J_b}$$

$$A(2, 4) = \frac{d_m(1 - r_i r_{fd})}{J_b}$$

$$A(2, 5..6) = 0$$

$$A(3, 1..2) = 0$$

$$A(3, 3) = -\frac{d_e + d_t}{J_e + J_t} - \frac{d_{isad}}{J_e + J_t}$$

$$A(3, 4) = -\frac{1}{J_e + J_t}$$

$$A(3, 5..6) = 0$$

$$A(4, 1) = k_{ds}$$

$$A(4, 2) = 0$$

$$A(4, 3) = k_{ds} r_i r_{fd}$$

$$A(4, 4) = 0$$

$$A(4, 5) = -k_{ds}$$

$$A(4, 6) = 0$$

$$A(5, 1..3) = 0$$

$$A(5, 4) = \frac{1}{2J_w}$$

$$A(5, 5) = -\frac{b_w v_{v0} m_{vr} g \cos \alpha_{grad}}{2J_w \omega_{w0}^2}$$

$$A(5, 6) = \frac{b_w m_{vr} g \cos \alpha_{grad}}{2J_w \omega_{w0}}$$

$$A(6, 1..4) = 0$$

$$A(6, 5) = \frac{R_w b_w v_{v0} m_{vr} g \cos \alpha_{grad}}{(m_v R_w^2 + 2J_{wheel}) \omega_{w0}^2}$$

$$A(6, 6) = -\frac{b_w R_w m_{vr} g \cos \alpha_{grad} + 2c_v R_w^2 v_{v0} \omega_{w0}}{(m_v R_w^2 + 2J_w) \omega_{w0}}$$

$$B(1, 1) = -\frac{1}{J_b}$$

$$B(2, 1) = \frac{d_m}{J_b}$$

$$B(3, 1) = \frac{1}{J_e + J_t}$$

$$B(4..6, 1) = 0$$

C.3   Model parameters

Variable	Description	Value	Unit
σ	Vehicle weight distribution with respect to front axle	0.5	$[-]$
ρ_{air}	Air density	1.2	$[kg/m^3]$
b_w	Tire-road friction coefficient	8.8	$[-]$
c_d	Drag coefficient	0.25	$[-]$
c_v	Air resistance constant	0.33	$[kg/m^2]$
d_e	Engine friction damping	0.19	$[Nms/rad]$
d_{isad}	ISAD damping constant	variable	$[Nms/rad]$
d_m	Powertrain mount damping constant	130	$[Nms/rad]$
d_{td}	Torsion damper damping	0.5	$[Nms/rad]$
d_t	Transmission friction damping	0.05	$[NMs/rad]$
g	Gravity constant	9.81	$[m/s^2]$
k_{ds}	Driveshaft stiffness	6200	$[Nm/rad]$
k_m	Powertrain mount stiffness	12000	$[Nm/rad]$
k_{td}	Torsion damper stiffness	1000	$[Nm/rad]$
m_v	Empty vehicle weight	850	$[kg]$
m_{vf}	Vehicle weight on front axle	σm_v	$[kg]$
m_{vr}	Vehicle weight on rear axle	$m_v - \sigma m_v$	$[kg]$
r_1	1st gear ratio	0.29	$[-]$
r_2	2nd gear ratio	0.43	$[-]$
r_3	3rd gear ratio	0.61	$[-]$
r_4	4th gear ratio	0.86	$[-]$
r_5	5th gear ratio	1.22	$[-]$
r_6	6th gear ratio	1.73	$[-]$
r_{fd}	Final gear ratio	0.23	$[-]$
x_l	Tire deformation length	0.0027	$[m]$
A_v	Frontal area	2.05	$[m^2]$
J_b	Powertrain unit inertia	12	$[kgm^2]$
J_e	Engine flywheel inertia	0.1	$[kgm^2]$
J_p	Primary transmission inertia	$9e^{-4}$	$[kgm^2]$
J_s	Secondary transmission inertia	varying	$[kgm^2]$
J_w	Wheel inertia	0.85	$[kgm^2]$
R_w	Wheel rolling radius	0.3	$[m]$

Table C.1: Numerical parameters for the TD and ISAD models. Data based upon the requirements for the "car of the future".

Appendix D

Frequency information

D.1 Power Spectral Density

The PSD (Power Spectral Density) figures show the engine input torque and the excitation modes the signal contains. The average engine torque is 50 [Nm] for all 5 systems. Lowering the average engine torque changes the modes due to the increasing influence of the inertia torque, which together with the gas pressure torque can result in increased modes.
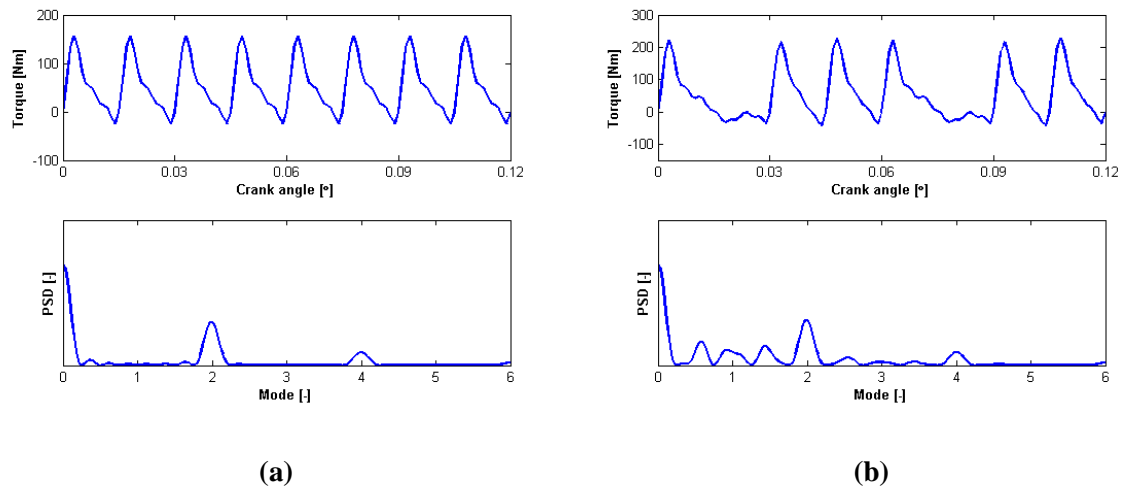

(a)   (b)

Figure D.1: Frequency content of the engine torque T_e for (a) 4 active cylinders (System 1234) and (b) 3 active cylinders (System 134).
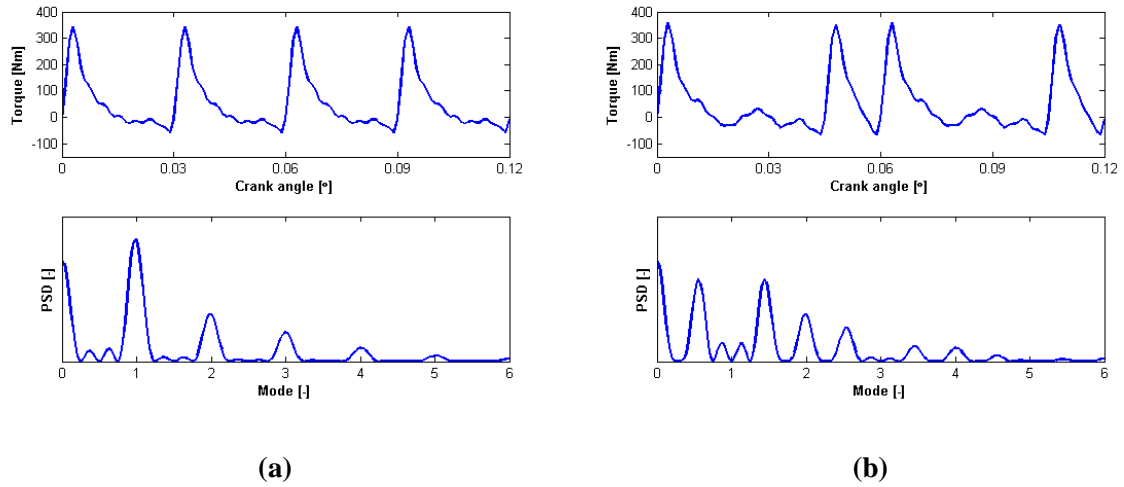
*Figure D.2: Frequency content of the engine torque T_e for (**a**) 2 active cylinders (System 14) and (**b**) 2 active cylinders (System 13).*
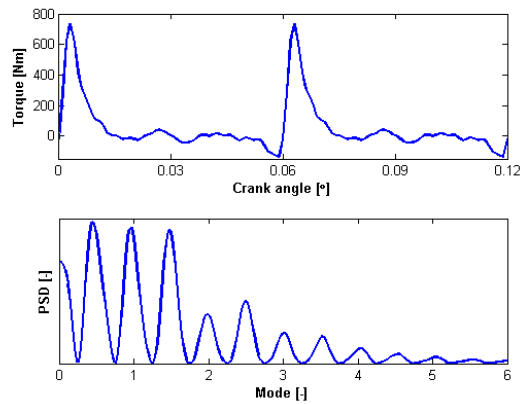
Figure D.3: Frequency content of the engine torque T_e for 1 active cylinder (System 1)

Appendix E

Frequency response results

The initial frequency response comparison between the TD setup and the ISAD setup showed that the first powertrain resonance shifted upwards in the case of the ISAD powertrain. The eigenfrequency felt inside the frequency band during deactivation. The reason for the shift is the reduced rotating engine inertia due to the lower rotor inertia compared to the flywheel inertia for the TD. The inertia can be simply raised by adding an additional flywheel or other inertia to the ISAD rotor. This can only be done at the cost of added weight, cost and build space and therefor is not desired. By investigating the influence of other vehicle parameters knowledge is gathered about the influence of these parameters and something can be said about how to suppress the resonances.

E.1 Parameters influence

The frequency responses of figures 7.1 to 7.2 are only correct for one operating condition, namely 5th gear, and for the used driveshaft stiffness, inertias etc. Powertrain parameters obviously have an influence on the dynamic behavior of the powertrain. It is of great value to know how these parameters will influence the dynamics, so that the correct parameters can be changed to improve the dynamic behavior if necessary. All responses are taken in 5th gear unless stated differently. Responses are obtained from models without powertrain mounts. The powertrain unit mounts cause a resonance frequency, which can interfere with other resonances. By leaving this mount resonance out, changes caused by other parameters are better visible.

E.1.1 Transmission ratio

Changing the gear ratio has influence on the lumped transmission inertia, explained by equation 6.8. Figure E.1 shows that the 1st resonance frequency increases, while the 2nd resonance frequency decreases when the transmission ratio is increased. Also the magnitude of the first resonance frequency raises with increasing ratio while the second resonance magnitude drops slightly with increasing ratio. The resonance frequency of the ISAD powertrain also increases with increased ratio, figure E.2. Typical values for driveshaft resonance lies between 1-10 $[Hz]$ ([4]) which is the case for these ratios apart from 6th gear, due to the relative high ratio.
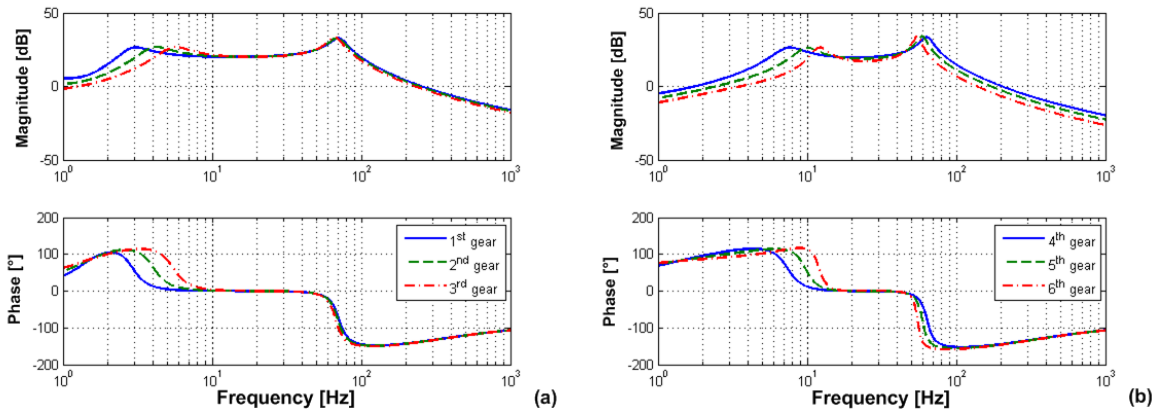
*Figure E.1: Frequency response of T_e to $\dot{\omega}_t$ for (**a**) ratios 1, 2 and 3 of the TD powertrain and (**b**) for ratios 4, 5 and 6 of the TD powertrain.*
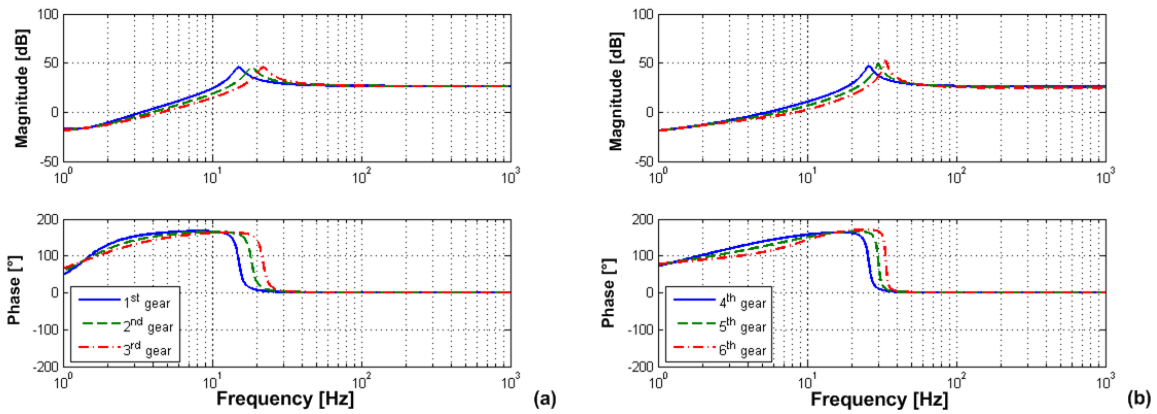

*Figure E.2: Frequency response of T_e to $\dot{\omega}_t$ for (**a**) ratios 1, 2 and 3of the ISAD powertrain and (**b**) for ratios 4, 5 and 6 of the ISAD powertrain.*

E.1.2   Vehicle mass

The vehicle mass is targeted at 950 [kg], including the driver and fluids with a maximum payload of 400 [kg]. The bode plots show that the vehicle mass only has a slight influence on the response, as can be seen in figure E.3. At low frequencies the loaded vehicle has a marginally better suppression. The FRF is obtained at 2000 RPM in 5th gear.
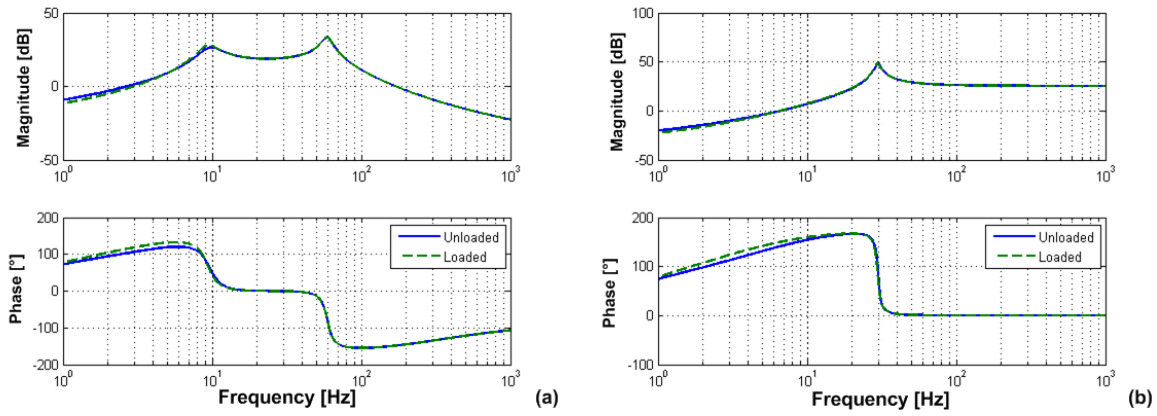
Figure E.3: *(a) Frequency response of T_e to $\dot{\omega}_t$ for unloaded en loaded vehicle of the TD powertrain. (b) Frequency response of T_e to $\dot{\omega}_t$ for unloaded en loaded vehicle of the ISAD powertrain.*

E.1.3   Powertrain inertia

Figures E.4 to E.6 show the influence of the engine inertia, transmission inertia and wheel inertia on the response. Inertias are 50% increased.

Increasing the engine inertia shifts the 1st resonance frequency of the TD powertrain down. The magnitudes at higher frequencies is slightly lower. The ISAD powertrain also shows a lower resonance frequency and reduced magnitudes after the eigenfrequency.

Increasing the transmission inertia shifts the 2nd resonance frequency of the TD powertrain down. The magnitude of the 1st resonance frequency is increased, while the magnitude at high excitation frequencies is lowered. The transmission inertia is relatively small compared to the engine inertia, therefor increasing the transmission inertia has little effect Increasing the wheel inertia has a larger effect on the ISAD powertrain compared to the TD powertrain.
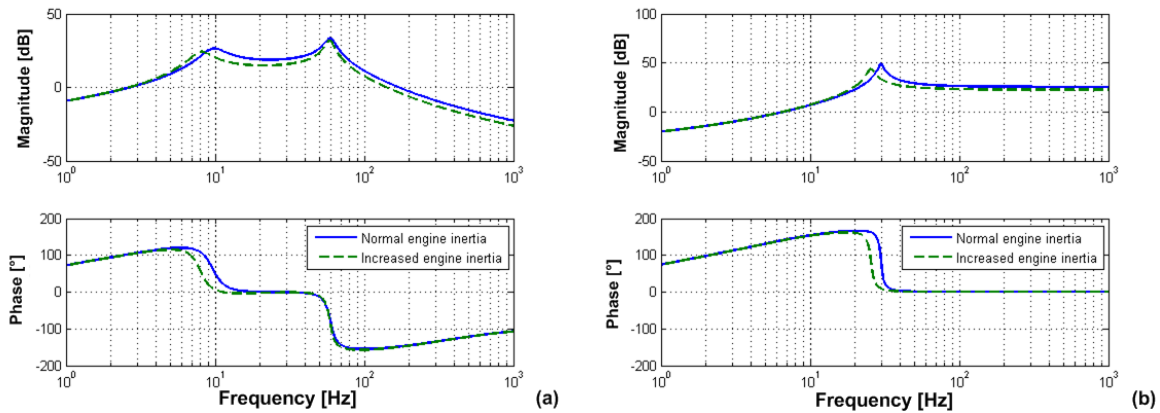
Figure E.4: Frequency response of T_e to $\dot{\omega}_t$ for engine inertia of (a) the TD powertrain and (b) the ISAD powertrain.
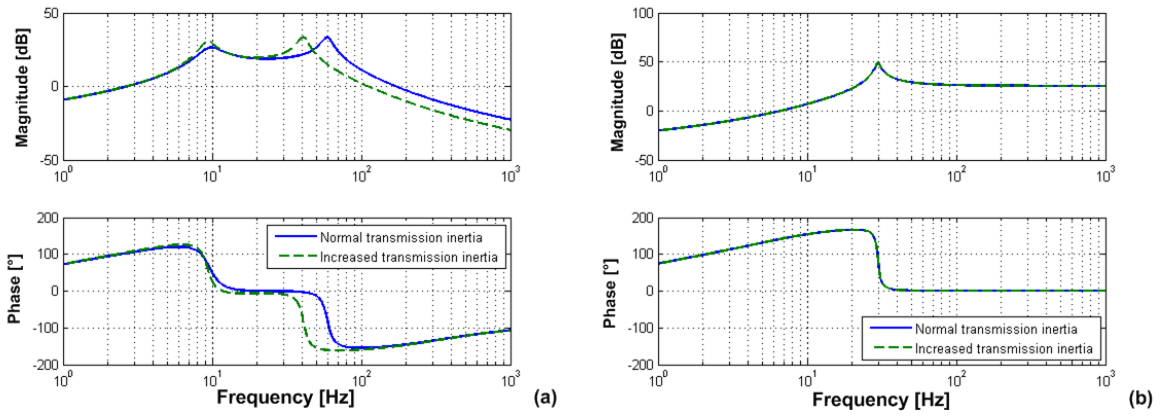
*Figure E.5: Frequency response of T_e to $\dot{\omega}_t$ for transmission inertia of (**a**) the TD powertrain and (**b**) the ISAD powertrain.*
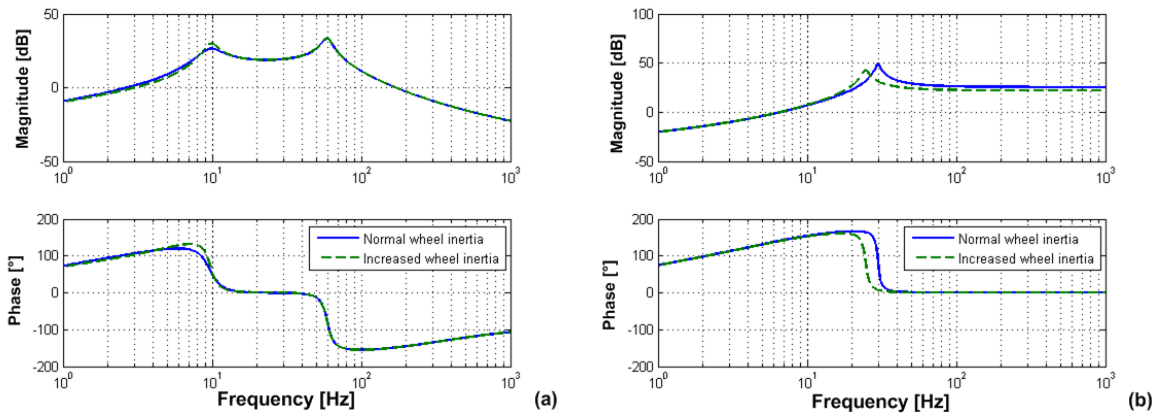
*Figure E.6: Frequency response of T_e to $\dot{\omega}_t$ for wheel inertia of (**a**) the TD powertrain and (**b**) the ISAD powertrain.*

E.1.4 Torsion damper

Increasing the stiffness of the torsion damper increases the 2nd resonance frequency of the TD powertrain. Increasing the damping of the torsion damper reduces the magnitude of the 2nd resonance frequency of the TD powertrain, see figure E.7.
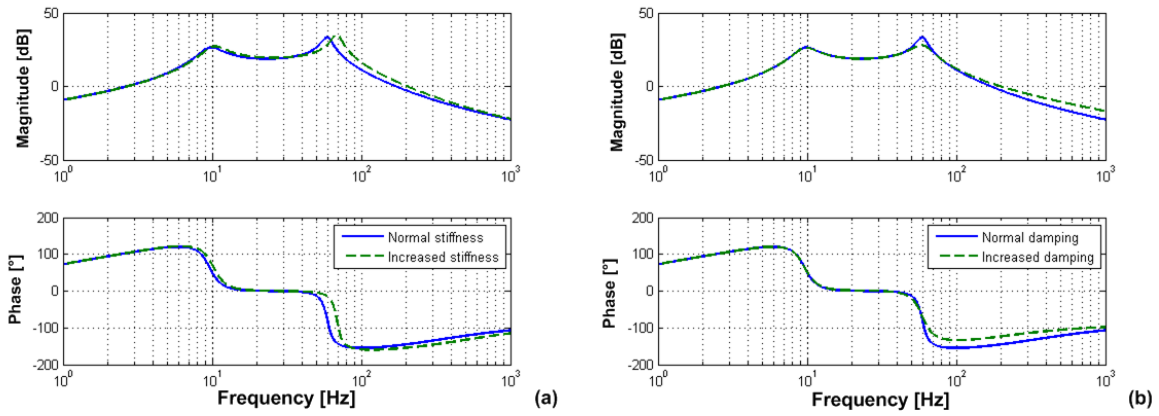
*Figure E.7: Frequency response of T_e to $\dot{\omega}_t$ for (**a**) change in torsion damper stiffness, (**b**) change in torsion damper damping of the TD powertrain.*

E.1.5   Driveshaft

Figure E.8 shows the effect of increasing the driveshaft stiffness. Both 1st and 2nd resonance frequencies are shifted upwards for the TD powertrain. The ISAD powertrain shows also an increased resonance frequency, figure E.8.
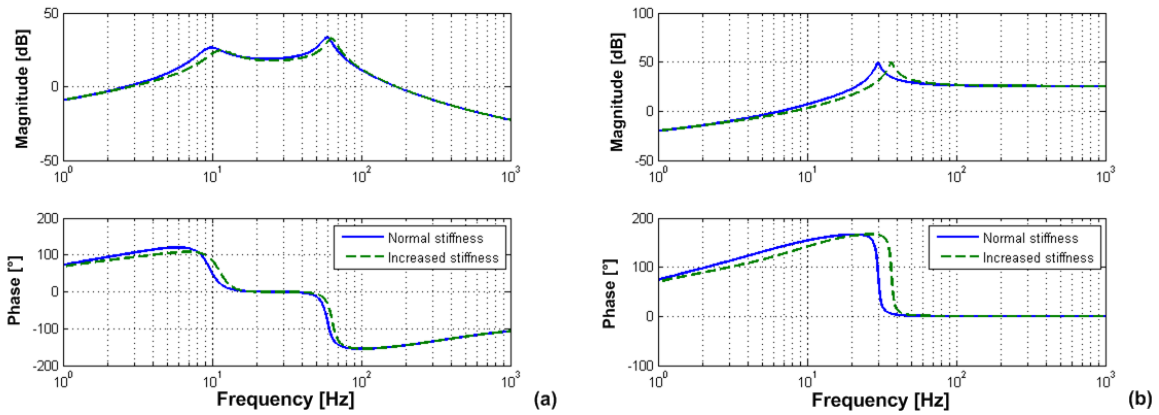
*Figure E.8: Frequency response of T_e to $\dot{\omega}_t$ for driveshaft stiffness of (**a**) the TD powertrain and (**b**) the ISAD powertrain.*

E.1.6 ISAD damper

Figure E.9 shows the effect of ISAD damping on the response. Due to ISAD damping the magnitude of the 1st resonance peak of the TD powertrain is reduced. The resonance peak of the ISAD powertrain also shows a reduction, figure E.9. Figure E.10 shows the response of T_e to ω_e and T_e to $\dot{v}_v$ for no damping and ISAD damping of the TD powertrain. The resonance peaks of the 1st resonance frequency are damped.
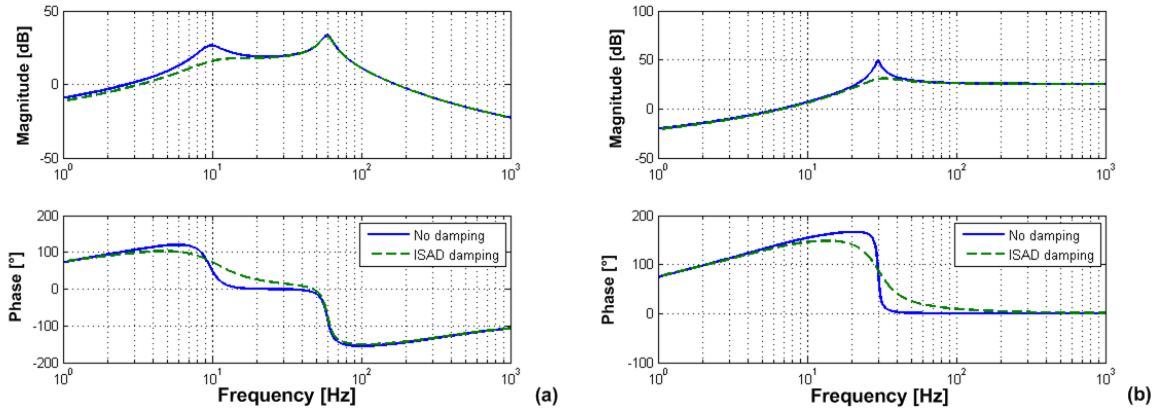
*Figure E.9: Frequency response of T_e to $\dot{\omega}_t$ for ISAD damping (**a**) the TD powertrain and (**b**) the ISAD powertrain.*
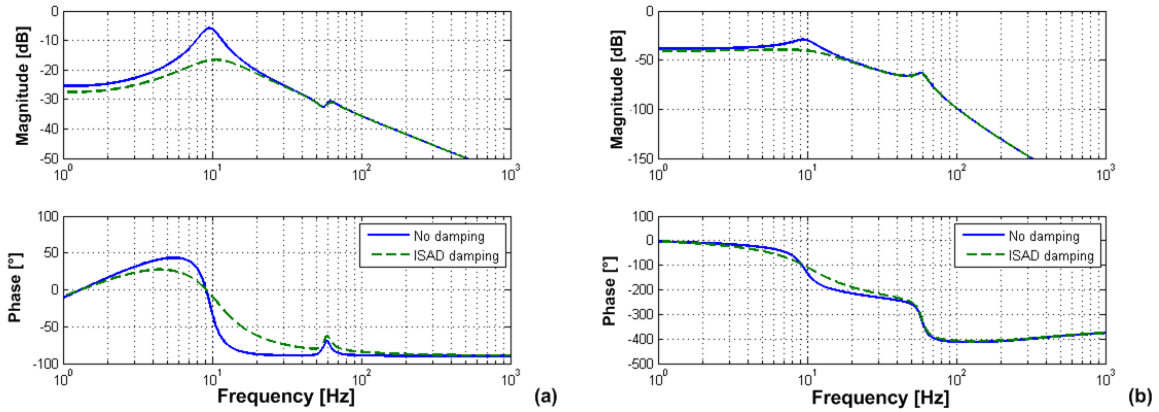
*Figure E.10: Frequency response showing the effect of ISAD damping for (**a**) T_e to ω_e and (**b**) T_e to $\dot{v}_v$ of the TD powertrain.*

Appendix F

Simulation results

F.1   Engine speed error plots
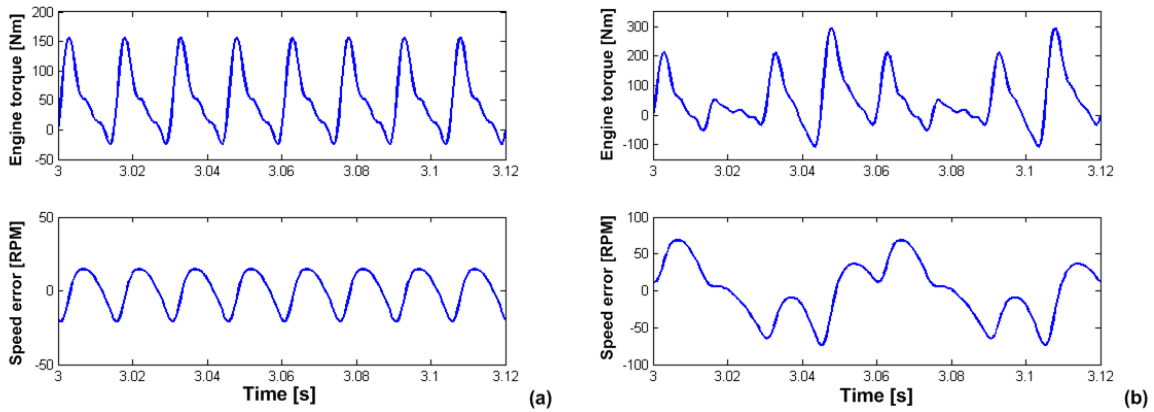
*Figure F.1: Engine speed fluctuation and engine torque for (**a**) System 1234 and (**b**) System 134.*
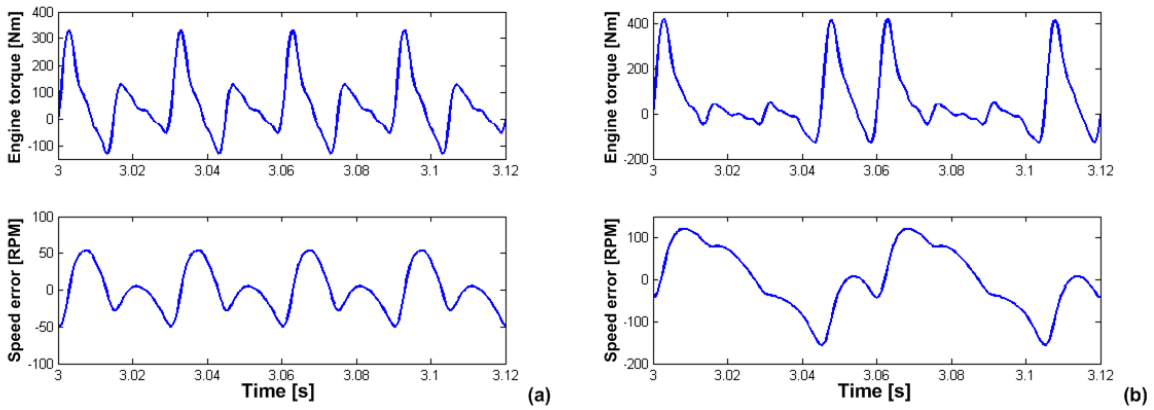

*Figure F.2: Engine speed fluctuation and engine torque for (**a**) System 14 and (**b**) System 13.*
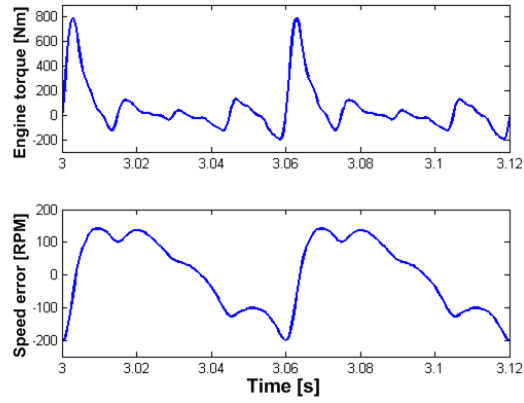
Figure F.3: Engine speed fluctuation and engine torque, cylinder 1 active undamped ISAD powertrain.
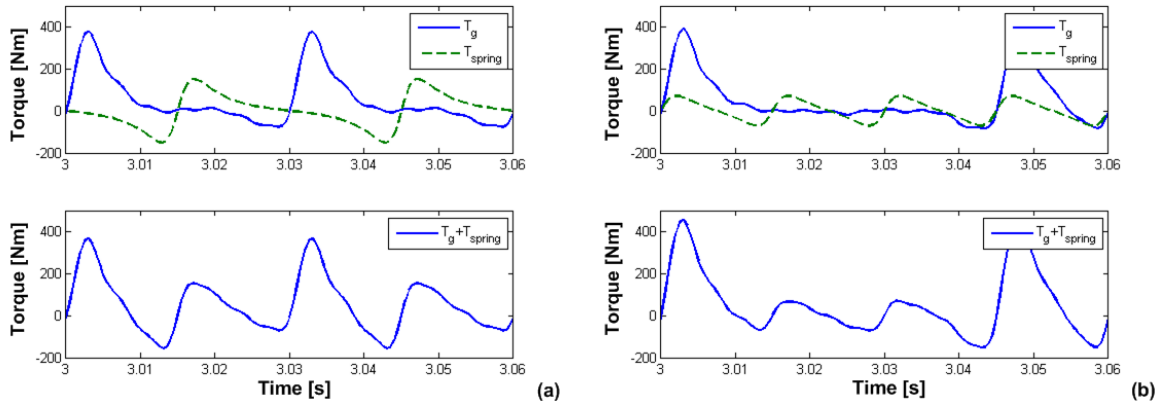
F.2 Air spring torque

*Figure F.4: Comparison between the gas pressure torque and air spring torque of (**a**) System 14 and (**b**) System 13.*

F.3 Simulation results

Figures F.5 to F.8 shows for three engine speeds, 1500, 2500 and 3500 [RPM] what the effect is of damping with the ISAD system on the 4 different systems. The effect, η_{ISAD}, is defined by equation F.1, with X_{damped} the magnitude of the damped system and X the magnitude of the undamped system.

$$\eta_{ISAD} = \frac{X_{damp} - X}{X} * 100\% \tag{F.1}$$

Also visible in the figures, is the effect of cylinder deactivation on the response magnitude related to the situation where no cylinders are deactivated. The effect is defined with f_x, where x stands for the deactivated system, see equations F.2 to F.4.

$$f_{134} = \frac{X_{134}}{X_{1234}} \tag{F.2}$$

$$f_{14} = \frac{X_{14}}{X_{1234}} \tag{F.3}$$
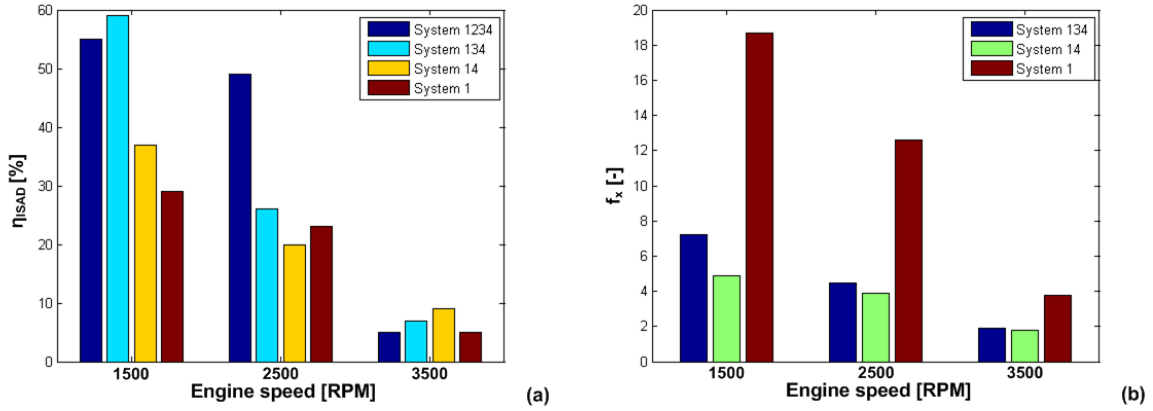
$$f_1 = \frac{X_1}{X_{1234}} \tag{F.4}$$

Figure F.5: **(a)** *Effect of ISAD damping on the cyclic speed fluctuation, related to the undamped situation.* **(b)** *Increase of cyclic speed fluctuation for* System 134, System 14 *and* System 1 *with respect to* System 1234.
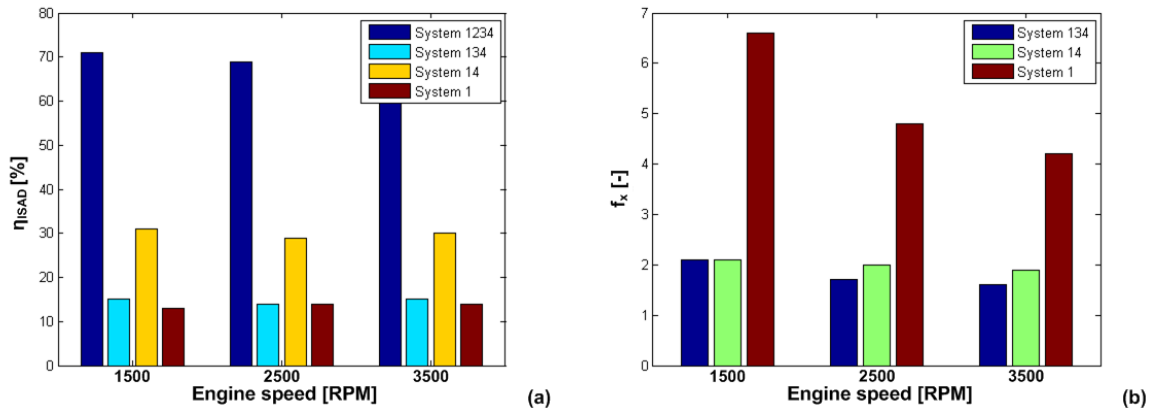
*Figure F.6: (**a**) Effect of ISAD damping on the transmission acceleration, related to the undamped situation. (**b**) Increase of transmission acceleration for* System 134, System 14 *and* System 1 *with respect to* System 1234.
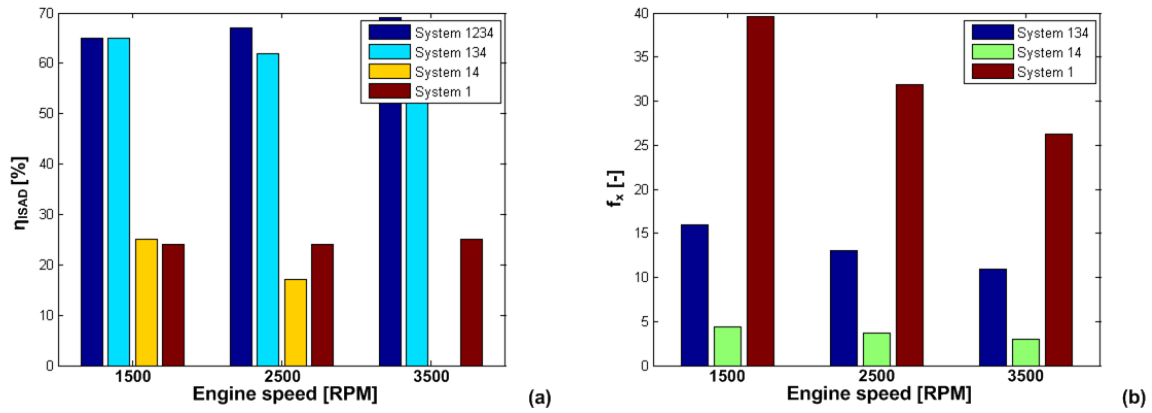

*Figure F.7: (**a**) Effect of ISAD damping on the vehicle acceleration, related to the undamped situation. (**b**) Increase of vehicle acceleration for* System 134, System 14 *and* System 1 *with respect to* System 1234.
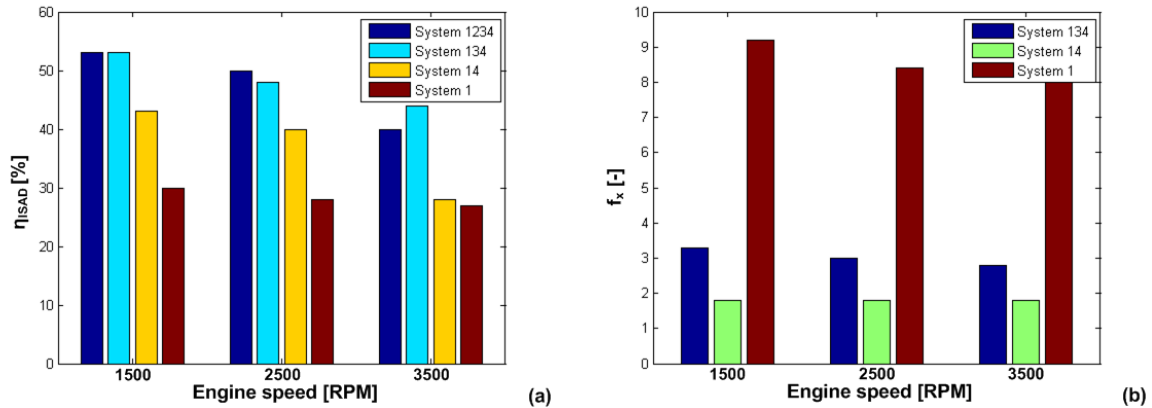

*Figure F.8: (**a**) Effect of ISAD damping on the powertrain unit acceleration, related to the undamped situation. (**b**) Increase of powertrain unit acceleration for* System 134, System 14 *and* System 1 *with respect to* System 1234.